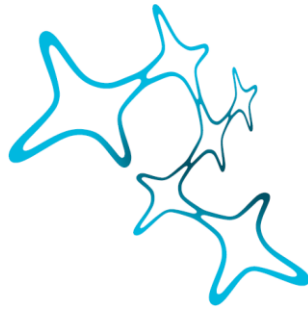


Dissertation an der
Graduate School of Systemic Neurosciences
der Ludwig-Maximilians-Universität München



Graduate School of
Systemic Neurosciences
LMU Munich

Modulation of the central vestibular networks through aging and high-strength magnetic fields

Implications for studies of vestibular function
with functional magnetic resonance imaging



vorgelegt von
Rainer E. Bögle
aus Gammertingen

München, den 20.02.2017

First reviewer: Prof. Dr. med. Marianne Dieterich

Second reviewer: Dr. rer. nat. Afra Wohlschläger

Day of submission: 20.02.2017

Date of Defense: 26.07.2017

“Discovery consists in seeing what everyone else has seen
and thinking what no one else has thought.”

- Albert Szent-Györgyi
(Hungarian Biochemist, 1893-1986, 1937 Nobel Prize for Medicine)

Abstract

The importance of the vestibular system usually goes unnoticed in our daily lives and its significance is only experienced by patients suffering from vestibular diseases. The vestibular system is essential for orientation in space, and perception of motion, as well as keeping balance, and maintaining stable visual perception while moving in a three-dimensional world.

Functional imaging has long been used to study the multisensory vestibular network in healthy subjects, as well as in patients with diseases of the vestibular system. The majority of these previous studies sought to associate brain areas with vestibular processing, by evaluating increases or decreases in blood-oxygen-level dependent signal (BOLD-signal) during application of artificial vestibular stimulations.

However, many basic network properties of the multisensory vestibular cortical network still remain unknown. Since it is now possible to infer networks from functional connectivity analysis, that associates areas into networks based on their spatiotemporal signal behavior, a few of the remaining questions can be addressed.

The dynamics of the vestibular networks and other co-activated networks in regard to the processing of a multisensory stimulation remain largely unknown. Do subjects of different ages respond differently to a vestibular challenge? Furthermore, a new form of vestibular stimulation, termed magnetic vestibular stimulation (MVS), has recently been discovered. It occurs in strong magnetic fields (≥ 1.5 tesla), that are commonly used in functional magnetic resonance imaging (fMRI), and raises questions about a possible modulation of vestibular networks during fMRI, potentially biasing functional neuroimaging results.

The purpose of this thesis is to develop suggestions for studying the multisensory vestibular network and the influence of vestibular modulations on resting-state networks with fMRI. The focus lies on basic scientific investigations of

- (1) the influence of aging on the ability of subjects to respond to a challenge of the multisensory vestibular network and
- (2) the modulatory influence of magnetic fields (the MR environment) on functional imaging and resting-state networks in general. To this end, we carried out two studies.

The first study was a cross-sectional aging study investigating the modulation of vestibular, somatosensory and motor networks in healthy adults (N=39 of 45 in total, age 20 to 70 years, 17 males). We used galvanic vestibular stimulation (GVS) to stimulate all afferences of the peripheral vestibular end organs or vestibular nerve in order to activate the entire multisensory vestibular network, as age-associated changes might be specific to sensory processing. We also controlled for changes of the motor network, structural fiber integrity (fractional anisotropy – FA), and volume changes to simultaneously compare the effects of aging across structure and function.

The second study investigated the influence of the static magnetic field of the MR environment in a group of healthy subjects (N=27 of 30 in total, age 21 to 38 years, 19 females), as it was recently shown that a strong magnetic field produces a vestibular imbalance in healthy subjects. We examined MVS at field strengths of 1.5 tesla and 3 tesla. The associated spontaneous nystagmus, the scaling of the nystagmus' slow phase velocity (SPV) across field strengths, the between subject variance of the SPV were analysed, and the analogous scaling relationship was identified in the modulation of resting-state network amplitudes, like the default mode network (DMN), between 1.5 tesla and 3 tesla to reveal its effect on fMRI results.

Aging and MVS modulated networks associated with vestibular function and resting-state networks known for vestibular interactions.

The results from our aging study imply that the dynamics of vestibular networks is limited by the influence of aging even in healthy adults without any noticeable vestibular deficit. Vestibular networks show a decline of functional connectivity with age and an increase of temporal variability (in excess of stimulation induced changes) with age. In contrast somatosensory and motor networks did not show any significant linear relationship with age or any significant changes between the youngest and oldest participants. Age-associated structural changes (gray matter volume changes or structural connectivity changes) did not explain the decline in functional connectivity or increase in temporal variability. Furthermore, stimulation thresholds did not change with age (nor did they correlate with the functional connectivity amplitudes or temporal variability), indicating that the age-associated changes that were found for the vestibular network, were not dependent on peripheral decline, as GVS is thought to directly stimulate the vestibular nerve.

The results from our study of the influence of the static magnetic field of the MR environment showed that MVS was already present at a field strength of 1.5 tesla, as evident from the induced nystagmus, indicating a state of vestibular imbalance. Furthermore, MVS scaled linearly with field strength between 1.5 tesla and 3 tesla, and identified the effects of MVS in the scaling of functional resting-state network fluctuations, showing that MVS does indeed influence resting-state networks due to vestibular imbalance. Specifically, MVS does influence DMN resting-state network dynamics in accordance with the predicted scaling of MVS based on the Lorentz-force model for MVS. These results taken together not only imply that subjects were in a vestibular state of imbalance, but also that the extent and direction of the state of imbalance showed more variance between subjects with increasing field strength.

In summary, the following suggestions for vestibular research can be delineated to extend the kind of questions that can be answered by functional MRI experiments and to improve these investigations for the benefit of clinically relevant research of healthy controls and patients.

Regarding the influence of age, we suggest that researchers comparing patients with vestibular deficits and healthy controls should separate the age-matched group into age-strata (non-overlapping subgroups with different age spans, e.g. 20-40 years, 40-60 years and above 60 years of age). Each stratum should be compared and interpreted separately given that different age-groups have different levels of vestibular network dynamics available for compensation (or responding to a challenge). This is particularly relevant when patients show a wide age-distribution, e.g. in the case of vestibular neuritis patients.

With respect to the influence of magnetic fields, we suggest that MVS should be seen as a new way of manipulating networks that either process vestibular information or show vestibular interactions, by using strong magnetic fields (≥ 1.5 tesla), as commonly used in MRI. The potential of modulating vestibular influences on networks via MVS lies in being able to induce or manipulate vestibular imbalances. In the healthy this can be used to create states that are similar to the diseased state, but without peripheral or central lesions. In patients this will allow to extend or reduce vestibular imbalances. In both cases this can be done while performing functional MRI simply by using the magnetic field of the MRI scanner and adjusting the head position of the subject in question. In studies that need to avoid vestibular perturbations MVS should be controlled by adjusting the head position of the subject and measuring the resulting eye movements. This should then be seen as an effort to remove unwanted variance, i.e., as an effort to homogenize the group, and achieve better

statistical results due to less (uncontrolled) MVS interference that increases bias and variance with increasing field strength.

In summary, these suggestions result in three short questions that researchers could ask themselves when thinking about vestibular research projects in the future.

Age-grouping:

“Is the response to a challenge different for younger adults than older adults, i.e., does each age-group compensate differently?”

MVS modulation:

“Can a manipulation of the imbalance state of our subjects with MVS help us to reveal more about the vestibular network’s response to a challenge or should we avoid interference by MVS in the imbalance state of our subjects?”

Sensitivity:

“Is the measure that I want to use sensitive enough to show the differences that I am looking for?” Connectivity and temporal variability might be sensitive enough, but many clinical tests might not be sufficient.

List of abbreviations

- MRI - magnetic resonance imaging
- fMRI - functional magnetic resonance imaging
- BOLD - blood-oxygen-level dependent
- CVS - caloric vestibular stimulation
- GVS - galvanic vestibular stimulation
- STB - short tone bursts
- MVS - magnetic vestibular stimulation
- SPV - slow phase velocity
- OKS - optokinetic stimulation
- OKN - optokinetic nystagmus
- VOR - vestibular ocular reflex
- MVN - medial vestibular nuclei
- SVN - superior vestibular nuclei
- LVN - lateral vestibular nuclei
- DVN - descending vestibular nuclei
- MST - middle superior temporal area
- VIP - ventral intraparietal area
- CSv - cingulated sulcus visual
- DTI - diffusion tensor imaging
- FA - fractional anisotropy
- DMN - default mode network

Table of contents

ABSTRACT	I
LIST OF ABBREVIATIONS	V
GENERAL INTRODUCTION	1
The vestibular system	1
The peripheral vestibular system	1
The multisensory central vestibular network	3
Vestibular stimulation methods and their neural correlates	6
Caloric vestibular stimulation	6
Galvanic vestibular stimulation	7
Short tone burst (“Clicks”) vestibular stimulation	8
Magnetic vestibular stimulation	8
Summary of the neural correlates for vestibular stimulations	9
The state of knowledge with respect to the cortical vestibular network	10
Open questions	10
Aim of the thesis	12
The effects of aging on the vestibular network	12
The effects of strong magnetic fields on resting state networks	12
CUMULATIVE THESIS	14
Age-related decline in functional connectivity of the vestibular cortical network	15
Abstract	15
Author contribution	16
Magnetic vestibular stimulation modulates default mode network fluctuations	17
Abstract	17
Author contribution	18
GENERAL DISCUSSION	19
Purpose of this thesis	19
Summary of the studies performed	19
Summary of the main results and conclusions of our two studies	20
Does aging impact vestibular research results?	22
Aging of peripheral and central vestibular structures	22
What approach is necessary for detecting aging effects?	23
Does functional connectivity represent a “reservoir of resilience”?	24

Does magnetic vestibular stimulation impact vestibular research results?	26
Overview of human and animal studies regarding magnetic vestibular stimulation	26
How neuroimaging studies of vestibular function might be affected by MVS	27
Potential implications for vestibular research with fMRI	30
Effects of age on vestibular research	30
Effects of strong magnetic fields on vestibular research	31
Summary of suggestions for study design	32
REFERENCES	33
APPENDIX	40
Acknowledgements	40
CV Rainer E. Bögle	41
List of all publications including copyright statements	43
Affidavit – Eidesstattliche Versicherung	44
Declaration of author contributions	45
Age-related decline in functional connectivity of the vestibular cortical network	45
Magnetic vestibular stimulation modulates default mode network fluctuations	46

General Introduction

The vestibular system

The importance of the vestibular system usually goes unnoticed in our daily lives and its significance is only experienced by people suffering from damages to one or several components of the vestibular system (Brandt et al., 2005; Cullen and Sadeghi, 2008; Dieterich and Brandt, 2008). The vestibular system is essential for orientation in space, and perception of motion, as well as keeping balance, and maintaining stable visual perception while moving in a three-dimensional world (Cullen and Sadeghi, 2008; Goldberg et al., 2012). Considering that these functions are essential for any animal's survival, it is not surprising that vestibular structures are one of the oldest structures that have developed during evolution, and are basically as old as the "Kingdom Animalia" (Metazoa) itself (Graf, 2009). Evidence for peripheral vestibular structures has been found in fossils that are over 400 million years old (Graf, 2009). For our purposes, we will distinguish the vestibular system into two parts, the peripheral vestibular end organs and the central nervous system with its multisensory vestibular network.

The peripheral vestibular system

The peripheral vestibular end organs are located in the temporal bone in direct vicinity of the cochlea, and are believed to be evolutionarily older than the cochlea (Graf, 2009). They are contained within a structure called the membranous labyrinth of the inner ear, (see figure 1A). The membranous labyrinth consists of five parts, the three semicircular canals and the two otolith organs, the utricle and the saccule (see figure 1B). The semicircular canals detect rotations while utricle and saccule detect translations of the head as well as head orientation with respect to gravity (Goldberg and Hudspeth, 2004; Goldberg et al., 2012).

Rotations of the head are sensed via detection of inertial flow (i.e., opposite to the head rotation) of endolymph fluid leading to deflections of the hair cells in the ampullary cupula of each respective semicircular canal (figure 1B). The membrane of the ampullary cupula is a gelatinous structure containing hair cells (i.e. cells with mechanosensitive ion channels) that influence the bipolar cells of the eighth cranial nerve (nervus vestibulocochlearis) in response to a deformation induced by inertial flow of the endolymph during head rotations (see detail inlays in figure 1B). The ion-channels of the hair cells are opened when the cells are bent in

one direction and closed when bent in the opposite direction, leading to an increase or decrease of their firing rate, respectively.

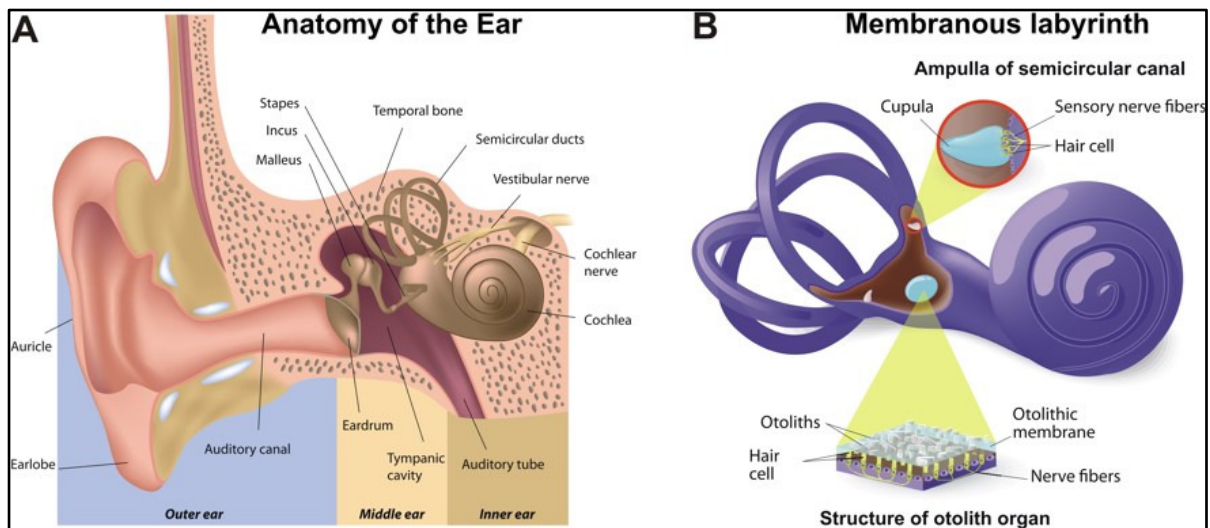


Figure 1: The anatomy of the ear (A) and the anatomy of the membranous labyrinth (B). [Images, used (and modified) under license from Shutterstock.com. (A) Alila Medical Media/Shutterstock.com, and (B) Designua/Shutterstock.com]

The three semicircular canals (horizontal, anterior, and posterior canals) of the left and right ear work in reciprocal pairs. The two horizontal canals work together, while each anterior canal is paired with the posterior canal of the opposite ear. This means that rotations can be sensed with “double” precision due to the reciprocal interaction of the pairs. If head motion occurs in a plane specific to a pair of canals, flow in one canal will lead to excitation while flow in the opposite paired canal will lead to inhibition.

In general, firing rate changes transmitted through the eighth cranial nerve are the way vestibular sensations are transmitted to the central nervous system. Note that the firing rate of the hair cells is reported to be near 100 Hz at rest, allowing for a wide range of modulation and the whole apparatus is sensitive to angular accelerations of $>0.1^\circ/s^2$ (Shumway-Cook and Woollacott, 2007). However, during continuous rotations a steady-state of zero flow can be reached and the cupula returns to its resting position, i.e., the cells go back to the resting firing rate, analogous to keeping the head still.

Translations and the orientation of the head relative to gravity are detected by the utricle and saccule. The utricle, by virtue of its orientation, senses linear accelerations and head-tilts in the horizontal plane. Analogously, the saccule is sensitive to vertical plane movements and head-tilts. Both structures together are termed the otolith organs (from the greek word “lithos”, meaning “stone”) containing hair cells that are surrounded by a gelatinous structure

with embedded calcium carbonate stones that by virtue of inertial acceleration allow sensing of the direction of gravitation or translation during movements (Goldberg and Hudspeth, 2004).

The multisensory central vestibular network

The multisensory vestibular cortical network interprets signals from the vestibular end organs, but it also does far more than just interpretation of these signals. Our sense of self motion and orientation in space, as well as a stable visual perception, and the control of posture and balance is dependent on a proper functioning of the multisensory vestibular network (Goldberg and Hudspeth, 2004; Shumway-Cook and Woollacott, 2007; Cullen and Sadeghi, 2008; Goldberg et al., 2012). To achieve these feats of perception and motor control, the multisensory vestibular cortical network has to engage in integration of information coming not only from the peripheral vestibular sensory end organs, but also from the visual, the proprioceptive, the somatosensory and the auditory systems (Cullen and Sadeghi, 2008).

The central multisensory vestibular network consists of the respective brain stem nuclei (mainly the medial (MVN), superior (SVN), lateral (LVN), and descending vestibular nuclei (DVN)), as well as cerebellar regions (nodulus, uvula, flocculus, and paraflocculus, as well as vermis, and fastigial deep cerebellar nucleus), and several cortical areas (e.g., the medial superior temporal (MST) area, posterior insula, parietal operculum, ventral intraparietal (VIP) area, anterior cingulum, and cingulate sulcus visual (CSv) area) which receive secondary input from the brain stem and cerebellum via the dorsolateral, and presumably the ventral anterior thalamus (Goldberg et al., 2012). It was recently shown that there might also be a direct ipsilateral connection bypassing the thalamus connecting the brain stem via the midbrain to the opercular-insular region (Kirsch et al., 2016).

The brain stem regions receive direct primary afferents from the vestibular periphery, as well as modulatory secondary inputs from the cerebellum, visual, somatosensory, proprioceptive and oculomotor regions of the cortex, making its processing truly multisensory even at the early stage (Goldberg et al., 2012).

The cerebellar regions receive direct afferents from the vestibular periphery and secondary inputs from the vestibular nuclei of the brain stem and provide an integrated signal back to the brain stem. One example of this feedback signal is the selective encoding of translational motion that remains relatively insensitive to changes in head orientation relative to gravity. It is generated via the processing in cerebellar regions nodulus and uvula as well as the fastigial

nucleus that provide an integration of signals from canal afferents which are activated during head tilt but not during pure translation. This signal is then combined with otolith signals to subtract out the influence of gravity from inertial motion, yielding a signal that selectively encodes translational motion (Cullen and Sadeghi, 2008; Goldberg et al., 2012).

The nodulus and uvula play a critical role in controlling the three-dimensional dynamics of the velocity storage system. In particular the integration of both canal and otolith inputs at the level of individual neurons facilitates the computation of head motion relative to space. The flocculus and adjacent paraflocculus are involved in the generation of ocular-visual following responses (i.e., optokinetic nystagmus (OKN) and pursuit). In addition, these regions are a critical component of the neural substrate underlying the plasticity of the optokinetic reflex and the VOR. The oculomotor vermis and anterior lobes make use of extra-vestibular inputs (visual and proprioceptive information, respectively) to ensure that the motor responses produced by vestibular pathways remain appropriately calibrated. Lastly, the deep nuclei, most notably the fastigial nucleus, play an important role in the generation of postural reflexes and orienting behaviors. Projections from the anterior lobe of the vermis and most medial zones of the nodulus and ventral uvula converge in the fastigial nucleus, which in turn projects to the brain stem structures (including the vestibular nuclei) to control and modulate behaviors (Cullen and Sadeghi, 2008; Goldberg et al., 2012).

Cortical processing of vestibular input is important for generating appropriate modulations of motor responses and the subjective sense of movement and orientation in three-dimensional space (Cullen and Sadeghi, 2008; Goldberg et al., 2012). The middle superior temporal area (MST) responds to optic flow and provides a signal for the direction of the visual signal or heading direction of the animal that allows smooth pursuit responses to follow and stay on target, but it does not respond to multiple patches of optical flow that are inconsistent with egomotion (Wall and Smith, 2008). The areas VIP (ventral intraparietal sulcus) and CSv (cingulate sulcus visual) are believed to be further processing stations in regard to egomotion, i.e., self-induced (visual) motion of the environment (Wall and Smith, 2008; Fischer et al., 2012). The posterior insula and the parietal operculum are believed to be multisensory integration hubs that receive strong vestibular input. They seem to act as the central vestibular relay regions in the cortex, i.e., all vestibular input goes into these regions and is integrated with all other sensory modalities from there as a central region “in the middle” of all these inputs (zu Eulenburg et al. 2012; Lopez et al. 2012). All these areas project back to the

vestibular nuclei and modulate the motor response depending of the behavioral context (Goldberg et al., 2012).

The functioning of the vestibular system as a whole is therefore based on the meaningful fusion of sensors. Vertigo and dizziness may occur if these multisensory interactions are disturbed, either at the periphery sensory end organs or the central level (Brandt et al., 2005; Dieterich and Brandt, 2008).

Thus, one main feature of the vestibular system is the integration of multisensory information and can best be understood in terms of interconnectivity of distant brain regions, i.e., networks in the brain.

Vestibular stimulation methods and their neural correlates

The functioning of the vestibular end organs and the neural correlates of the multisensory vestibular system have previously been studied using stimulations of the vestibular end organs during neuroimaging (e.g. see (Dieterich and Brandt, 2008; Lopez et al., 2012; zu Eulenburg et al., 2012; Wiest, 2015)). The most common forms of vestibular stimulation are caloric irrigation (CVS) of the horizontal semicircular canal with water or air, galvanic vestibular stimulation (GVS) of the irregular and to a lesser extend also regular afferents in the vestibular nerve, or “Clicks”, loud short tone burst (STB) vestibular stimulation, i.e., sound pressure induced otolith stimulation (for an overview see (zu Eulenburg et al. 2012; Lopez et al. 2012)). A more recent variant of stimulating the vestibular end organs with strong magnetic fields (>1 T), termed magnetic vestibular stimulation (MVS) has recently emerged (Roberts et al., 2011), although it was long known that strong magnetic fields cause dizziness (Schenck, 1992). Due to the multisensory nature of the vestibular network and the interaction with other sensory systems different sensory stimuli can be used to create vestibular (e.g. dizziness) or self-motion sensations. Optokinetic stimulation (OKS) for example can be applied to elicit nystagmus and induce a vection sensation (the feeling of self-motion), by exploiting visual-vestibular interactions (Brandt et al., 1998; Dieterich et al., 1998; Bense et al., 2006; Dieterich, 2007).

It is important to note here, that all these stimulations have confounding effects but they have to be used during functional neuroimaging, because more natural stimulation of the vestibular periphery via actual head movements will lead to severe artifacts in MRI and correction methods for free movement are still under development (for a review see Zaitsev et al. 2015).

Caloric vestibular stimulation

It is mostly believed that caloric vestibular stimulation (CVS) acts upon the semicircular canals by inducing a convective flow caused by temperature changes relative to the body temperature (Barany, 1906; Friberg et al., 1985; Aw et al., 2000; Arai, 2001; Maes et al., 2007). However, it was also demonstrated that CVS induced nystagmus occurs in microgravity, suggesting that there might also be another mechanism of stimulation, possibly shifting discharge rates of hair cells (Scherer and Clarke, 1987). The stimulation can be done by using hot ($>40^{\circ}\text{C}$) or cold ($\leq 30^{\circ}\text{C}$) water (air) irrigation of one (monothermal stimulation) or both ears (bithermal stimulation). A maximal stimulation of the horizontal canal with CVS can be achieved by putting subjects in a supine position with their head tilted 30° forward in

order to align the horizontal canal perpendicular to the direction of gravity. CVS then leads to a horizontal-rotatory nystagmus and a profound rotatory vertigo.

The confounding effects of CVS are the simultaneous stimulation of the vagal nerve, the somatosensory (tactile, thermal, pain), and auditory system due to the injection of water into the external ear canal.

Galvanic vestibular stimulation

Galvanic vestibular stimulation uses electrical current flow (>1 mA) with an electrode placed over the mastoid bone. It was suggested that it stimulates the entire vestibular nerve (eighth cranial nerve) at the axon hillock, where the electrical potential needed for generating action potentials is lowest (Goldberg et al., 1982, 1984; Zink et al., 1998; Schneider et al., 2002; Fitzpatrick and Day, 2004; Curthoys and MacDougall, 2012). This means GVS influences the firing rate at the eighth nerve to cause vestibular sensations. Note that this can result in a stimulation of all afferents of the vestibular end organs, canals and otolith organs alike, as the whole nerve is stimulated. It is believed that GVS increases the firing rate at the side of the cathode and decreases the firing rate at the side of the anode at those time intervals of the stimulation when the stimulation current is changing (Goldberg et al., 1984). This implies that a constant or direct current stimulation will change the firing rate only during the onset (or offset) of the direct current galvanic vestibular stimulation (DC-GVS), but not during the phase of the stimulation when the current is constant. This also means that the firing rate changes continuously during an alternating current galvanic vestibular stimulation (AC-GVS), e.g., when applying a sinusoidal stimulation current (Goldberg et al., 1982, 1984; Schneider et al., 2002; Fitzpatrick and Day, 2004; Stephan et al., 2005, 2009; Lopez et al., 2012). GVS modulates and excites all aspects of the vestibular network, as it stimulates the whole nerve and leads to vertigo, ocular torsion and rotatory nystagmus in the case of AC stimulation (Schneider et al., 2002; Fitzpatrick and Day, 2004; Stephan et al., 2005). In the case of DC stimulation, GVS leads to a feeling of head tilt, and torsion of the eyes around the gaze direction (Zink et al., 1997, 1998). The perceptual effect is akin to feeling “pushed” or “nudged”, and occurs in the onset and offset phase of the stimulation, and subsides over the course of the constant stimulation when the current does not change (Zink et al., 1998; Schneider et al., 2002; Stephan et al., 2009).

The confounding effects of GVS are the stimulation of the skin around the electrodes leading to tactile and nociceptive sensations activating the somatosensory system and possibly a

stimulation of the vagus nerve, metallic taste on the tongue and increased saliva production due to stimulation of the chorda tympani, as well as the potential elicitation of phosphenes due to the electrode placement in the vicinity of the inferior occipital cortex. Using sustained DC-GVS it was possible to distinguish the vestibular and somatosensory response in fMRI (Stephan et al., 2009). This is possible due to the different time courses of the vestibular sensation, occurring especially at the onset and offset of stimulation, in contradistinction to the somatosensory sensations that are continuously present throughout the stimulation (Stephan et al., 2009).

Short tone burst (“Clicks”) vestibular stimulation

Tone burst “clicks” (usually 500 Hz sounds of 110 dB-SPL or louder) are believed to influence mainly the otolith organ saccule, (probably also to a smaller amount the utricle), due to the differential pressure of the sound waves leading to motion of the otoliths (Colebatch et al., 1994; Rosengren et al., 2005). Tone burst “clicks” do not influence the flow in the semicircular canals of the labyrinth, but the stimulation of the otoliths have been shown to create interactions with signals from the semi-circular canals. This means tone burst “clicks” only interfere with signals from semi-circular canals by virtue of stimulating the otoliths, but do not stimulate the canals themselves (Miyamoto et al., 2007; Janzen et al., 2008; Schlindwein et al., 2008; Lopez et al., 2012).

Tone bursts and “clicks” are confounded by the activation of the auditory system and, if loud enough, may be experienced as a painful sensation.

Magnetic vestibular stimulation

Magnetic vestibular stimulation (MVS), has recently been proposed as another form of vestibular stimulation that occurs in the presence of strong magnetic fields (>1 tesla). MVS might potentially be present during all fMRI experiment (Roberts et al., 2011; Antunes et al., 2012; Glover et al., 2014; Ward et al., 2014a, 2015; Boegle et al., 2016). It was shown that healthy subjects exposed to the static magnetic field of a MR scanner developed a persistent nystagmus (in total darkness), while patients with bilateral peripheral vestibular failure did not show any nystagmus (Roberts et al., 2011). This supports the hypothesis that MVS actually originates in the inner ear. It was proposed that the ionic currents coming from hair cells in the inner ear are diverted by a Lorentz-force (Roberts et al., 2011). This creates an endolymph flow diverting the cupula, “the rotatory motion sensor” of the inner ear, resulting in a nystagmus akin to an accelerating rotatory stimulation (Glover et al., 2014; Jareonsettasin et

al., 2016). The orientation-dependency of the Lorentz-force in the magnetic field of an MRI scanner also explains why the nystagmus' slow phase velocity (SPV) depends on the subject's head orientation within the magnetic field (Roberts et al., 2011). This model was further supported by several studies (Antunes et al., 2012; Glover et al., 2014; Ward et al., 2014a; Jareonsettasin et al., 2016). Analogous behavioral and neural effects were reported for animals (e.g. see: (Saunders, 2005; Houpt et al., 2013; Ward et al., 2015)).

Consequently, it was speculated that this magnetic vestibular stimulation (MVS) might influence fMRI results (Roberts et al., 2011), as nystagmus is indicative of an imbalance in the vestibular system, potentially influencing also other systems via multisensory vestibular interactions (Boegle et al., 2016).

Summary of the neural correlates for vestibular stimulations

Functional imaging has long been used to study the multisensory vestibular network in healthy subjects, as well as diseases of the vestibular system (e.g. for review see: Dieterich & Brandt 2008; zu Eulenburg et al. 2012; Lopez et al. 2012; Besnard et al. 2015).

While neural correlates due to MVS had not been investigated until our study (Boegle et al., 2016), there are a many studies with respect to the other three stimulation methods CVS (Bottini et al., 1994, 2001; Suzuki et al., 2001; Becker-Bense, 2003; Dieterich et al., 2003; Marcelli et al., 2009), GVS (Lobel et al., 1998; Bense et al., 2001; Stephan et al., 2005; Eickhoff et al., 2006; Cyran and Boegle et al., 2016), and STB "Clicks" (Miyamoto et al., 2007; Janzen et al., 2008; Schlindwein et al., 2008).

These show a convergence of activated areas over a larger network with activations mainly in the insular, and retroinsular cortex, parietal operculum, the superior temporal gyrus, the supramarginal gyrus, the inferior parietal lobe, the inferior frontal gyrus, the anterior cingulate gyrus, the thalamus, the cerebellum, the basal ganglia, and the hippocampus in both hemispheres, with a particular preponderance of activation on the right hemisphere for right-handed individuals, and on the left hemisphere for left-handed individuals (Bottini et al., 1994; Lobel et al., 1998; Brandt and Dieterich, 1999; Bense et al., 2001; Dieterich et al., 2003; Stephan et al., 2005; Schlindwein et al., 2008; Lopez and Blanke, 2011; Lopez et al., 2012; zu Eulenburg et al., 2012).

The state of knowledge with respect to the cortical vestibular network

Many basic network properties of the multisensory vestibular cortical network remain unknown, despite multiple studies researching the neural correlates of stimulations of the vestibular end organs. This is mainly due to the fact that the areas that have been found in terms of “analysis of co-activation”. This means that the areas were identified with vestibular processing by evaluating increases or decreases in activation level during application of CVS, GVS, and STBs (“clicks”). The association of these areas into networks was previously inferred by considering other sources, e.g. animal research. However, it is now also possible to infer networks from fMRI functional connectivity analysis that associates areas into networks based on their spatiotemporal signal behavior (Beckmann and Smith, 2004; Beckmann et al., 2005; Smith et al., 2009; Garrett et al., 2010, 2011).

Open questions

The network relationship of the aforementioned co-activated areas is not established. The dynamics of the networks in regard to the progression of the stimulation remain largely unknown. Furthermore, the confounding effects of the stimulation methods (see above) make a distinction of vestibular and other influences difficult.

Therefore, the following questions were addressed:

“Is it possible to distinguish networks associated with the confounding effects from networks associated with the vestibular response?”

“Which areas overlap between these networks, i.e., which areas are potentially multisensory, or integration areas?”

“Is there a purely vestibular area in the cortex or are all cortical areas receiving vestibular input multisensory, i.e., mixed with other sensory signals?”

The dynamics of the networks over the lifespan remain unknown. Note that any effects that occur during healthy aging can have important implications for the various studies that have investigated responses for patient versus controls. Most of the patients involved in such studies have already reached a stage of advanced age post-maturation (>50 years of age), but patients suffering from an acute vestibular failure (e.g. vestibular neuritis) can be of any age and the status of their network dynamics may be an important factor in how they respond to this challenge during rehabilitation.

The associated questions here were:

“Is the response from the network under a challenge different across the lifespan?”

“Does the compensation in response to disease change over the ages based on the underlying properties of the network across the ages?”

For almost 25 years dizziness in MR-scanners has been reported and linked with the strong magnetic fields used in MRI (e.g. Schenck 1992), but it is still unclear how this affects the vestibular system and BOLD-responses in functional imaging. It has recently been shown that healthy subjects develop a persistent nystagmus in the magnetic field of a MR environment (Roberts et al., 2011). The presence of a spontaneous nystagmus is indicative of a vestibular imbalance and it was speculated that this magnetic vestibular stimulation (MVS) might lead to modulations of fMRI results, given that modulations of resting-state networks have been shown in response to vestibular imbalances caused by peripheral vestibular dysfunctions (Roberts et al., 2011; Göttlich et al., 2014; Helmchen et al., 2014; Klingner et al., 2014).

Therefore, the question remains

“Does MVS influence network dynamics via an interaction due to vestibular imbalance as indicated by the spontaneous nystagmus?”

Aim of the thesis

The thesis focuses on the study of vestibular function and vestibular interaction with an array of brain areas, and sensory systems by means of functional neuroimaging. We have conducted basic scientific research to fill some of the knowledge gaps with regard to network properties, the influence of aging, and strong magnetic fields encountered in a MR environment upon these network properties.

The purpose of this doctoral thesis is to derive suggestions for researchers interested in the vestibular system, to extend the kind of questions that can be answered by functional MRI experiments and improve these investigations for the benefit of clinically relevant research of patients and healthy controls.

The effects of aging on the vestibular network

A cross-sectional aging study of 45 mature subjects (>20 years of age to 70 years of age) was performed with DC-GVS (Cyran and Boegle et al., 2016). The aim was to explore the changes of the connectivity and temporal variability of brain networks that are available to the average healthy adult throughout their post-adolescence lifespan. This is based on the idea that connectivity can be interpreted as the foundation for responding to challenges, be it either to an artificial stimulation or compensating a peripheral vestibular disease. The study used DC-GVS to activate all afferents of the vestibular end organs and employs a square-shape time course for the stimulation, i.e., a sustained current. This stimulation shape allows the differentiation of vestibular and somatosensory responses, as it was previously shown that the perceived vestibular sensations occur at the onset and offset while the somatosensory sensations occur continuously during the stimulation (Stephan et al., 2009). We set out to characterize the stimulated networks across the lifespan. For this we went beyond the usual examination of response amplitudes, and included analysis of spatiotemporal correlatedness, as well as temporal dispersion of the responses (Beckmann and Smith, 2005; Garrett et al., 2010; Cyran and Boegle et al., 2016). The study also included a motor-task control experiment, as well as analysis of anatomical changes in grey matter volume, and structural fiber integrity using diffusion tensor imaging (DTI) to account for non-specific changes with age (general vascular, atrophic, or structural changes).

The effects of strong magnetic fields on resting state networks

This experiment aimed to identify and delineate the modulatory effects of magnetic vestibular stimulation (MVS) on resting-state network fluctuations of 30 healthy adults (Boegle et al.,

2016). This study also wanted to verify the effects of previous studies suggesting a Lorentz-force model as the cause for the nystagmus slow phase velocity in a magnetic environment (Roberts et al., 2011) and established that MVS does scale linearly with field strength giving further support to the Lorentz-force model of MVS (Boegle et al., 2016). We recorded eye movements as well as resting-state fMRI of 30 healthy subjects in darkness at 1.5 tesla and 3.0 tesla magnetic field strength. We hypothesized that the scaling of MVS, as established from the nystagmus' SPV, should be identifiable in the scaling of the resting-state network fluctuations, indicating modulations due to a varying vestibular arousal. We demonstrated that this is indeed the case, focusing on the default mode network (DMN). This network was previously shown to be modulated in patients with peripheral vestibular dysfunction, i.e., the DMN was indicated to be modulated due to vestibular imbalances and therefore MVS was also expected to have a similar effect on this network (Göttlich et al., 2014; Helmchen et al., 2014; Klingner et al., 2014; Boegle et al., 2016).

Cumulative Thesis

This cumulative thesis consists of two articles published in peer-reviewed journals. The title and abstract of each publication are presented together with the author contributions. The full publications with the copyright forms can be found in the appendix of this thesis.

Age-related decline in functional connectivity of the vestibular cortical network

*C.A.M. Cyran^{1,2}, *R. Boegle^{3,4}, T. Stephan^{1,3,4,7}, M. Dieterich^{1,3,4,5}, S. Glasauer^{3,4,6,7}

*C.A.M. Cyran and R. Boegle contributed equally to the study.

¹Dept. of Neurology, Klinikum der Universität, Ludwig-Maximilians-University Munich, Marchioninstr. 15, 81377 Munich, Germany

²Institute of Neurology, University College London, Queen Square, London WC1N 3BG, UK

³Graduate School of Systemic Neurosciences, Ludwig-Maximilians-University Munich, Marchioninstr. 15, 81377 Munich, Germany

⁴German Center for Vertigo and Balance Disorders (IFB^{LMU}), Klinikum der Universität, Ludwig-Maximilians-University Munich, Marchioninstr. 15, 81377 Munich, Germany

⁵SyNergy: Cluster for Systems Neurology, Munich, Germany

⁶Center for Sensorimotor Research, Ludwig-Maximilians-University Munich, Marchioninstr. 15, 81377 Munich, Germany

⁷Institute for Clinical Neurosciences, Ludwig-Maximilians-University Munich, Marchioninstr. 15, 81377 Munich, Germany

Abstract

In the elderly, major complaints include dizziness and an increasing number of falls, possibly related to an altered processing of vestibular sensory input. In this study, we therefore investigate age-related changes induced by processing of vestibular sensory stimulation. While previous functional imaging studies of healthy aging have investigated brain function during task performance or at rest, we used galvanic vestibular stimulation during functional MRI in a task-free sensory stimulation paradigm to study the effect of healthy aging on central vestibular processing, which might only become apparent during stimulation processing. Since aging may affect signatures of brain function beyond the BOLD-signal amplitude -such as functional connectivity or temporal signal variability- we employed independent component analysis and partial least squares analysis of temporal signal variability. We tested for age-associated changes unrelated to vestibular processing, using a motor paradigm, voxel-based morphometry and diffusion tensor imaging. This allows us to control for general age-related modifications, possibly originating from vascular, atrophic or structural connectivity changes. Age-correlated decreases of functional connectivity and increases of BOLD-signal variability were associated with multisensory vestibular networks. In contrast, no age-related functional connectivity changes were detected in somatosensory

networks or during the motor paradigm. The functional connectivity decrease was not due to structural changes but to a decrease in response amplitude. In synopsis, our data suggest that both the age-dependent functional connectivity decrease and the variability increase may be due to deteriorating reciprocal cortico-cortical inhibition with age and related to multimodal vestibular integration of sensory inputs. (Cyran and Boegle et al., 2016)

Author contribution

The Author of this thesis participated in measuring the subjects, analyzed the functional imaging data for functional connectivity and performed the data denoising for the analysis of temporal variability, as well as writing substantial parts of the manuscript, and created figures 2, 3, and 4 of the attached publication.

Magnetic vestibular stimulation modulates default mode network fluctuations

R. Boegle^{a,b}, T. Stephan^{a,b,c}, M. Ertl^{b,c}, S. Glasauer^{a,b,d}, and M. Dieterich^{a,b,c,e}

^aGerman Center for Vertigo and Balance Disorders (DSGZ-IFBLMU),
Ludwig-Maximilians-University Munich, Marchioninstr. 15, 81377 Munich, Germany

^bGraduate School of Systemic Neurosciences,
Ludwig-Maximilians-University Munich, Marchioninstr. 15, 81377 Munich, Germany

^cDepartment of Neurology,
Ludwig-Maximilians-University Munich, Marchioninstr. 15, 81377 Munich, Germany

^dCenter for Sensorimotor Research,
Ludwig-Maximilians-University Munich, Marchioninstr. 15, 81377 Munich, Germany

^eSyNergy: Cluster for Systems Neurology, Munich, Germany

Abstract

Strong magnetic fields (>1 Tesla) can cause dizziness and it was recently shown that healthy subjects (resting in total darkness) developed a persistent nystagmus even when remaining completely motionless within a MR tomograph. Consequently, it was speculated that this magnetic vestibular stimulation (MVS) might influence fMRI results, as nystagmus is indicative of an imbalance in the vestibular system, potentially influencing other systems via multisensory vestibular interactions. The objective of our study was to investigate whether MVS does indeed modulate BOLD signal fluctuations. We recorded eye movements, as well as, resting-state fMRI of 30 volunteers in darkness at 1.5 T and 3.0 T to answer the question whether MVS modulated parts of the default mode resting-state network (DMN) in accordance with the Lorentz-force model for MVS, while distinguishing this from the known signal increase due to field strength related imaging effects. Our results showed that modulation of the default mode network occurred mainly in areas associated with vestibular and ocular motor function, and was in accordance with the Lorentz-force model, i.e., double than the expected signal scaling due to field strength alone. We discuss the implications of our findings for the interpretation of studies using resting-state fMRI, especially those concerning vestibular research. We conclude that MVS needs to be considered in vestibular research to avoid biased results, but it might also offer the possibility of manipulating network dynamics and may thus help in studying the brain as a dynamical system. (Boegle et al., 2016)

Author contribution

The Author of this thesis planned the experiment, measured the subjects, performed the data analysis, wrote major parts of the manuscript, and created all figures.

General Discussion

Purpose of this thesis

The purpose of this thesis is to develop suggestions for studying the multisensory vestibular network and the influence of vestibular modulations on resting-state networks with functional magnetic resonance imaging (fMRI). The focus lies on basic scientific investigations of (1) the influence of aging on the ability of subjects to respond to a challenge of the multisensory vestibular network, and (2) the modulatory influence of magnetic fields (the MR environment) on functional imaging and resting-state networks in general. To this end, two studies were carried out, one focusing on the effects of galvanic vestibular stimulation (GVS) on the multisensory vestibular network across the lifespan, and another study focusing on the effects of magnetic vestibular stimulation (MVS) on resting-state networks, in particular the default mode network (DMN).

Summary of the studies performed

The first study was a cross-sectional aging study investigating the modulation of vestibular, somatosensory and motor networks in healthy adults (N=39 of 45 in total, age 20 to 70 years, 17 males; of the total N=14 with age 20 to 40 years, mean age=27.3±4.4 years, 6 males; N=12 with age 40 to 60 years, mean age=52.3±5.0 years, 5 males, and N=13 with age >60 years, mean age= 67.1±2.4 years, 6 males). We used GVS to stimulate all afferences of the peripheral vestibular end organs in order to activate the entire multisensory vestibular network as age-associated changes might be specific to sensory processing (Goldberg et al., 1982, 1984; Zink et al., 1998; Schneider et al., 2002; Stephan et al., 2005, 2009; Cyran and Boegle et al., 2016). The time course of stimulation was designed to allow for a separation of vestibular and somatosensory processing based on the temporal properties of sustained DC-GVS (Stephan et al., 2009). In addition to vestibular and somatosensory stimulation, we also controlled for changes of the motor network, structural fiber integrity (fractional anisotropy – FA), and volume changes to simultaneously compare the effects of aging across structure and function.

The second study investigated the influence of the static magnetic field of the MR environment in a group of healthy subjects (N=27 of 30 in total, age 21 to 38 years, mean age= 26.5±4.6 years, 19 females), as it was recently shown that a strong magnetic field produces a vestibular imbalance in healthy subjects (Roberts et al., 2011). It was speculated

that this magnetic vestibular stimulation (MVS) might influence fMRI results (Roberts et al., 2011; Boegle et al., 2016). We examined MVS at field strengths of 1.5 tesla, and 3 tesla and analyzed the associated spontaneous nystagmus, the scaling of the nystagmus' slow phase velocity (SPV) across field strengths, and identified the analogous scaling relationship in the modulation of DMN amplitudes between 1.5 tesla, and 3 tesla to reveal its effect on fMRI results (Boegle et al., 2016). Furthermore, the between subject variance associated with MVS across field strengths was investigated by analyzing the nystagmus' SPV in four different head positions across field strengths of 1.5 tesla, and 3 tesla.

Summary of the main results and conclusions of our two studies

We were able to demonstrate that aging and MVS modulate networks associated with vestibular function and resting-state networks known for vestibular interactions (Göttlich et al., 2014; Helmchen et al., 2014; Klingner et al., 2014; Boegle et al., 2016; Cyran and Boegle et al., 2016).

The results from our aging study imply that the dynamics of vestibular networks are limited by the influence of aging even in healthy adults without any noticeable vestibular deficit (Cyran and Boegle et al., 2016). Vestibular networks show a decline of functional connectivity with age and an increase of temporal variability (in excess of stimulation induced changes) with age (Cyran and Boegle et al., 2016). Most notably, aging modulates vestibular networks differently than somatosensory or motor networks. Somatosensory and motor networks did not show any significant linear relationship with age, or any significant changes between the youngest and oldest participants, in contradistinction to the vestibular networks (Cyran and Boegle et al., 2016). We were also able to show that the somatosensory and vestibular networks overlap in a region covering the posterior insula, which we infer as an indication of multisensory integration in this area (Cyran and Boegle et al., 2016). We were able to demonstrate that age-associated structural changes (gray matter volume changes or structural connectivity changes) did not explain the decline in functional connectivity or increase in temporal variability (Cyran and Boegle et al., 2016). Furthermore, stimulation thresholds did not change with age (nor did they correlate with the functional connectivity amplitudes or temporal variability), indicating that the age-associated changes that were found for the vestibular network, were not dependent on peripheral decline, as GVS is thought to directly stimulate the vestibular nerve (Goldberg et al., 1982, 1984, 2012).

The results from our study of the influence of the static magnetic field of the MR environment showed that MVS was already present at a field strength of 1.5 tesla, as evident from the induced nystagmus (Boegle et al., 2016). Furthermore, we were able to show that MVS scaled linearly with field strength between 1.5 tesla, and 3 tesla (Boegle et al., 2016). We identified the effects of MVS in the scaling of functional resting-state network fluctuations, showing that MVS does indeed influence resting-state networks due to vestibular imbalance (Boegle et al., 2016). Specifically, MVS does influence DMN resting-state network dynamics in accordance with the predicted scaling of MVS based on the Lorentz-force model for MVS (Roberts et al., 2011). The between subject variance in SPV was increased with magnetic field strength, which further supports the Lorentz-force model that posits a multiplicative influence of the magnetic field (Roberts et al., 2011). Taken together, these results not only imply that subjects were in a vestibular state of imbalance, but also that the extent and direction of the state of imbalance showed more variance between subjects with increasing field strength. This is in line with a multiplicative relationship with the magnetic field strength, as expected for an effect governed by a Lorentz-force relationship (Roberts et al., 2011; Boegle et al., 2016).

Does aging impact vestibular research results?

Aging of peripheral and central vestibular structures

It is well known that peripheral vestibular end organs, like any other sensory organ, deteriorate with age (for an overview see (Ishiyama, 2009; Fernández et al., 2015; Maheu et al., 2015)). Peripheral vestibular structures such as hair cell counts, the number of nerve fibers, and the size of the otoconia have been demonstrated to decrease with age (Bergström, 1973; Rosenhall, 1973; Ross et al., 1976; Igarashi et al., 1993; Lopez et al., 2005; Walther and Westhofen, 2007). Behavioral testing of physiology such as head thrust dynamic visual acuity testing, ocular and cervical vestibular evoked myogenic potentials, as well as timed balance tests show declining trends (in the case of timed balance tests it is an increase in time needed for stable execution) (Bohannon et al., 1984; Furman and Redfern, 2001; Welgampola and Colebatch, 2001; Agrawal et al., 2012; Wiesmeier et al., 2015). However, it is interesting to note that some clinical tests such as caloric testing or video head impulse test (HIT) remain relatively unaffected during aging, e.g., gain reduction was estimated to be 0.012 per decade and significant gain difference has only been found from 90 years of age (Matiño-Soler et al., 2015). In other words, the behavioral function of the overall system is maintained until high age. This means that central mechanisms have adapted to preserve performance despite the change in nerve cells at the periphery.

It is important to note here that most of what is known about compensation in the vestibular system is known from studies regarding the response of the system to vestibular disease, i.e., sudden and dramatic changes of vestibular input to the system, e.g., following unilateral peripheral vestibular failure. The compensatory mechanisms mainly involve shifts towards other sensory inputs as the system as a whole is multisensory in nature (Bles et al., 1983, 1984; Möller and Ödkvist, 1989; Cass and Goshgarian, 1991; Curthoys and Halmagyi, 1995; Curthoys, 2000; Bense et al., 2004a, 2004b; Dieterich et al., 2007; zu Eulenburg et al., 2010; McCall and Yates, 2011; Devèze et al., 2015; Micarelli et al., 2016; Lacour et al., 2016). It is therefore possible that such a shift, i.e., a reweighting of the inputs in the multisensory processing may also occur during age-associated deterioration of the vestibular end organs. In the case of disease, if the vestibular nerve is severely and permanently damaged, this shift towards other sensory inputs is especially strong as the input from the vestibular system is either permanently lacking or very noisy (Curthoys and Halmagyi, 1995; Dieterich et al., 2007; zu Eulenburg et al., 2010; Lacour et al., 2016). It has been shown that this shift first occurs towards visual inputs (Bense et al., 2004a, 2004b; Dieterich, 2007; zu Eulenburg et al.,

2010; Becker-Bense et al., 2013) which are especially dominant in humans and other apes, and that this can also be followed by a shift towards the somatosensory system (Bles et al., 1983, 1984), and even the auditory system if special prosthetics are used (Hegeman et al., 2005), that deliver meaningful input for the auditory system (head motion transformed to sound). In squirrel monkeys it has been shown that exercise is beneficial for compensation (Igarashi et al., 1979, 1989). For humans reweighting towards visual signals are the first and fastest changes, as patients perform significantly better in eyes-open condition one month after disease onset while eyes-closed performance has not improved much at that point and can be shown to need a longer time and depends strongly on somatosensory input (Lacour et al., 1997, 2016; Gauchard et al., 2001; Devèze et al., 2015).

There are two interpretations for these results in relation to our aging study. Either, these results imply that the sensitivity of the system (as a whole) is only slightly reduced, indicating that an adaptation of vestibular gains or compensation via sensory substitution has occurred that has stabilized the overall sensitivity despite cell loss (Maheu et al., 2015). The alternative interpretation is that the aforementioned measures may not have been sensitive enough to detect early or subtle age-related changes that occur before disease onset (Dowiasch et al., 2015; Scheltinga et al., 2016). In other words, the function is preserved because central adaptations, possibly by compensation via sensory substitution has occurred that cannot be detected in behavior.

What approach is necessary for detecting aging effects?

The results from our neuroimaging aging study imply that the dynamics of vestibular networks were already limited by the influence of aging in healthy subjects (Cyran and Boegle et al., 2016). The change in connectivity and temporal variability might on one hand be related to the preservation of the behavioral response only leading to a slow decline prior to age 90 (Matiño-Soler et al., 2015). In other words our results might indicate that a form of central vestibular compensation has taken place. This might have slowed the decline, but it also cannot fully preserve the function of the balance system, hence the slow decline in functional connectivity. On the other hand, the decline in connectivity (and temporal variability increase) might be an early sign of a reduced ability to respond to a challenge when clinical behavioral tests still show little to no deficits (Dowiasch et al., 2015; Cyran and Boegle et al., 2016; Scheltinga et al., 2016).

Note that aging may be defined as ongoing damage and compensation that will eventually lead to a state where further damage cannot be compensated adequately, and nonlinear descent into chaos occurs, i.e. disease.

Two recent studies have shown that clinical laboratory tests (e.g., head impulse test and caloric stimulation test of canal paresis) are not as sensitive as real world tests such as free gaze while walking or stance balance tests (Dowiasch et al., 2015; Scheltinga et al., 2016). Subtle changes, specifically that older patients with unilateral peripheral deficits recover balance control slower than younger patients, have been missed in previous studies (Scheltinga et al., 2016). This corroborates our hypothesis of early asymptomatic vestibular decline as indicated by the functional connectivity changes (Cyran and Boegle et al., 2016; Scheltinga et al., 2016). It is particularly noteworthy that Scheltinga and coauthors showed that their patients did not recover peripheral function, as canal paresis could be shown to persist while patients improved in stance balance test performance, indicating central compensation (Scheltinga et al., 2016). In fact, younger patients showed almost no difference from normal controls for stance balance tasks in the course of a unilateral peripheral failure. This indicates that their balance control was very robust early on while the balance control of the middle-aged and elderly was strongly affected and needed a substantial amount of time to recover, and the time to recovery increased with the age of participants (Scheltinga et al., 2016).

As noted above, studies examining the same parameters as assessed in vestibular disease did not find any significant changes during most of the lifespan, although it is known that cell loss occurs, suggesting that compensation must have happened, and that the changes found in neuroimaging may be related to the reported longer recovery time for balance tests (Cyran and Boegle et al., 2016; Scheltinga et al., 2016).

Does functional connectivity represent a “reservoir of resilience”?

Thus, we interpret the vestibular network dynamics as the central “reservoir of resilience” that is available for adjusting responses when facing a vestibular challenge. The idea is that the remaining functional connectivity of the vestibular system can be used as a “reserve” for compensation and therefore a greater “reserve” is present (on average) at a younger age. This does also imply that monitoring of the functional connectivity of a subject could be used as a predictor for how well that subject can respond to a vestibular challenge.

Patients with unilateral hypofunction or complete loss of one side (i.e., loss of 50% vestibular sensory input) have the capability to adjust their central processing to respond to this enormous change in peripheral sensory input (e.g. see (Bense et al., 2004a; Becker-Bense et al., 2014; Göttlich et al., 2014; Helmchen et al., 2014; Klingner et al., 2014)). That is by far a more extensive and sudden change that has to be adjusted for via central adaptation and sensory substitution than the age-related decline of the vestibular end organs. This also reinforces the view that the pattern of decline seen in our study is an early sign of central compensation even when no behavioral effects are noticeable (Cyrn and Boegle et al., 2016; Scheltinga et al., 2016).

Based on this idea of functional connectivity strength as a “reservoir of resilience”, we predict that younger patients that suffer from a peripheral vestibular failure should also (on average) recover better due to the (on average) higher functional connectivity of the vestibular system and (on average) lower temporal variability, than older patients who should have (on average) lower functional connectivity and (on average) higher temporal variability.

Therefore, in consideration of our results and the literature it is clear that the initial question, whether vestibular research is influenced by age, should be answered in the affirmative.

Does magnetic vestibular stimulation impact vestibular research results?

The study of the influence of magnetic fields on biological systems has a long history and many significant advances have only been made in the last 25 years since the advent of MRI (Schenck, 1992). Even before MRI was available, effects of magnetic stimulation and associated vertigo were described ever since the advent of MR-spectroscopy using high magnetic field strengths (Schenck, 1992). However, MRI made the application of strong magnetic fields on a large area that humans can enter possible and necessitates the study of its effects for safety regulations (Schenck, 1992).

Overview of human and animal studies regarding magnetic vestibular stimulation

Studies with mammals (e.g., rats, mice, and humans) have revealed signs of vestibular imbalance and dizziness in magnetic fields above 1.5 tesla (Weiss et al., 1992). For rats and mice in particular it has been shown that the behavioral effects in response to magnetic field exposure depend on the intact labyrinth of the animals (Haupt et al., 2007). Furthermore, neuronal activity in the brain stem due to the presence of a magnetic field was indicated via immunohistochemistry labeling of c-fos, (a protein associated with the generation of action potentials), and it was shown that this signal was abolished by labyrinthectomy (Cason et al., 2009). Motion seemed to intensify the effects, but the effects were also present when the animals were restrained (Lockwood et al., 2003; Haupt et al., 2011).

Since the proposal of the Lorentz-force model (Roberts et al., 2011) all the behavioral and neuronal correlates in animals can be explained more thoroughly (Haupt et al., 2013). Specifically, the distribution of c-fos in the vestibular nuclei of the rats was shown to depend on the angle of the rat's inner ear relative to the field, and this was also reflected in the behavior of the rats, i.e., they swam in circles ("circling behavior") after 15 min exposure to the magnetic field (Haupt et al., 2013). If the mice were oriented 90° relative to the field, no significant c-fos induction (relative to sham treatment group) could be shown and these mice did not show circling behaviors. In contrast, an orientation at 0° and 180° relative to the field produced significant c-fos induction in the vestibular nuclei with a left-right asymmetry. This asymmetry was reverse for 180° vs 0° orientation and reflected in the circling behavior which was either clockwise or counter-clockwise, respectively (Haupt et al., 2013).

In humans it was shown that the temporal dynamics of the nystagmus' SPV are similar to those known from rotational stimulation or caloric irrigation studies (Glover et al. 2014; Jareonsettasin et al. 2016). A simulation study regarding the magneto-hydrodynamic forces acting on the cupula showed that the expected Lorentz-force should be strong enough to cause nystagmus (Antunes et al., 2012). A study of patients with unilateral labyrinthine disorders showed that the nystagmus direction is dependent on the interaction of signals from the semicircular canals from both ears, further supporting the idea that the labyrinth is the part of the inner ear that is mainly affected by the magnetic field (Ward et al. 2014). More specifically, MVS stimulates all three canals of both ears, but due to the reciprocal interaction of the anterior and posterior canals of opposite ears, only healthy subjects show a horizontal nystagmus, while patients with unilateral loss show an additional vertical component in the nystagmus because the inhibitory opposite side is lost (Ward, Roberts, et al. 2014). This supports the idea that the labyrinth is the part of the inner ear that is mainly affected by the magnetic field (Roberts et al., 2011; Glover et al., 2014; Ward et al., 2014a).

In short, various animal and human studies using behavioral and neural correlates showed that magnetic fields influence the peripheral vestibular end organs, and that the central nervous system is affected via the multisensory vestibular system (e.g. (Weiss et al., 1992; Schenck, 1992; Snyder et al., 2000; Lockwood et al., 2003; Saunders, 2005; Glover et al., 2007, 2014; Cason et al., 2009; Roberts et al., 2011; Houpt et al., 2013; Ward et al., 2014a, 2014b; Boegle et al., 2016; Jareonsettasin et al., 2016)).

How neuroimaging studies of vestibular function might be affected by MVS

These results support that our approach for identifying the modulations due to MVS in resting-state fMRI data, based on transferring the scaling relationship of the Lorentz-force model to fMRI modulations, was well justified (Triantafyllou et al., 2005; Duyn, 2012; Boegle et al., 2016).

Our results raise questions about the influence of MVS on fMRI above 1.5T field strength, and in particular about fMRI studies on the function of the vestibular system and the influence of vestibular deficits. It is important to keep in mind that the effect of MVS is not like the constant acoustic noise stimulation during fMRI. MVS induces an imbalance state with a directional preponderance, i.e., has a signed difference effect, unlike acoustic noise that can be supposed to be equal and balanced for the auditory network and its connections. Thus, healthy subjects measured under MVS influence (i.e., in a MR scanner) might be more like a

“special patient group with a vestibular imbalance” but without lesions in the inner ear or central nervous system (Boegle et al., 2016).

Recent studies examining patients with vestibular deficits using resting-state fMRI showed widespread changes in various networks that also included the DMN similar to our findings for MVS (Göttlich et al., 2014; Helmchen et al., 2014; Klingner et al., 2014; Boegle et al., 2016). Our results suggest caution when interpreting such studies.

In the case of bilateral vestibular loss (Göttlich et al., 2014), it should be noted that the patients will not show a MVS influence (Roberts et al., 2011), but the healthy control group will be under the influence of MVS (Boegle et al., 2016). This might then lead to changes in the comparison of differences between the two groups as examined with fMRI that are not expected to appear in imaging methods without the use of strong magnetic fields. In this case, the healthy controls might be more akin to patients with acute unilateral vestibular neuritis, given that such patients also show a directional imbalance with a horizontal nystagmus, not unlike that evoked by MVS (Roberts et al., 2011; Ward et al., 2014a; Boegle et al., 2016).

For studies of vestibular neuritis patients versus healthy controls (e.g. (Helmchen et al., 2014; Klingner et al., 2014)), MVS effects should be expected for both, the patients and the healthy controls (Ward et al., 2014a; Boegle et al., 2016). However, MVS will affect patients with unilateral vestibular deficits differently than healthy controls (Ward et al. 2014), which will then further obscure the real differences between the two groups. This means that the reported differences at every time interval during the compensation period relative to the healthy control group will be obscured or biased by MVS (Boegle et al., 2016). However, the trajectory of recovery of the patients and therefore the trajectory of associated relative differences to the healthy controls might not be affected by MVS influence. Thus, the trend of the change of the differences over the time intervals of compensation should be unaffected by MVS (Boegle et al., 2016). This requires, however, that the subjects are imaged in, at least, very similar head positions and field strength at every time interval of compensation to stay comparable over the time intervals (Boegle et al., 2016). In the resting-state study on vestibular neuritis patients (Klingner et al., 2014) it is interesting to note that no significant correlations were found for the caloric testing covariate, although this is usually a good indicator of impairment or restoration of vestibular function. One might speculate that MVS had obscured this correlation, because MVS seems to share important characteristics in terms of temporal dynamics with caloric stimulation (Glover et al., 2014; Jareonsettasin et al., 2016).

In summary, in a sufficiently strong (e.g. ≥ 1.5 tesla) magnetic field, MVS will induce a state of vestibular imbalance in each healthy subject. The variability between subjects will increase with field strength due to the multiplicative nature of the Lorentz-force. These effects may lead to biased results and reduced statistical significance when testing for the statistical significance of mean responses related to vestibular stimulation (Boegle et al., 2016).

Potential implications for vestibular research with fMRI

We derive suggestions for studies of the vestibular system with fMRI in healthy controls and patients from the results of our studies and the associated literature.

Effects of age on vestibular research

In regard to the influence of age, we suggest that researchers comparing patients with vestibular deficits and healthy controls should separate the age-matched group into age-strata (non-overlapping subgroups with different age spans, e.g. 20-40 years, 40-60 years and above 60 years of age). Each stratum should be compared and interpreted separately given that different age-groups have different levels of vestibular network dynamics available for compensation (or responding to a challenge). This is particularly relevant when patients show a wide age-distribution, e.g., in the case of patients with unilateral vestibulopathy.

Further research should be directed towards uncovering factors related to the decline, and if possible for improving network dynamics and its relationship to subject performance. This may also include an exploration of questions we could not answer with our cross-sectional aging study. For example, by performing prospective aging studies including training or interventions together with follow up examination. Possible questions which could be addressed are:

“What prevents a connectivity or behavioral decline at higher age?”

“Can network dynamics be elevated again by training and is this related to balance improvements at any age?”

The idea for an experiment would be to determine the connectivity and temporal variability via fMRI during rest and vestibular stimulation (e.g. GVS) and then have the subjects train and evaluate them again in several time intervals.

Furthermore, it is important to note that the sensitivity of brain and behavioral measures should be considered when planning a study. As discussed before, certain behavioral measures or clinical tests are not sensitive enough to reveal age-related changes, while functional neuroimaging is only sensitive enough when measures of network dynamics are considered (Garrett et al., 2010; Dowiasch et al., 2015; Cyran and Boegle et al., 2016; Scheltinga et al., 2016).

Effects of strong magnetic fields on vestibular research

In regard to the influence of magnetic fields, we suggest that MVS should be seen as a new way of manipulating networks that either process vestibular information or show vestibular interactions, by using strong magnetic fields (≥ 1.5 tesla), as commonly used in MRI. The potential of modulating vestibular influences on networks via MVS lies in being able to induce or manipulate vestibular imbalances. In the healthy this can be used to create states that are similar to the diseased state, but without peripheral or central lesions. In patients this will allow to extend or reduce vestibular imbalances. In both cases this can be done while performing functional MRI simply by using the magnetic field of the MRI and adjusting the head position of the subject.

In studies that need to avoid vestibular perturbations, MVS might be considered a side effect or nuisance during functional imaging and should be controlled by adjusting the head position and measuring the resulting eye movements. This should then be seen as an effort to remove unwanted variance, i.e., as an effort to homogenize the group and achieve better statistical results due to less (uncontrolled) MVS interference that increases bias and variance with increasing field strength.

In general, MVS as a method allows the investigation of brain states from the viewpoint of “the brain as a dynamic system”. The assumption here is similar to the ideas regarding aging and the “connectivity reservoir” available for responding to challenges, in the sense that the brain has a vast complex dynamic that is for the most part “invisible” unless a response to a challenge is examined. Given methods like MVS it is possible to exert influences on this “invisible” dynamic and then examine how the response to a challenge is differing, as a way of examining the “invisible” dynamics of the system. This will also present an opportunity to study the influences of vestibular imbalance on higher cognitive functions and multisensory interaction that has been raised previously as an important research topic by various authors (Hanes and McCollum, 2006; Smith and Zheng, 2013; Mast et al., 2014).

One exemplary idea regarding the study of patients with an imbalance state would be the study of patients that show an upbeat nystagmus when lying down. MVS can be used to compensate their nystagmus via an adjustment of the head position (moving ear to shoulder induces vertical, i.e., upbeat nystagmus in healthy subjects) while acquiring resting fMRI. These subjects can then be compared with healthy controls without the respective nystagmus. Another interesting condition would be the comparison of healthy controls that lie in a position that produces a nystagmus akin to the patients and have the patients place in such a

way that MVS have no influence on their nystagmus and compare these states as well. With these comparisons one could account for the effect of the pure nystagmus of patients and controls to examine the residual differences that are not related to the pure eye movement but the imbalance state itself.

Summary of suggestions for study design

In summary, we can rephrase all our suggestions into three short questions that researchers could ask themselves when thinking about vestibular research projects in the future.

Age-grouping:

“Is the response to a challenge different for younger adults than older adults, i.e., does each age-group compensate differently?”

MVS modulation:

“Can a manipulation of the imbalance state of our subjects with MVS help us to reveal more about the vestibular network’s response to a challenge or should we avoid interference by MVS in the imbalance state of our subjects?”

Sensitivity:

“Is the measure that I want to use sensitive enough to show the differences that I am looking for?” Connectivity and temporal variability might be sensitive enough, but many clinical tests might not be sufficient.

References

- Agrawal, Y., Zuniga, M.G., Davalos-Bichara, M., Schubert, M.C., Walston, J.D., Hughes, J., Carey, J.P., 2012. Decline in semicircular canal and otolith function with age. *Otol. Neurotol.* 33, 832–839. doi:10.1097/MAO.0b013e3182545061
- Antunes, A., Glover, P.M., Li, Y., Mian, O.S., Day, B.L., 2012. Magnetic field effects on the vestibular system: calculation of the pressure on the cupula due to ionic current-induced Lorentz force. *Phys. Med. Biol.* 57, 4477–87. doi:10.1088/0031-9155/57/14/4477
- Arai, Y., 2001. A new light on caloric test--what was disclosed by three dimensional analysis of caloric nystagmus? *Biol. Sci. Sp.* 15, 387–92.
- Aw, S.T., Haslwanter, T., Fetter, M., Dichgans, J., 2000. Three-dimensional spatial characteristics of caloric nystagmus. *Exp. Brain Res.* 134, 289–294. doi:10.1007/s002210000460
- Barany, R., 1906. Untersuchungen über den vom Vestibularapparat des Ohres reflektorisch ausgelösten rhythmischen Nystagmus und seine Begleiterscheinungen. *Monatschrift Ohrenheilkd.* 4, 193–297.
- Becker-Bense, S., 2003. three determinants vestibular dominance during caloric stimulation. *Ann. N. Y. Acad. Sci.* 1004, 1–9. doi:10.1196/annals.1303.001
- Becker-Bense, S., Buchholz, H.-G., Best, C., Schreckenberger, M., Bartenstein, P., Dieterich, M., 2013. Vestibular compensation in acute unilateral medullary infarction: FDG-PET study. *Neurology* 80, 1103–1109. doi:10.1212/WNL.0b013e31828868a6
- Becker-Bense, S., Dieterich, M., Buchholz, H.G., Bartenstein, P., Schreckenberger, M., Brandt, T., 2014. The differential effects of acute right- vs. left-sided vestibular failure on brain metabolism. *Brain Struct. Funct.* 219, 1355–1367. doi:10.1007/s00429-013-0573-z
- Beckmann, C.F., DeLuca, M., Devlin, J.T., Smith, S.M., 2005. Investigations into resting-state connectivity using independent component analysis. *Philos. Trans. R. Soc. Lond. B. Biol. Sci.* 360, 1001–13. doi:10.1098/rstb.2005.1634
- Beckmann, C.F., Smith, S.M., 2005. Tensorial extensions of independent component analysis for multisubject fMRI analysis. *Neuroimage* 25, 294–311. doi:10.1016/j.neuroimage.2004.10.043
- Beckmann, C.F., Smith, S.M., 2004. Probabilistic independent component analysis for functional magnetic resonance imaging. *IEEE Trans. Med. Imaging* 23, 137–52. doi:10.1109/TMI.2003.822821
- Bense, S., Bartenstein, P., Lochmann, M., Schlindwein, P., Brandt, T., Dieterich, M., 2004a. Metabolic changes in vestibular and visual cortices in acute vestibular neuritis. *Ann. Neurol.* 56, 624–630. doi:10.1002/ana.20244
- Bense, S., Deutschländer, A., Stephan, T., Bartenstein, P., Schwaiger, M., Brandt, T., Dieterich, M., 2004b. Preserved visual–vestibular interaction in patients with bilateral vestibular failure. *Neurology* 63, 122–128. doi:10.1212/01.WNL.0000129545.79566.6A
- Bense, S., Janusch, B., Vucurevic, G., Bauermann, T., Schlindwein, P., Brandt, T., Stoeter, P., Dieterich, M., 2006. Brainstem and cerebellar fMRI-activation during horizontal and vertical optokinetic stimulation. *Exp. brain Res.* 174, 312–23. doi:10.1007/s00221-006-0464-0
- Bense, S., Stephan, T., Yousry, T. a, Brandt, T., Dieterich, M., 2001. Multisensory cortical signal increases and decreases during vestibular galvanic stimulation (fMRI). *J. Neurophysiol.* 85, 886–899.
- Bergström, B., 1973. Morphology of the vestibular nerve: II. The number of myelinated vestibular nerve fibers in man at various ages. *Acta Otolaryngol.* 76, 173–179. doi:10.3109/00016487309121496

- Besnard, S., Lopez, C., Brandt, T., Denise, P., Smith, P.F., 2015. Editorial: The vestibular system in cognitive and memory processes in mammals. *Front. Integr. Neurosci.* 9. doi:10.3389/fnint.2015.00055
- Bles, W., de Jong, J.M., de Wit, G., 1984. Somatosensory compensation for loss of labyrinthine function. *Acta Otolaryngol.* 97, 213–21.
- Bles, W., Vianney de Jong, J.M., de Wit, G., 1983. Compensation for labyrinthine defects examined by use of a tilting room. *Acta Otolaryngol.* 95, 576–9.
- Boegle, R., Stephan, T., Ertl, M., Glasauer, S., Dieterich, M., 2016. Magnetic vestibular stimulation modulates default mode network fluctuations. *Neuroimage* 127, 409–421. doi:10.1016/j.neuroimage.2015.11.065
- Bohannon, R.W., Larkin, P.A., Cook, A.C., Gear, J., Singer, J., 1984. Decrease in timed balance test scores with aging. *Phys. Ther.* 64, 1067–70.
- Bottini, G., Karnath, H.O., Vallar, G., Sterzi, R., Frith, C.D., Frackowiak, R.S., Paulesu, E., 2001. Cerebral representations for egocentric space: Functional-anatomical evidence from caloric vestibular stimulation and neck vibration. *Brain* 124, 1182–96.
- Bottini, G., Sterzi, R., Paulesu, E., Vallar, G., Cappa, S.F., Erminio, F., Passingham, R.E., Frith, C.D., Frackowiak, R.S., 1994. Identification of the central vestibular projections in man: a positron emission tomography activation study. *Exp. Brain Res.* 99, 164–9.
- Brandt, T., Bartenstein, P., Janek, A., Dieterich, M., 1998. Reciprocal inhibitory visual-vestibular interaction. Visual motion stimulation deactivates the parieto-insular vestibular cortex. *Brain* 121, 1749–1758. doi:10.1093/brain/121.9.1749
- Brandt, T., Dieterich, M., 1999. The vestibular cortex: Its locations, functions, and disorders. *Ann. N. Y. Acad. Sci.* 871, 293–312. doi:10.1111/j.1749-6632.1999.tb09193.x
- Brandt, T., Dieterich, M., Strupp, M., 2005. Vertigo and dizziness: Common complaints, *Vertigo and Dizziness: Common Complaints*. Springer-Verlag London Ltd, London. doi:10.1097/00000441-195902000-00023
- Cason, A.M., Kwon, B., Smith, J.C., Houpt, T. a, 2009. Labyrinthectomy abolishes the behavioral and neural response of rats to a high-strength static magnetic field. *Physiol. Behav.* 97, 36–43. doi:10.1016/j.physbeh.2009.01.018
- Cass, S.P., Goshgarian, H.G., 1991. Vestibular compensation after labyrinthectomy and vestibular neurectomy in cats. *Otolaryngol. Head. Neck Surg.* 104, 14–9.
- Colebatch, J.G., Halmagyi, G.M., Skuse, N.F., 1994. Myogenic potentials generated by a click-evoked vestibulocollic reflex. *J. Neurol. Neurosurg. Psychiatry* 57, 190–7.
- Cullen, K., Sadeghi, S., 2008. Vestibular system. *Scholarpedia* 3, 3013. doi:10.4249/scholarpedia.3013
- Curthoys, I.S., 2000. Vestibular compensation and substitution. *Curr. Opin. Neurol.* 13, 27–30.
- Curthoys, I.S., Halmagyi, G.M., 1995. Vestibular compensation: a review of the oculomotor, neural, and clinical consequences of unilateral vestibular loss. *J. Vestib. Res.* 5, 67–107.
- Curthoys, I.S., MacDougall, H.G., 2012. What galvanic vestibular stimulation actually activates. *Front. Neurol.* JUL, 1–5. doi:10.3389/fneur.2012.00117
- Cyran, C.A.M., Boegle, R., Stephan, T., Dieterich, M., Glasauer, S., 2016. Age-related decline in functional connectivity of the vestibular cortical network. *Brain Struct. Funct.* 221, 1443–1463. doi:10.1007/s00429-014-0983-6
- Devèze, A., Montava, M., Lopez, C., Lacour, M., Magnan, J., Borel, L., 2015. Vestibular compensation following vestibular neurotomy. *Eur. Ann. Otorhinolaryngol. Head Neck Dis.* 132, 197–203. doi:10.1016/j.anorl.2015.04.003
- Dieterich, M., 2007. Functional brain imaging: a window into the visuo-vestibular systems. *Curr. Opin. Neurol.* 20, 12–18. doi:10.1097/WCO.0b013e328013f854
- Dieterich, M., Bauermann, T., Best, C., Stoeter, P., Schlindwein, P., 2007. Evidence for cortical visual substitution of chronic bilateral vestibular failure (an fMRI study). *Brain*

- 130, 2108–2116. doi:10.1093/brain/awm130
- Dieterich, M., Bense, S., Lutz, S., Drzezga, a, Stephan, T., Bartenstein, P., Brandt, T., 2003. Dominance for vestibular cortical function in the non dominant hemisphere. *Cereb. Cortex* 994–1007.
- Dieterich, M., Brandt, T., 2008. Functional brain imaging of peripheral and central vestibular disorders. *Brain* 131, 2538–2552. doi:10.1093/brain/awn042
- Dieterich, M., Bucher, S.F., Seelos, K.C., Brandt, T., 1998. Horizontal or vertical optokinetic stimulation activates visual motion-sensitive, ocular motor and vestibular cortex areas with right hemispheric dominance. An fMRI study. *Brain* 121 (Pt 8, 1479–95.
- Dowiasch, S., Marx, S., Einhäuser, W., Bremmer, F., 2015. Effects of aging on eye movements in the real world. *Front. Hum. Neurosci.* 9, 46. doi:10.3389/fnhum.2015.00046
- Duyn, J.H., 2012. The future of ultra-high field MRI and fMRI for study of the human brain. *Neuroimage* 62, 1241–1248. doi:10.1016/j.neuroimage.2011.10.065
- Eickhoff, S.B., Weiss, P.H., Amunts, K., Fink, G.R., Zilles, K., 2006. Identifying human parieto-insular vestibular cortex using fMRI and cytoarchitectonic mapping. *Hum. Brain Mapp.* 27, 611–621. doi:10.1002/hbm.20205
- Fernández, L., Breinbauer, H.A., Delano, P.H., 2015. Vertigo and Dizziness in the Elderly. *Front. Neurol.* 6. doi:10.3389/fneur.2015.00144
- Fischer, E., Bühlhoff, H.H., Logothetis, N.K., Bartels, A., 2012. Visual motion responses in the posterior cingulate sulcus: A comparison to V5/MT and MST. *Cereb. Cortex* 22, 865–876. doi:10.1093/cercor/bhr154
- Fitzpatrick, R.C., Day, B.L., 2004. Probing the human vestibular system with galvanic stimulation. *J. Appl. Physiol.* 96, 2301–16. doi:10.1152/jappphysiol.00008.2004
- Friberg, L., Olsen, T.S., Roland, P.E., Paulson, O.B., Lassen, N.A., 1985. Focal increase of blood flow in the cerebral cortex of man during vestibular stimulation. *Brain* 108 (Pt 3, 609–23.
- Furman, J.M., Redfern, M.S., 2001. Effect of aging on the otolith-ocular reflex. *J. Vestib. Res.* 11, 91–103.
- Garrett, D.D., Kovacevic, N., McIntosh, A.R., Grady, C.L., 2011. The importance of being variable. *J. Neurosci.* 31, 4496–4503. doi:10.1523/JNEUROSCI.5641-10.2011
- Garrett, D.D., Kovacevic, N., McIntosh, A.R., Grady, C.L., 2010. Blood Oxygen Level-Dependent Signal Variability Is More than Just Noise. *J. Neurosci.* 30, 4914–4921. doi:10.1523/JNEUROSCI.5166-09.2010
- Gauchard, G.C., Jeandel, C., Perrin, P.P., 2001. Physical and sporting activities improve vestibular afferent usage and balance in elderly human subjects. *Gerontology* 47, 263–70. doi:52810
- Glover, P.M., Cavin, I., Qian, W., Bowtell, R., Gowland, P. a., 2007. Magnetic-field-induced vertigo: A theoretical and experimental investigation. *Bioelectromagnetics* 28, 349–361. doi:10.1002/bem.20316
- Glover, P.M., Li, Y., Antunes, A., Mian, O.S., Day, B.L., 2014. A dynamic model of the eye nystagmus response to high magnetic fields. *Phys. Med. Biol.* 59, 631–45. doi:10.1088/0031-9155/59/3/631
- Goldberg, A.J., Hudspeth, M.E., 2004. The vestibular system., in: Kandel, E.R., Schwartz, J.H., Jessell, T.M. (Eds.), *Principles of Neural Science*. McGraw-Hill, New York, pp. 801–815.
- Goldberg, J.M., Fernández, C., Smith, C.E., 1982. Responses of vestibular-nerve afferents in the squirrel monkey to externally applied galvanic currents. *Brain Res.* 252, 156–60.
- Goldberg, J.M., Smith, C.E., Fernández, C., 1984. Relation between discharge regularity and responses to externally applied galvanic currents in vestibular nerve afferents of the squirrel monkey. *J. Neurophysiol.* 51, 1236–56.

- Goldberg, J.M., Wilson, V.J., Cullen, K.E., Angelaki, D.E., Broussard, D.M., Buttner-Ennever, J., Fukushima, K., Minor, L.B., 2012. The Vestibular System. Oxford University Press. doi:10.1093/acprof:oso/9780195167085.001.0001
- Göttlich, M., Jandl, N.M., Wojak, J.F., Sprenger, A., Der Gablentz, J. Von, Münte, T.F., Krämer, U.M., Helmchen, C., 2014. Altered resting-state functional connectivity in patients with chronic bilateral vestibular failure. *NeuroImage Clin.* 4, 488–499. doi:10.1016/j.nicl.2014.03.003
- Graf, W.M., 2009. Evolution of the Vestibular System, in: *Encyclopedia of Neuroscience*. Springer Berlin Heidelberg, Berlin, Heidelberg, pp. 1440–1448. doi:10.1007/978-3-540-29678-2_3175
- Hanes, D. a, McCollum, G., 2006. Cognitive-vestibular interactions: a review of patient difficulties and possible mechanisms. *J. Vestib. Res.* 16, 75–91.
- Hegeman, J., Honegger, F., Kupper, M., Allum, J.H.J., 2005. The balance control of bilateral peripheral vestibular loss subjects and its improvement with auditory prosthetic feedback. *J. Vestib. Res.* 15, 109–17.
- Helmchen, C., Ye, Z., Sprenger, A., Münte, T.F., 2014. Changes in resting-state fMRI in vestibular neuritis. *Brain Struct. Funct.* 1–12. doi:10.1007/s00429-013-0608-5
- Haupt, T.A., Carella, L., Gonzalez, D., Janowitz, I., Mueller, A., Mueller, K., Neth, B., Smith, J.C., 2011. Behavioral Effects on Rats of Motion within a High Static Magnetic Field. *Physiol Behav* 103, 338–346. doi:10.1115/1.3071969.Automating
- Haupt, T.A., Cassell, J.A., Cason, A.M., Riedell, A., Golden, G.J., Riccardi, C., Smith, J.C., 2007. Evidence for a cephalic site of action of high magnetic fields on the behavioral responses of rats. *Physiol. Behav.* 92, 665–74. doi:10.1016/j.physbeh.2007.05.011
- Haupt, T.A., Kwon, B., Haupt, C.E., Neth, B., Smith, J.C., 2013. Orientation within a high magnetic field determines swimming direction and laterality of c-Fos induction in mice. *Am. J. Physiol. Regul. Integr. Comp. Physiol.* 305, R793-803. doi:10.1152/ajpregu.00549.2012
- Igarashi, M., Levy, J.K., Takahashi, M., Alford, B.R., Homick, J.L., 1979. Effect of exercise upon locomotor balance modification after peripheral vestibular lesions (unilateral utricular neurotomy) in squirrel monkeys. *Adv. Otorhinolaryngol.* 25, 82–7.
- Igarashi, M., Ohashi, K., Yoshihara, T., MacDonald, S., 1989. Effect of physical exercise prelabrynthectomy on locomotor balance compensation in the squirrel monkey. *Percept. Mot. Skills* 68, 407–414. doi:10.2466/pms.1989.68.2.407
- Igarashi, M., Saito, R., Mizukoshi, K., Alford, B.R., 1993. Otoconia in Young and Elderly Persons: A Temporal Bone Study. *Acta Otolaryngol.* 113, 26–29. doi:10.3109/00016489309128117
- Ishiyama, G., 2009. Imbalance and vertigo: the aging human vestibular periphery. *Semin. Neurol.* 29, 491–9. doi:10.1055/s-0029-1241039
- Janzen, J., Schlindwein, P., Bense, S., Bauermann, T., Vucurevic, G., Stoeter, P., Dieterich, M., 2008. Neural correlates of hemispheric dominance and ipsilaterality within the vestibular system. *Neuroimage* 42, 1508–18. doi:10.1016/j.neuroimage.2008.06.026
- Jareonsettasin, P., Otero-Millan, J., Ward, B.K., Roberts, D.C., Schubert, M.C., Zee, D.S., 2016. Multiple time courses of vestibular set-point adaptation revealed by sustained magnetic field stimulation of the labyrinth. *Curr. Biol.* 26, 1359–1366. doi:10.1016/j.cub.2016.03.066
- Kirsch, V., Keiser, D., Hergenroeder, T., Erat, O., Ertl-Wagner, B., Brandt, T., Dieterich, M., 2016. Structural and functional connectivity mapping of the vestibular circuitry from human brainstem to cortex. *Brain Struct. Funct.* doi:10.1007/s00429-014-0971-x
- Klingner, C.M., Volk, G.F., Brodoehl, S., Witte, O.W., Guntinas-Lichius, O., 2014. Disrupted functional connectivity of the default mode network due to acute vestibular deficit. *NeuroImage. Clin.* 6, 109–14. doi:10.1016/j.nicl.2014.08.022

- Lacour, M., Barthelemy, J., Borel, L., Magnan, J., Xerri, C., Chays, A., Ouaknine, M., 1997. Sensory strategies in human postural control before and after unilateral vestibular neurotomy. *Exp. Brain Res.* 115, 300–310. doi:10.1007/PL00005698
- Lacour, M., Helmchen, C., Vidal, P.-P., 2016. Vestibular compensation: the neuro-otologist's best friend. *J. Neurol.* S54-64. doi:10.1007/s00415-015-7903-4
- Lobel, E., Kleine, J.F., Bihan, D.L., Leroy-Willig, A., Berthoz, A., 1998. Functional MRI of galvanic vestibular stimulation. *J. Neurophysiol.* 80, 2699–709.
- Lockwood, D.R., Kwon, B., Smith, J.C., Houpt, T.A., 2003. Behavioral effects of static high magnetic fields on unrestrained and restrained mice. *Physiol. Behav.* 78, 635–640. doi:10.1016/S0031-9384(03)00040-4
- Lopez, C., Blanke, O., 2011. The thalamocortical vestibular system in animals and humans. *Brain Res. Rev.* 67, 119–146. doi:10.1016/j.brainresrev.2010.12.002
- Lopez, C., Blanke, O., Mast, F.W., 2012. The human vestibular cortex revealed by coordinate-based activation likelihood estimation meta-analysis. *Neuroscience* 212, 159–179. doi:10.1016/j.neuroscience.2012.03.028
- Lopez, I., Ishiyama, G., Tang, Y., Tokita, J., Baloh, R.W., Ishiyama, A., 2005. Regional estimates of hair cells and supporting cells in the human crista ampullaris. *J. Neurosci. Res.* 82, 421–31. doi:10.1002/jnr.20652
- Maes, L., Dhooge, I., De Vel, E., D'haenens, W., Bockstael, A., Vinck, B.M., 2007. Water irrigation versus air insufflation: a comparison of two caloric test protocols. *Int. J. Audiol.* 46, 263–9. doi:10.1080/14992020601178147
- Maheu, M., Houde, M.S., Landry, S.P., Champoux, F., 2015. The effects of aging on clinical vestibular evaluations. *Front. Neurol.* 6. doi:10.3389/fneur.2015.00205
- Marcelli, V., Esposito, F., Aragri, A., Furia, T., Riccardi, P., Tosetti, M., Biagi, L., Marciano, E., Di Salle, F., 2009. Spatio-temporal pattern of vestibular information processing after brief caloric stimulation. *Eur. J. Radiol.* 70, 312–316. doi:10.1016/j.ejrad.2008.01.042
- Mast, F.W., Preuss, N., Hartmann, M., Grabherr, L., 2014. Spatial cognition, body representation and affective processes: the role of vestibular information beyond ocular reflexes and control of posture. *Front. Integr. Neurosci.* 8, 44. doi:10.3389/fnint.2014.00044
- Matiño-Soler, E., Esteller-More, E., Martin-Sanchez, J.-C., Martinez-Sanchez, J.-M., Perez-Fernandez, N., 2015. Normative Data on Angular Vestibulo-Ocular Responses in the Yaw Axis Measured Using the Video Head Impulse Test. *Otol. Neurotol.* 36, 466–471. doi:10.1097/MAO.0000000000000661
- McCall, A.A., Yates, B.J., 2011. Compensation Following Bilateral Vestibular Damage. *Front. Neurol.* 2, 88. doi:10.3389/fneur.2011.00088
- Micarelli, A., Chiaravalloti, A., Schillaci, O., Ottaviani, F., Alessandrini, M., 2016. Aspects of cerebral plasticity related to clinical features in acute vestibular neuritis: a "starting point" review from neuroimaging studies. *ACTA Otorhinolaryngol. Ital. Acta Otorhinolaryngol Ital* 3636, 75–8475. doi:10.14639/0392-100X-642
- Miyamoto, T., Fukushima, K., Takada, T., de Waele, C., Vidal, P.-P., 2007. Saccular stimulation of the human cortex: a functional magnetic resonance imaging study. *Neurosci. Lett.* 423, 68–72. doi:10.1016/j.neulet.2007.06.036
- Möller, C., Ödkvist, L.M., 1989. The plasticity of compensatory eye movements in bilateral vestibular loss: A study with low and high frequency rotatory tests. *Acta Otolaryngol.* 108, 345–354. doi:10.3109/00016488909125538
- Roberts, D.C., Marcelli, V., Gillen, J.S., Carey, J.P., Della Santina, C.C., Zee, D.S., 2011. MRI magnetic field stimulates rotational sensors of the brain. *Curr. Biol.* 21, 1635–40. doi:10.1016/j.cub.2011.08.029
- Rosengren, S.M., McAngus Todd, N.P., Colebatch, J.G., 2005. Vestibular-evoked extraocular potentials produced by stimulation with bone-conducted sound. *Clin. Neurophysiol.* 116,

- 1938–1948. doi:10.1016/j.clinph.2005.03.019
- Rosenhall, U., 1973. Degenerative patterns in the aging human vestibular neuro-epithelia. *Acta Otolaryngol.* 76, 208–220. doi:10.3109/00016487309121501
- Ross, M.D., Peacor, D., Johnsson, L.G., Allard, L.F., 1976. Observations on normal and degenerating human otoconia. *Ann. Otol. Rhinol. Laryngol.* 85, 310–26.
- Saunders, R., 2005. Static magnetic fields: Animal studies. *Prog. Biophys. Mol. Biol.* 87, 225–239. doi:10.1016/j.pbiomolbio.2004.09.001
- Scheltinga, A., Honegger, F., Timmermans, D.P.H., Allum, J.H.J., 2016. The effect of age on improvements in vestibulo-ocular reflexes and balance control after acute unilateral peripheral vestibular loss. *Front. Neurol.* 7, 18. doi:10.3389/fneur.2016.00018
- Schenck, J.F., 1992. Health and physiological effects of human exposure to whole-body four-tesla magnetic fields during MRI. *Ann. N. Y. Acad. Sci.* 649, 285–301. doi:10.1111/j.1749-6632.1992.tb49617.x
- Scherer, H., Clarke, A.H., 1987. Thermal stimulation of the vestibular labyrinth during orbital flight. *Arch. Otorhinolaryngol.* 244, 159–66.
- Schlindwein, P., Mueller, M., Bauermann, T., Brandt, T., Stoeter, P., Dieterich, M., 2008. Cortical representation of saccular vestibular stimulation: VEMPs in fMRI. *Neuroimage* 39, 19–31. doi:10.1016/j.neuroimage.2007.08.016
- Schneider, E., Glasauer, S., Dieterich, M., 2002. Comparison of human ocular torsion patterns during natural and galvanic vestibular stimulation. *J. Neurophysiol.* 87, 2064–2073. doi:10.1152/jn.00558.2001
- Shumway-Cook, A., Woollacott, M.H., 2007. *Motor control : translating research into clinical practice.* Lippincott Williams & Wilkins, Philadelphia [u.a.].
- Smith, P.F., Zheng, Y., 2013. From ear to uncertainty: vestibular contributions to cognitive function. *Front. Integr. Neurosci.* 7, 84. doi:10.3389/fnint.2013.00084
- Smith, S.M., Fox, P.T., Miller, K.L., Glahn, D.C., Fox, P.M., Mackay, C.E., Filippini, N., Watkins, K.E., Toro, R., Laird, A.R., Beckmann, C.F., 2009. Correspondence of the brain's functional architecture during activation and rest. *Proc. Natl. Acad. Sci. U. S. A.* 106, 13040–5. doi:10.1073/pnas.0905267106
- Snyder, D.J., Jahng, J.W., Smith, J.C., Houpt, T. a, 2000. c-Fos induction in visceral and vestibular nuclei of the rat brain stem by a 9.4 T magnetic field. *Neuroreport* 11, 2681–5.
- Stephan, T., Deutschländer, A., Nolte, A., Schneider, E., Wiesmann, M., Brandt, T., Dieterich, M., 2005. Functional MRI of galvanic vestibular stimulation with alternating currents at different frequencies. *Neuroimage* 26, 721–732. doi:10.1016/j.neuroimage.2005.02.049
- Stephan, T., Hüfner, K., Brandt, T., 2009. Stimulus profile and modeling of continuous galvanic vestibular stimulation in functional magnetic resonance imaging. *Ann. N. Y. Acad. Sci.* 1164, 472–5. doi:10.1111/j.1749-6632.2008.03715.x
- Suzuki, M., Kitano, H., Ito, R., Kitanishi, T., Yazawa, Y., Ogawa, T., Shiino, A., Kitajima, K., 2001. Cortical and subcortical vestibular response to caloric stimulation detected by functional magnetic resonance imaging. *Cogn. Brain Res.* 12, 441–449. doi:10.1016/S0926-6410(01)00080-5
- Triantafyllou, C., Hoge, R.D., Krueger, G., Wiggins, C.J., Potthast, a., Wiggins, G.C., Wald, L.L., 2005. Comparison of physiological noise at 1.5 T, 3 T and 7 T and optimization of fMRI acquisition parameters. *Neuroimage* 26, 243–250. doi:10.1016/j.neuroimage.2005.01.007
- Wall, M.B., Smith, A.T., 2008. The representation of egomotion in the human brain. *Curr. Biol.* 18, 191–194. doi:10.1016/j.cub.2007.12.053
- Walther, L.E., Westhofen, M., 2007. Presbyvertigo-aging of otoconia and vestibular sensory cells. *J. Vestib. Res.* 17, 89–92.
- Ward, B.K., Roberts, D.C., Della Santina, C.C., Carey, J.P., Zee, D.S., 2015. Vestibular

- stimulation by magnetic fields. *Ann. N. Y. Acad. Sci.* 1343, 69–79.
doi:10.1111/nyas.12702
- Ward, B.K., Roberts, D.C., Della Santina, C.C., Carey, J.P., Zee, D.S., 2014a. Magnetic vestibular stimulation in subjects with unilateral labyrinthine disorders. *Front. Neurol.* 5, 28. doi:10.3389/fneur.2014.00028
- Ward, B.K., Tan, G.X.J., Roberts, D.C., Della Santina, C.C., Zee, D.S., Carey, J.P., 2014b. Strong static magnetic fields elicit swimming behaviors consistent with direct vestibular stimulation in adult zebrafish. *PLoS One* 9. doi:10.1371/journal.pone.0092109
- Weiss, J., Herrick, R.C., Taber, K.H., Contant, C., Plishker, G.A., 1992. Bio-effects of high magnetic fields: a study using a simple animal model. *Magn. Reson. Imaging* 10, 689–694. doi:10.1016/S0891-5849(02)01354-0
- Welgampola, M.S., Colebatch, J.G., 2001. Vestibulocollic reflexes: normal values and the effect of age. *Clin. Neurophysiol.* 112, 1971–9.
- Wiesmeier, I.K., Dalin, D., Maurer, C., 2015. Elderly use proprioception rather than visual and vestibular cues for postural motor control. *Front. Aging Neurosci.* 7. doi:10.3389/fnagi.2015.00097
- Wiest, G., 2015. The origins of vestibular science. *Ann. N. Y. Acad. Sci.* 1343, 1–9. doi:10.1111/nyas.12706
- Zaitsev, M., Maclaren, J., Herbst, M., 2015. Motion artifacts in MRI: A complex problem with many partial solutions. *J. Magn. Reson. Imaging* 42, 887–901. doi:10.1002/jmri.24850
- Zink, R., Bucher, S.F., Weiss, A., Brandt, T., Dieterich, M., 1998. Effects of galvanic vestibular stimulation on otolithic and semicircular canal eye movements and perceived vertical. *Electroencephalogr. Clin. Neurophysiol.* 107, 200–205. doi:10.1016/S0013-4694(98)00056-X
- Zink, R., Stedding, S., Weiss, A., Brandt, T., Dieterich, M., 1997. Galvanic vestibular stimulation in humans: effects on otolith function in roll. *Neurosci. Lett.* 232, 171–4.
- zu Eulenburg, P., Caspers, S., Roski, C., Eickhoff, S.B., 2012. Meta-analytical definition and functional connectivity of the human vestibular cortex. *Neuroimage* 60, 162–169. doi:10.1016/j.neuroimage.2011.12.032
- zu Eulenburg, P., Stoeter, P., Dieterich, M., 2010. Voxel-based morphometry depicts central compensation after vestibular neuritis. *Ann. Neurol.* 68, 241–249. doi:10.1002/ana.22063

Appendix

Acknowledgements

Firstly, I want to express my gratitude to my thesis advisory committee members Prof. Dr. Marianne Dieterich, Prof. Dr. Stefan Glasauer, and Dr. Afra Wohlschläger for their intellectual guidance, specifically for teaching me that “science is as much about message than it is about methods” and generally for their support during this dissertation.

Besides my thesis committee, I would like to thank all my colleagues for their support.

Dr. Thomas Stephan and Dr. Virginia Flanagin for helping me with all technical questions during this thesis and their awesome fMRI methods course.

Prof. Dr. Peter zu Eulenburg for teaching me “how to write good”, and eating healthier. 😊

I thank Dr. Matthias Ertl for his spiritual guidance in times of need, and teaching me how to distinguish good science from bad science, junk science, pseudoscience and psychology. 😊

Dr. Valerie Kirsch for helping me translate “Physicist - Doctor” and “Doctor - Physicist”. 😊

I thank the whole GSN team for providing an intellectually stimulating environment in which PhD students of different backgrounds can interact and grow.

Finally, I want to express my love and deep thankfulness to my whole family.

Especially, to my father and my mother who always supported me and taught me that with persistence and determination, great things can be achieved, and to my wife Jing for her love, kindness and for giving me the greatest gifts of all, our beautiful daughter Magdalena 楚楚 who can light up a room with her smile.

CV Rainer E. Bögle

Date of Birth: 02.10.1981
Nationality: German
Academic Title: Dipl.Phys. (Master of Science); PhD cand. Systemic Neuroscience
Position: Research scientist at the German Center for Vertigo and Balance Disorders (DSGZ IFB-LMU), LMU, Munich

Academic education and career

March 2010 – present **PhD Student** in the neuroimaging group of Prof. Dr. Marianne Dieterich at the German Center for Vertigo and Balance Disorders (DSGZ).
June 2009 – February 2010 **Diploma Student** in the fMRI group of Prof. Dr. Jürgen Hennig, at the University Hospital Freiburg.

Education

2001-2009 Student of Physics at the Karlsruhe Institute of Technology (TH)
 Received Diploma of Physics (equivalent to a Masters degree)
1998-2001 Highschool student at the Technisches Gymnasium Sigmaringen
 (oriented towards technology in preparation for University studies)
1992-1998 Realschule Gammertingen (german system preparatory school with the option
 of attending Highschool afterwards, similar to junior high or secondary school)
1989-1992 Grundschule Gammertingen (primary school)

Publications

Boegle R, Stephan T, Ertl M, Glasauer S and Dieterich M.

“Magnetic vestibular stimulation modulates default mode network fluctuations”,

NeuroImage 2016; 127:409-21. DOI: 10.1016/j.neuroimage.2015.11.065.

*Cyrano CAM, ***Boegle R**, Stephan T, Dieterich M, Glasauer S.

“Age-related decline in functional connectivity of the vestibular cortical network”,

BSAF, 2015, DOI: 10.1007/s00429-014-0983-6

*These authors contributed equally to the study

Computer Skills

Distinguished programmer in MATLAB, JavaScript and C/C++ incl. MRI sequence programming for Siemens VB15. Fluent in LaTeX, Windows Office (Word, Excel, etc)

Languages

German (native), English (fluent), French (basic), Chinese (basic)

List of all publications including copyright statements

This thesis resulted in two publications and was written in cumulative style.

1. *Cyran, C.A.M., ***Boegle, R.**, Stephan, T., Dieterich, M., Glasauer, S., 2016.
Age-related decline in functional connectivity of the vestibular cortical network.
Brain Struct. Funct. 221, 1443–1463. doi:10.1007/s00429-014-0983-6
**indices equal contributions*
2. **Boegle, R.**, Stephan, T., Ertl, M., Glasauer, S., Dieterich, M., 2016.
Magnetic vestibular stimulation modulates default mode network fluctuations.
Neuroimage 127, 409–421. doi:10.1016/j.neuroimage.2015.11.065

Copies of the publications and copyright statements are attached on the following pages.

Age-related decline in functional connectivity of the vestibular cortical network

Carolin Anna Maria Cyran · Rainer Boegle ·
Thomas Stephan · Marianne Dieterich ·
Stefan Glasauer

Received: 18 November 2013 / Accepted: 28 December 2014 / Published online: 8 January 2015
© Springer-Verlag Berlin Heidelberg 2015

Abstract In the elderly, major complaints include dizziness and an increasing number of falls, possibly related to an altered processing of vestibular sensory input. In this study, we therefore investigate age-related changes induced by processing of vestibular sensory stimulation. While previous functional imaging studies of healthy aging have investigated brain function during task performance or at rest, we used galvanic vestibular stimulation during functional MRI in a task-free sensory stimulation paradigm to study the effect of healthy aging on central vestibular processing, which might only become apparent during stimulation processing. Since aging may affect signatures of brain function beyond the BOLD-signal amplitude—such as functional connectivity or temporal signal variability—we employed independent component analysis and partial least squares analysis of temporal signal

variability. We tested for age-associated changes unrelated to vestibular processing, using a motor paradigm, voxel-based morphometry and diffusion tensor imaging. This allows us to control for general age-related modifications, possibly originating from vascular, atrophic or structural connectivity changes. Age-correlated decreases of functional connectivity and increases of BOLD-signal variability were associated with multisensory vestibular networks. In contrast, no age-related functional connectivity changes were detected in somatosensory networks or during the motor paradigm. The functional connectivity decrease was not due to structural changes but to a decrease in response amplitude. In synopsis, our data suggest that both the age-dependent functional connectivity decrease and the variability increase may be due to deteriorating reciprocal cortico-cortical inhibition with age and related to multimodal vestibular integration of sensory inputs.

C. A. M. Cyran and R. Boegle contributed equally to the study.

Present Address:

C. A. M. Cyran
Institute of Neurology, University College London,
Queen Square, London WC1N 3BG, UK

C. A. M. Cyran (✉) · T. Stephan · M. Dieterich
Department of Neurology, Ludwig-Maximilians-University
Munich, Marchioninstr. 15, 81377 Munich, Germany
e-mail: carolin.cyran.14@ucl.ac.uk

R. Boegle · T. Stephan · M. Dieterich · S. Glasauer
Graduate School of Systemic Neurosciences, Ludwig-
Maximilians-University Munich, Marchioninstr. 15,
81377 Munich, Germany

R. Boegle · T. Stephan · M. Dieterich · S. Glasauer
German Center for Vertigo and Balance Disorders, (IFBLMU),
Ludwig-Maximilians-University Munich, Marchioninstr. 15,
81377 Munich, Germany

T. Stephan · S. Glasauer
Institute for Clinical Neurosciences, Ludwig-Maximilians-
University Munich, Marchioninstr. 15, 81377 Munich, Germany

M. Dieterich
SyNergy: Cluster for Systems Neurology, Munich, Germany

S. Glasauer
Center for Sensorimotor Research, Ludwig-Maximilians-
University Munich, Marchioninstr. 15, 81377 Munich, Germany

Keywords Aging · Vestibular · fMRI · Functional connectivity · Independent component analysis · Temporal BOLD-signal variability

Introduction

Most fMRI studies examining the effects of healthy aging on brain activity have so far focused on the traditional analysis of the BOLD amplitude of task-related responses (Aizenstein et al. 2004). More recently, however, imaging research has emphasized the importance of other aspects of brain activity like spontaneous fluctuations of the BOLD signal, expressed as functional connectivity (Fox and Raichle 2007) or temporal variability (e.g. see Garrett et al. 2010). Studies of age-related brain activity in particular have demonstrated the importance of underlying dynamic functional networks and of temporal BOLD-signal variability to the performance of the aging brain (Grady and Garrett 2014; Madhyastha and Grabowski 2014). Measures of functional connectivity such as the independent component analysis (ICA) reveal the strength of relations between spatially distinct regions of the brain. Imaging of the resting-state brain demonstrated spatially distinct, but temporally correlated neural systems also called functional connectivity maps, which have been shown to depend on age (Biswal et al. 2010). Balance and spatial orientation have long been known to involve various sensory systems, integrating information from the visual, vestibular and proprioceptive systems (Angelaki and Cullen 2008). Consequently, cerebral vestibular processing seems predestined to be examined in terms of functional network behavior. Furthermore, increases and decreases of temporal variability of the BOLD signal have been demonstrated to be a signature of the aging brain (Garrett et al. 2010). Notably, although temporal variability is increasing and decreasing with age in different parts of the brain and can generally be used as a predictor of age (Garrett et al. 2010), an interaction seems to exist between task performance and aging (Garrett et al. 2011, 2013; Samanez-Larkin et al. 2010; Wutte et al. 2011). However, since task performance is often confounded with age, it can be difficult to disentangle task-related and age-related effects. Several studies, therefore, strove to avoid this confound altogether by investigating resting-state activity (Allen et al. 2011; Meier et al. 2012) involving no task and only minimal sensory input. Nevertheless, many age-related problems in the elderly are explicitly linked to the processing of sensory information and may thus only become evident with stimulation.

In the elderly, major problems are complaints about dizziness and the increasing number of falls with age (Sturnieks et al. 2008; Barin and Dodson 2011), which, among other reasons, may be related to changes in central

processing of vestibular sensory input (Jahn et al. 2003). Besides many seniors suffering from peripheral vestibular deficits, their balance may be influenced by various age-dependent modifications such as changes in the supraspinal locomotor network (Zwergal et al. 2012). Given that changes of sensory processing may be a key aspect in the aforementioned deficits, possibly starting to occur prior to the deficits, this study aimed to assess age-related modifications of central vestibular sensory processing in healthy aging from a young age. Since several studies report that age-related brain changes vary in the context of more or less preserved function (Cabeza et al. 2002; Garrett et al. 2010, 2011, 2013; Samanez-Larkin et al. 2010; Wutte et al. 2011), we recruited volunteers who had maintained a healthy vestibular function in their daily lives and had no history of vestibular dysfunction or falls. Furthermore, we chose a task-free paradigm to activate brain networks specifically devoted to the processing of vestibular sensory input while avoiding confounds with task-related activations. Consequently, we used galvanic vestibular stimulation (GVS) (Schneider et al. 2002; Stephan et al. 2005; Dieterich and Brandt 2008) inside the MRI scanner to engage the vestibular system in sensory processing, focusing our volunteers on the feeling of being “nudged” or tilted. Vestibular stimulation in healthy volunteers has been shown to consistently activate a widespread cortical network including areas such as the insular cortex, the superior temporal gyrus, the supramarginal gyrus, the inferior parietal lobe, the inferior frontal gyrus, the anterior cingulate gyrus, and the hippocampus (Lobel et al. 1998; Brandt and Dieterich 1999; Stephan et al. 2005; Schindwein et al. 2008; Lopez et al. 2012).

Vestibular cerebral processing is fundamentally multimodal and dependent on the integration of several sets of sensory information. Hence, we hypothesized that the effect of healthy aging on cortical processing of sensory information in the brain may not simply result in a change in relative amplitude of BOLD signal, but may affect functional connectivity as well as temporal variability of the BOLD signal (Biswal et al. 2010; Garrett et al. 2013; Wutte et al. 2011). Functional connectivity is a measure for the relationship of distinct areas interacting during multimodal integration. Temporal variability is a measure for variations in either input-related noise or in noise associated with deteriorating neuronal processing of specific areas in the vestibular network. We therefore used, in addition to the standard GLM analysis of BOLD-signal amplitudes, ICA and partial least squares (PLS) analysis of temporal BOLD-signal variability to investigate these signatures of brain function for age-related changes. To be misled by age-related changes unrelated to vestibular processing, we performed a simple motor paradigm, voxel-based morphometry and diffusion tensor imaging as a

control to detect age-related changes that might be unrelated to vestibular processing, due to vascular modifications, atrophy of brain structures or structural connectivity changes. Jointly, these methods permitted us to characterize our networks more precisely, both locally and temporally. In combination with our experiment setup aimed at creating a subjectively equal level of stimulation, our methods of temporal analysis in particular lead us to consider the possibility of a peripheral vestibular or general cerebral effect as the reason for our findings unlikely.

Methods

Volunteers

Forty-five healthy right-handed Caucasian healthy volunteers aged 20–70 years were recruited by newspaper ads and word-of-mouth. All were screened by telephone to exclude health problems and/or medications that might affect cognitive function and brain activity, such as strokes, previous balance problems, antihypertensive drugs and antidepressants. Only volunteers with no previous history of falls or dizziness were accepted to partake in the study. Due to the reasons stated below, 39 of these 45 volunteers aged 20–70 were included in the final analysis. These were divided into three age groups [Group 1 (20–40 years of age, $n = 14$, average age 27.3 ± 4.4 years, 6 were male), Group 2 (40–60 years of age, $n = 12$, average age 52.3 ± 5.0 years, 5 were male) and Group 3 (over 60 years of age, $n = 13$, average age 67.1 ± 2.4 years, 6 were male)]. The average age of these participants was 48.3 years, 17 were male. The ethics committee of the medical faculty of the Ludwig-Maximilians University approved the investigation. All volunteers gave their written informed consent.

In addition to the fMRI examination of GVS-related activity, volunteers were asked to complete a short-handledness test (Salmaso and Longoni 1985) and a Montreal Cognitive Assessment (MoCA) test (Nasreddine et al. 2005) to investigate age-correlated cognitive impairment. None of the volunteers had a known history of vestibular deficits; nonetheless, we additionally performed a head-impulse test (Halmagyi and Curthoys 1988; Halmagyi 2005) to assure normal horizontal vestibular-ocular reflex functioning. No further vestibular testing was performed, since feeling “nudged” or tilted by switching on the stimulus was a prerequisite of taking part in the study, thereby testing the peripheral function and assuring a sufficient level of stimulation. Volunteers were informed beforehand that the vestibular sensation was the subject of examination and one volunteer did not partake because of an insufficient vestibular feeling even at higher amplitudes.

Six volunteers had to be excluded due to technical problems or strong motion artefacts in the scanner, among them one from the young age group, three middle-aged volunteers and two over the age of 60. Thus, 39 volunteers (age 20–70) were included in the subsequent analysis. For the motor paradigm, one additional female volunteer from the young age group had to be excluded due to motion artefacts, for this analysis a total of 38 datasets were taken into account.

fMRI experimental design

Tasks and stimuli

Volunteers were stimulated by unilateral GVS with direct current, i.e. rectangular sustained stimulation with constant current over whole duration of a stimulation block. Two pairs of MRI-compatible cup electrodes (MRI-compatible electromyography-cup electrodes, Brain Products) with an integrated 5 k Ω resistance for added safety were applied to the volunteer’s mastoid bone and neck after careful skin preparation and connected to custom-made stimulators placed inside the Faraday cage to allow independent stimulation of the right or left vestibular nerve. Simultaneous timing of stimulation and MRI data acquisition was controlled from the control room via optical data transmission. The cathode was placed over the mastoid bone and the anode on the neck paravertebrally of C7.

It is known that GVS induces both vestibular sensation and cutaneous pain at the electrode site, both intensifying with increasing current amplitude (Lobel et al. 1998; Bense et al. 2001). To maximize the vestibular stimulus intensity in different individuals and minimize somatosensory sensation, thereby optimizing the vestibular/somatosensory sensation ratio, volunteers were asked after demonstration to choose the lowest amplitude that would still produce a distinct vestibular sensation of being tilted or “nudged”. This individual current amplitude varied between 1.25 and 2.75 mA and was established while volunteers lay supine on the scanner bed before being transported into the MRI bore. Current intensity was gradually increased in steps of 0.25 mA and volunteers were asked after every three steps if they had already experienced a feeling of being tilted. If the vestibular sensation felt comparable at two different amplitudes, the lower one was chosen for stimulation. Before testing, all volunteers were informed that the vestibular sensation was the one of interest and should be maximized, while cutaneous pain should be minimized. Volunteers were therefore asked during demonstration to choose the amplitude that elicited a maximally intense feeling of being tilted while only causing a non-distracting amount of pain. They were instructed to opt for the weaker current amplitude if two intensities were perceived as

almost equal in terms of vestibular and cutaneous sensations. While the actual current intensity differed between individuals, this procedure ensured that a comparable intensity of perception could be assumed.

A motor paradigm was employed to account for possible general effects of aging in our group of volunteers. Volunteers were first shown a cross flashing at 1 Hz and then asked during scanning to reproduce the speed tapping their right index finger when instructed to do so by visual verbal cues (“Go” and “Stop”). Data from the motor paradigm were then analyzed for age-dependent changes in BOLD-signal amplitude, in functional connectivity and in temporal variability. As explained below, general cerebral volume changes as well as changes in fractional anisotropy were controlled by the analysis of the anatomical images of all volunteers. All of these may possibly be affected by vascular aging. In this case, this should have become evident in both, the control motor paradigm and the vestibular stimulation paradigm.

Hearing protection was provided and volunteers’ heads were fixated by means of adhesive tape and cushions to keep head movements to a minimum.

fMRI data acquisition

MRI scans were acquired on a 3-Tesla scanner using an eight-channel standard head coil (Signa Hdx platform; GE Medical Systems, Milwaukee, WI, USA). Functional MRI images were obtained by a T2 × weighted echo-planar imaging (EPI) sequence (TE = 40 ms, TR = 2,800 ms, flip angle 90°, FOV = 200 mm, matrix 64 × 64 × 44, voxel size 3.125 × 3.125 × 3.5 mm). Additionally, we used a FSPGR sequence (TE out of phase, preparation time 500 ms, flip angle 15 ms, FOV 22 cm, Locs per Slap 128, matrix 256 × 256, voxel size 0.86 × 0.86 × 0.7 mm) to obtain a high resolution T1 weighted whole brain anatomical scan of all volunteers. Diffusion tensor imaging (DTI) data were acquired using a diffusion-weighted single shot spin echo sequence (15 diffusion directions, matrix 256 × 256 × 39, b value = 1,000 s/mm², FOV 240 mm, slice thickness 3 mm).

Two GVS runs of 120 functional images each were acquired for each volunteer. An alternating block design of stimulation and rest was used. Block lengths for both stimulation and rest were randomized in the range from two to five scans of 2.8 s lengths starting with a block of GVS after six scans. Two runs were acquired each with 18 stimulation blocks (9 left and 9 right-sided stimulations).

For the motor paradigm, 84 functional images were acquired in a single run, while volunteers tapped in blocks of six scans of 2.8 s each, interjected with six scans of rest. Seven blocks of finger tapping were performed.

Data analysis

fMRI data pre-processing

Data processing was performed in MATLAB (The MathWorks Inc., Natick, MA) using the SPM5 toolbox (revision 3381, <http://www.fil.ion.ucl.ac.uk/spm/>). For each volunteer, all functional images from all runs were realigned to the first image of the first run. The anatomical image was coregistered to the mean image of the functional images. The coregistered anatomical and functional MRI data were normalized to MNI space using the unified segmentation and normalization method (Ashburner and Friston 2005) implemented in SPM5. The voxel size after normalization was 2 × 2 × 2 mm³ for the functional, and 1 × 1 × 1 mm³ for the anatomical image. The functional images were spatially smoothed by convolving the voxel values of the images with an isotropic Gaussian kernel of 8 mm FWHM. Statistical analysis included high-pass filtering of each voxel’s time course with a cutoff frequency of 0.009 Hz (i.e. a cutoff period of 108.8 s). We determined the cutoff period in consideration of the Nyquist-Shannon sampling theorem as the double of the longest time interval (i.e. the lowest frequency) between the onsets of two identical stimulation or task conditions. The principle at the base of this approach is that any variation that is based on longer cycles than this can be assumed not to be stimulation or task related and hence can be removed by the high-pass filter.

General linear model-based analysis

Functional MRI data The data were analyzed using the general linear model (GLM) as implemented in SPM5 with all updates installed (revision 3381). In the first-level analysis, effects of DC-GVS were modeled separately with a combination of event- and block-regressors as described in (Stephan et al. 2009). Periods of stimulation were modeled as block regressors convolved with the canonical HRF, separately for blocks of left and right stimulation (Left block, Right block). In addition to that, the phases of switching the DC-GVS on and off were modeled as events convolved with the canonical HRF, separately for left and right-sided stimulation and switching on and off (Left on, Right on, Left off, and Right off). Therefore, the first-level design matrix contained 6 regressors for the stimulation and one constant regressor per imaging run. Linear contrasts were defined to compute representative maps (contrast images) for the effects of: Left on, Right on, Left off, Right off, Left block, Right block, Left on and Right on for each subject.

The contrast images from the first-level analysis were entered into the second-level analysis to test for group

effects on a between subject basis (Frison and Pocock 1992; Woods 1996). We used an ANOVA (analysis of variance) and included the factors “stimulation side” (Left or Right) and “stimulation phase” (on, block, and off), as well as the factor “subject” and the covariates “age” and “current amplitude”. Data were evaluated with regard to localization of BOLD effect increases and decreases, as well as their linear correlations with age or amplitude.

In addition, we tested for differences between age groups in the conditions Left on and Right on using two-sample t tests. Separate second-level models were constructed for each comparison (Group 1 vs Group 2, Group 1 vs Group 3, Group 2 vs Group 3) and for the stimulus conditions Left on and Right on.

For all analyses, results exceeding a threshold of $p \leq 0.05$, corrected for multiple comparisons (FWE) were considered significant.

Voxel-based morphometry The VBM8 toolbox (<http://dbm.neuro.uni-jena.de/vbm/>) was used to test for changes in the local amount of gray matter with age. The high resolution T1-weighted images (FSPGR) of all subjects were analyzed using the default parameters of the VBM8 toolbox. To ensure a good starting point for the spatial normalization and segmentation procedures, we manually set the origin (i.e. the coordinate $x, y, z = 0, 0, 0$ mm) to the anterior commissure. Then, images were segmented, registered to the MNI space, followed by a non-linear normalization to the MNI template space using the high-dimensional DARTEL algorithm (Ashburner 2007) and the DARTEL templates included in the toolbox. The normalized and bias-corrected gray matter images were modulated using the non-linear components of the applied spatial transformations. This modulation step changes the voxel values in the images based on the amount of expansion or contraction applied during normalization. Modulation using the non-linear components only (without the affine components) allows to analyse the absolute amount of tissue corrected for individual brain sizes. Prior to statistical analysis, the images were smoothed with a 12-mm FWHM Gaussian kernel (Ashburner and Friston 2000, 2005; Good et al. 2001). Age-associated local changes in gray matter volume were tested for by multiple regression using the SPM implementation of the GLM. Using a design matrix that contained age, sex, and MoCA test results (compare Behavioral data in Results) as covariates, we tested for increases and decreases in the local amount of tissue associated with age. Results exceeding a threshold of $p < 0.05$ corrected for multiple comparisons (FWE) were considered significant.

Diffusion tensor imaging data analysis DTI data pre-processing and analyses were performed using the FMRIB

Software Library FSL, version 4.1.8 (<http://www.fmrib.ox.ac.uk/fsl/>) following the protocol described in (Smith et al. 2007). Diffusion data from every subject were corrected for head motion and eddy current effects using affine registration to a brain extracted b_0 volume (without diffusion weighting). Voxelwise statistical analysis of the fractional anisotropy (FA) data was carried out using TBSS [Tract-Based Spatial Statistics, (Smith et al. 2006)], part of FSL (Smith et al. 2004). First, FA images were created by fitting a tensor model to the raw diffusion data using FDT (FMRIB’s diffusion toolbox, part of FSL), and then brain extracted using BET (Smith 2002). All subjects’ FA data were then aligned into a common space (defined by the FMRIB58_FA template included in FSL) using the non-linear registration tool FNIRT (Andersson et al. 2007a, b) that uses a b-spline representation of the registration warp field (Rueckert et al. 1999). Next, the mean FA image was created and thresholded at 0.3 to create a mean FA skeleton, which represents the centers of all tracts common to the group. Each subject’s aligned FA data were then projected onto this skeleton and the resulting data fed into voxelwise cross-subject statistics.

Hypothesis testing for the DTI data was performed using permutation testing in Randomize (part of FSL) with 5,000 permutations. A model containing age as a covariate of interest was used to test for changes of skeletonized FA with age. Maps of the statistical results were generated as p value statistical images using threshold-free cluster enhancement ($p < 0.05$, FWE corrected) (Smith and Nichols 2009).

Model-free analysis

Functional connectivity analysis (Tensor independent component analysis) We analyzed our multi-volunteer fMRI data using TICA, the tensorial extension of probabilistic independent component analysis as described by Beckmann and Smith (2004, 2005) and implemented in the FSL toolbox MELODIC (<http://www.fmrib.ox.ac.uk/fsl/melodic/>). Before TICA was conducted, a voxelwise demeaning and normalization of the voxelwise variance were performed. Pre-processed data were whitened and projected into a subspace using probabilistic principal component analysis. The number of dimensions for the subspace was estimated using the Laplace approximation to the Bayesian evidence of the model order (Minka 2000; Beckmann and Smith 2004). Component maps were then estimated and afterwards normalized using the residual noise standard deviation. These normalized component maps were then thresholded by fitting a mixture model to the histogram of intensity values (Beckmann et al. 2003; Beckmann and Smith 2004).

Tensor-independent component analysis allows us to extract functional networks from the data, as well as

associated relative weighting factors for the volunteers in the group which enable us to evaluate general trends of increase or decrease of this functional network weighting (and therefore a change in functional connectivity) with age (or other covariates) via correlation testing.

A functional network is defined here as “multi-voxel structured responses with one shared time course”, i.e. the spatial-independent component maps (ICs) in combination with their associated time courses called temporal modes. It is important to note here that based on this analysis alone, it cannot be distinguished if every voxel in the network is driven in the same way by the periphery sensory inputs or if they all communicate with each other and only one receives input from the periphery sensory inputs. The collection of the relative weighting factors for all volunteers per IC is called volunteer modes. It should be noted that the functional networks (ICs and temporal modes) are representative for the group and that the variation over the group is captured in the volunteer modes (the relative weighting factors), due to the formulation of the tensor ICA model for trilinear expansion of the multi-volunteer fMRI data.

Determination of covariate-related variations in functional network responses

We can, therefore, test for (linear) changes in the functional network responses with respect to volunteer covariates by correlating the volunteer modes with covariate values (e.g. correlation of the volunteer modes with the age of the volunteers). All volunteer-wise covariates were tested for significant correlation between each other using SPSS 16.

Analysis of temporal modes via event-related averaging (ERA)

We will show in the results section that the volunteer modes (the relative weighting factors for functional connectivity) obtained from the tensor ICA correlate with age for certain networks and will visualize the cause of this correlation in terms of temporal stimulus responses. Furthermore, we will demonstrate that the statistical significance of this correlation with age (or absence thereof, depending on the IC), is caused by a statistically significant decline in average temporal stimulus response amplitudes (or absence thereof, depending on the IC) from the youngest (Group 1) to the oldest volunteers (Group 3) in our sample.

The temporal responses of a functional network (IC) associated with stimulation (e.g. GVS) or task execution (e.g. finger tapping) were evaluated, via averaging the time courses of the respective temporal mode taken from a window of 1 TR before and 10 TRs after the onset of each event, respectively (also known as event-related averaging,

ERA). Furthermore, we applied ERA on the time courses of each single volunteer taken from the mixing matrix of the ICA. We used these ERA to calculate the representative responses of each age group by assigning subjects to the age groups Group 1 (20–40 years of age), Group 2 (40–60 years of age) and Group 3 (over 60 years of age) and calculating the mean and standard deviation of the ERAs for all subjects of each group, respectively. This resulted in one average ERA per age group for displaying. We also used the single volunteer ERA amplitudes in two-sample t tests between the age groups Group 1 and Group 3 to test for significant differences between age group response amplitudes, as a demonstration that a significant negative correlation of age with volunteer modes does correspond to a decline in response amplitudes. All time courses were shifted prior to averaging to set the onset values to zero.

Criteria for selection of independent components of interest

Selection of ICs proceeded in three steps. First, all ICs were selected which individually describe more than 1 % of the total variance. In the second step, all ICs corresponding to head motion, head motion and magnetic field inhomogeneity interaction, physiological artefacts (e.g. pulsation), registration error or CSF fluctuations were removed from the list generated in the first step. In the third step, those ICs were selected which show spatial overlap with vestibular, somatosensory or motor areas corresponding with the respective experiment (GVS or motor paradigm). In the case of the GVS experiment, this resulted in eight ICs. In the case of the motor paradigm this resulted in one IC.

IC residual analysis

So as to test if ICA sufficiently modeled all age dependency in the fMRI data, we adopted the partial least squares (PLS) method introduced by Garrett et al. (2010) and McIntosh et al. (1996) to investigate IC residuals for eventual age dependence, beyond the aging effects found in ICA. We calculated the single volunteer time course for each voxel from the group-average tensor ICA results via dual regression (Beckmann 2009; Filippini et al. 2009) and subtracted each IC of interest from the volunteer’s raw data to get the residual time series per volunteer. We then determined regions of interest using the thresholded spatial maps of each IC of interest (see above). For each of these eight ROIs, we calculated the voxelwise residual temporal variability as standard deviation of the residual time series. The correlation of this residual variability to age was determined using the PLS analysis. For none of the ROIs

we found any significant age dependence (permutation test, 1,000 permutations).

Temporal variability analysis We also used the partial least squares (PLS) method (McIntosh et al. 1996; Garrett et al. 2010) with a slight modification to investigate possible age-related changes of BOLD signal variability. As a first step, we removed extra variability, that we considered noise, from the fMRI data of each individual run of each individual volunteer. This was done using the results of the group ICA and performing a dual regression analysis (Beckmann CF 2009; Filippini et al. 2009) to obtain the individual time courses and residuals of the ICA associated with each functional imaging run of each volunteer corresponding to all group ICs and subtracting the residuals artefacts, judged as noise. Additionally, instead of using the block normalization procedure introduced by Garrett et al. (2010) to remove stimulus-related variability, we adopted a different method. In contrast to block normalization, which relies on block design with BOLD responses mirroring the block design, our group-mean normalization method is hypothesis free and only requires identical stimulation time courses for all subjects, as in the present study. For the group-mean normalization, we first masked the spatially aligned functional images using a gray matter mask [gray matter definition from the Talairach daemon database (www.talairach.org) as a binary mask, dilated by smoothing with a Gaussian kernel (FWHM 2 mm) and thresholding at 0.2], then normalized the voxel time series by subtracting the individual voxel means, and determined the average time course of each voxel over the whole group. We then regressed these group-mean time courses into the individual time series to get a residual time series for each voxel and participant. The variability of these residual time series was then analyzed using the PLS method for age dependence as described in Garrett et al. (2010). The significance of the correlation between the resulting brain scores and age was determined by permutation analysis (1,000 permutations). To further investigate which voxels contributed most to the age dependence, we thresholded the brain saliences resulting from the PLS analysis by a bootstrap ratio of 3 corresponding approximately to a 99 % confidence interval (Garrett et al. 2010).

Results

Unilateral galvanic vestibular stimulation

Behavioral data

After the experiment, the volunteers reported a feeling of their head being nudged every time the current was

switched on; this feeling subsided gradually over the stimulation period. Statements concerning the turning direction differed and were generally inconsistent. Cutaneous pain was reported to be sharp, pinpoint like at the beginning of stimulation, but then continued as a slightly burning sensation. Current amplitude did not generally increase with age and no correlation between age and amplitude could be observed ($R = 0.04$; $p = 0.79$). Volunteers had an average current amplitude of 1.6 mA (1.64 mA with standard deviation of 0.4 mA), in Group 1 the average current amplitude was 1.7 mA (1.67 mA with standard deviation of 0.47 mA), in Group 2 it was 1.5 mA (1.5 mA with standard deviation of 0.31 mA) and in Group 3 it was 1.7 mA (1.73 mA with standard deviation of 0.37 mA).

Volunteers averaged 27 (26.97 with standard deviation of 2.5) points in the MoCA test. In Group 1 the average number of points scored in the MoCA was 28 (28.29 with standard deviation of 1.8), in Group 2 27 (26.7 with standard deviation of 3) and in Group 3 26 (25.85 with standard deviation of 2.1). MoCA showed a significant negative linear correlation with age, as expected, but the relationship was only weakly present ($R = -0.36$; $p = 0.02$).

General linear model analysis

The following BOLD signal increases could be found during GVS. Only the subjectively more intense effects of switching the current on or off induced significant BOLD signal changes, bilaterally in the posterior insula, the cerebellum, the hippocampus, the thalamus, the cingulus and the inferior and superior parietal lobe (see Table 1; Fig. 1 for more detail). Both switching the current on and off induced a similar activation pattern involving the typical multisensory areas.

More specifically, for the contrast “Left On”, activations included the right middle frontal gyrus, the right middle temporal gyrus, the right and left premotor cortex, the right secondary somatosensory cortex in the parietal operculum, the right insula, the right inferior parietal lobule, the right anterior intra-parietal sulcus, as well as the left Broca’s area, the left middle frontal gyrus, left cerebellar culmen, tonsil and pyramis as well as the right cerebellar uvula. Cluster dimensions also encompassed the insula and the thalamus bilaterally, as well as the posterior cingulum.

The contrast “Right On” showed activations in the left superior frontal gyrus, the left premotor cortex, the left secondary somatosensory cortex in the parietal operculum OP1, OP2, OP3 and OP4, the left superior (7M, 7L) and inferior (PFop) parietal lobule, the left inferior occipito-frontal fascicle, the left Insula (Ig2, Id1), left Cuneus, the callosal body, the right middle temporal gyrus, the right temporal lobe, as well as the right cerebellar uvula, tonsil and pyramis.

Table 1 Significant increases in BOLD signal induced by GVS and detected by GLM analysis

MNI coordinates x, y, z (mm)	Voxel	<i>p</i> (FWE corrected)	Anatomical location	BA
Activations induced by powering on the current on the left hand side				
64, -18, 24	25,815	0.000	Right inferior parietal lobule PFop and PFt, secondary somatosensory cortex/parietal operculum OP1 and OP4	3ab
38, -14, 20		0.000	Right secondary somatosensory cortex/parietal operculum OP3, OP2, OP4; right Insula	13
52, -28, 28		0.000	Right inferior parietal lobule PFop and Pfc right secondary somatosensory cortex/parietal operculum OP1; right anterior intra-parietal sulcus HIP2	
-28, -66, -28	2,744	0.000	Left cerebellar culmen	
-2, -62, -34		0.000	Left cerebellar tonsil	
-8, -80, -30		0.000	Left cerebellar pyramis	
50, -50, 0	657	0.000	Right middle temporal gyrus	
-46, 8, 38	331	0.000	Left Broca's area, left premotor cortex, left middle frontal gyrus	44, 6
-32, 0, 46		0.011	Left premotor cortex, left middle frontal gyrus	6
32, -74, -24	203	0.001	Right cerebellar uvula	
-4, 6, 62	48	0.005	Left premotor cortex, left medial frontal gyrus	6
4, 8, 62,		0.006	Right premotor cortex, right medial frontal gyrus	6
Activations induced by powering on the current on the right				
-60, -24, 16	23,207	0.000	Left secondary somatosensory cortex/parietal operculum OP1, left inferior parietal lobule PFop	40
-38, -2, -14		0.000	Insula Id1	
-38, -18, 16		0.000	Left Insula Ig1 and Ig2, left secondary somatosensory cortex/parietal operculum OP3, OP2, OP4	13
28, -70, -24	1,768	0.000	Right cerebellar uvula	
-2, -62, -40		0.000	Left cerebellar tonsil	
14, -78, -26		0.000	Right cerebellar pyramis	
0, -24, 26	579	0.000	Callosal body	
0, -36, 16		0.001	Callosal body	
-10, 18, 54	160	0.001	Left premotor cortex, left superior frontal gyrus	6
62, -52, 0	168	0.001	Right middle temporal gyrus	
54, -48, -4		0.001	Right temporal gyrus	
56, -56, -10		0.013	Right middle temporal gyrus	
-6, -76, 36	17	0.024	Left superior parietal lobule 7M, 7L, left Cuneus	
Activations induced by powering off the current on the left				
No significant activations at FWE $p < 0.05$				
Activations induced by powering off the current on the right				
62, -2, 24	29	0.019	Right premotor somatosensory cortex, right primary motor cortex, right precentral gyrus	4a, 6
Activations induced by sustained GVS on the left				
No significant activations at FWE $p < 0.05$				
Activations induced by sustained GVS on the right				
No significant activations at FWE $p < 0.05$				

All results are FWE corrected for false positives. Clusters containing more than 15 voxels are displayed. Anatomical locations determined using the Juelich Histological Atlas and the Tailarach Demon Atlas as in the FSL Atlas toolbox

Among the other contrasts, only “right off” showed a significant activation in the right primary somatosensory cortex, and the right primary motor cortex in the precentral gyrus.

The BOLD signal increases induced by switching the current on either on the left (A) or on the right (B) hand side are shown in Fig. 1. During the block stimulation, no

significant effects could be found. Furthermore, no negative BOLD signal changes could be detected at any time during GVS. BOLD signal changes were not correlated significantly to age or amplitude.

In the following text, BOLD signal increases will be denominated as “activations”, while BOLD signal decreases will be denominated as “deactivations”.

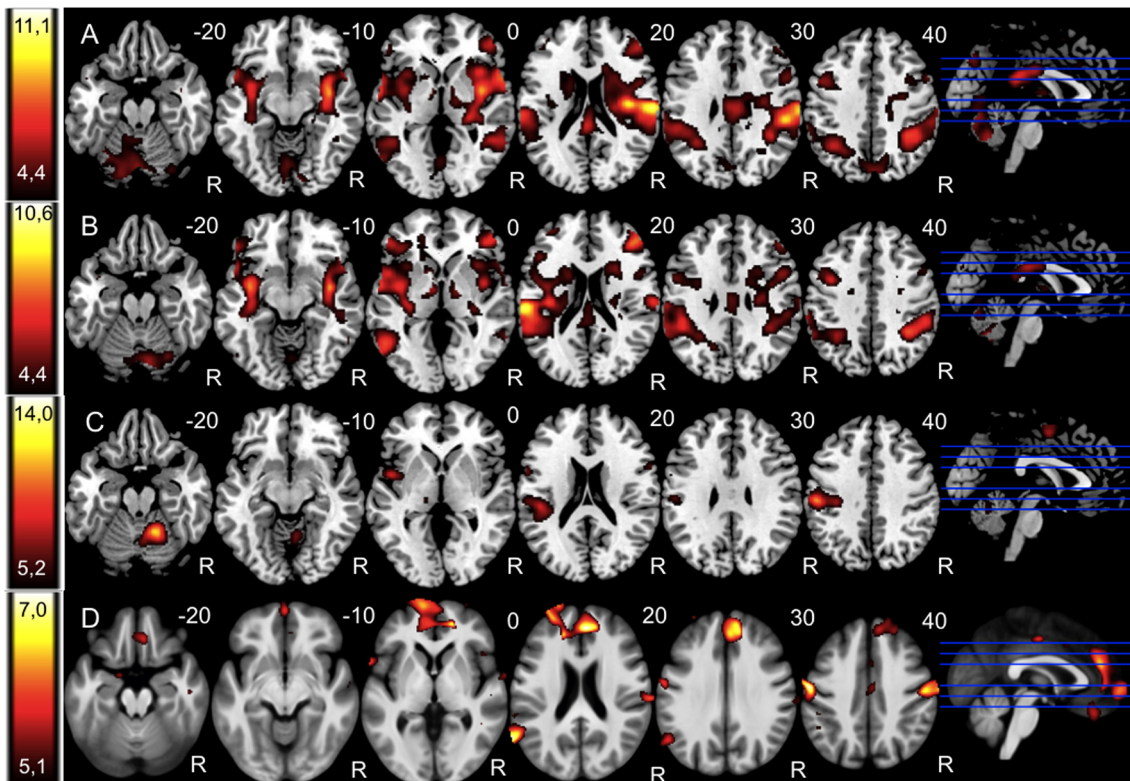


Fig. 1 Significant activations in the GLM analysis induced by switching on the direct current mediating the galvanic vestibular stimulation on the *left* (a) and *right* (b) hand side, as well as

significant activations induced by tapping of the right index finger at approx. 1 Hz (c). Significant negative correlation of brain volume with increasing age (d). All results FWE corrected, $p < 0.05$

Functional connectivity analysis (Tensor ICA)

The final estimated dimensionality for the tensor ICA expansion was 44 retaining 83.99 % of total variance. Of these 44 ICs, 13 ICs described less than 1 % of total variance and 14 were identified as artefacts, i.e. noise sources. The artefacts included ten ICs, which were identified as head motion or head motion and magnetic field inhomogeneity interaction artefacts, two ICs were identified as pulsation artefacts and two ICs were identified as CSF fluctuations. From the remaining 17 ICs, we chose eight ICs for further study, which collectively explained 32.83 % of the total variance of the group data (the other nine ICs were labeled as “not interpretable” in the above sense). The first six of these eight ICs of interest (all eight in order of their respective percentage of variance explained) overlapped with vestibular areas (also identified by means of the GLM analysis) and furthermore showed an event-like transient response associated with switching of the current, collectively explaining 26.88 % of the total variance. The remaining last two ICs of interest, collectively explaining 5.95 % of the total variance, overlapped mainly with somatosensory areas. Each of these two ICs showed block-like, (i.e. sustained) reciprocal responses in the

respective left or right somatosensory areas, whereas the “first six” ICs of interest were bilateral and largely symmetric, i.e. the right somatosensory cortex (responding with a positive block-like response associated with direct current stimulation of the left side and negative block-like response associated with direct current stimulation of the right side) was represented solely in IC-9 whereas the left somatosensory cortex (responding with a positive block-like response associated with direct current stimulation of the right side and negative block-like response associated with direct current stimulation of the left side) was solely represented in IC-12. Details on the retained ICs are shown in Table 3. All volunteer modes of the “first six” ICs showed significant negative correlations with age, while neither of the other two exhibited a significant correlation with age. Consistent with this finding, the ERAs for the age groups Group 1 and Group 3 differed significantly in their amplitudes for all of the “first six” ICs, while neither of the last two ICs showed a significant difference of ERA amplitudes between age groups Group 1 and Group 3. Figure 2 shows two ICs from the “first six” ICs with a significant correlation with age [$R(\text{IC-2}) = -0.64$, $p < 0.001$ and $R(\text{IC-3}) = -0.57$, $p < 0.001$] in their volunteer modes, displayed in Fig. 2 parts d₁ and d₂ as well as

a significant difference between ERA amplitudes of age groups Group 1 and Group 3 [$p(\text{IC-2}) < 0.001$ and $p(\text{IC-3}) < 0.001$], displayed in Fig. 2 parts c_1 and c_2 . Figure 3 shows the last two ICs which show no significant correlation with age [$R(\text{IC-9}) = -0.072$, $p = 0.66$ and $R(\text{IC-12}) = -0.19$, $p < 0.22$] in their volunteer modes, displayed in Fig. 3 parts D_1 and D_2 as well as no significant differences between age groups Group 1 and Group 3 [$p(\text{IC-9}) = 0.85$ and $p(\text{IC-12}) = 0.31$] displayed in Fig. 3 parts C_1 and C_2 . The other four of the “first six” ICs (not shown) all had significant negative correlations with age for their volunteer modes, $R(\text{IC-1}) = -0.50$ ($p = 0.0011$), $R(\text{IC-4}) = -0.54$ ($p < 0.001$), $R(\text{IC-5}) = -0.58$ ($p < 0.001$), and $R(\text{IC-6}) = -0.53$ ($p < 0.001$), the differences in ERA amplitudes between age groups Group 1 and Group 3 were all significant [$p(\text{IC-1}) < 0.001$, $p(\text{IC-4}) < 0.001$, $p(\text{IC-5}) < 0.001$ and $p(\text{IC-6}) = 0.0016$]. All statistical tests were multiple comparison corrected according to the number of ICs tested using the Bonferroni correction method.

In the two ICs representing the “first six” networks (IC-2 and IC-3), increased BOLD-signal activity could be detected in IC-2 bilaterally in the superior temporal gyrus, the middle temporal gyrus, the thalamus (right medial dorsal nucleus, left ventral posterior lateral nucleus, ventral lateral nucleus bilaterally, left ventral posterior lateral nucleus) and the posterior insula, as well as in the left inferior parietal lobe, the midbrain bilaterally, the left cuneus, the right superior frontal gyrus and the right caudate body. In IC-3, activated areas comprised the right inferior frontal gyrus, the complete insula bilaterally, the thalamus (including the right and left ventral lateral, medial dorsal nuclei) bilaterally and parts of the midbrain down to the substantia nigra and subthalamic nucleus, the parahippocampal gyrus bilaterally (left more than right), the lingual gyrus bilaterally, the right middle temporal gyrus, the left superior temporal gyrus, the inferior parietal lobe bilaterally and the posterior cingulate gyrus.

In the ICs exemplifying the remaining two networks (IC-9 and IC-12), increased BOLD-signal activity could be detected in IC-9 in the left postcentral gyrus and in the left paracentral lobule, as well as in IC-12 in the right precentral gyrus, the right postcentral gyrus, the right superior parietal lobe, the right inferior parietal lobe and the right posterior insula.

Analysis of the residual time series (see “Methods”) showed that the residual BOLD variability unexplained by the tensor ICA was not significantly related to age, thus corroborating that the ICs modeled BOLD variability for young and old subjects equally well. Consequently, it appears implausible that analysis-related factors such as an insufficient number of ICs could be the reason for the described age dependence.

Temporal variability analysis

As demonstrated by the PLS analysis, the temporal variability of the BOLD signal expressed as PLS brain scores derived from the voxelwise standard deviation of the group-mean normalized BOLD signal time series exhibited a significant correlation with age ($R = 0.68$, $p = 0.034$). Further analysis of the PLS brain saliences revealed that local BOLD variability increased with age bilaterally in the thalamus and the posterior insula (see Fig. 4). Decreases in variability were observed in regions of the frontal cortex. The regions with increasing variability partly overlap with the ROIs of the “first six” ICs described above, which showed significant age dependence of the associated ICs. Regions of interest are detailed in Table 2. To further investigate whether age-dependent variability was associated with the stimulus, we separated the time series into stimulation periods and rest periods. Temporal variability analysis of these separated time series showed a significant effect for stimulation ($R = 0.71$, $p = 0.016$) but not for rest ($R = 0.58$, $p = 0.082$), although it should be noted that this result for the rest periods was near significance. To further illustrate the temporal variability of the BOLD signal, we extracted the BOLD time course of a voxel in the insula (which also coincides with the networks of the “first six” ICs described above) that contributed strongly to the correlation between age and temporal variability (see Fig. 5). While the group-mean time series of this exemplary voxel resembles the event-like response of the “first six” ICs (Fig. 5a, cf. Fig. 2), the group-mean normalized BOLD signal (Fig. 5b, c) suggests that temporal BOLD-variability is neither time locked to stimulus onset nor does it show a direct relation to the IC time series, suggesting that the effect of increasing temporal variability occurs over the whole time course equally and is not very different during rest periods than it is during stimulation periods.

Motor paradigm

General linear model analysis The GLM analysis of the finger tapping motor paradigm showed BOLD signal increases in the corresponding motor cortex (left precentral gyrus), the anterior lobe of the right cerebellum, in the left medial frontal gyrus, left medial insula, the right inferior frontal gyrus and the left ventral posterior medial thalamic nucleus.

Functional connectivity analysis (Tensor ICA) A tensor ICA of the “finger tapping data” conducted in the same manner as for the GVS experiment showed similar activations in the spatial components as in the GLM results and a blocked response associated with blocks of finger tapping, but no significant linear age correlations ($R = -0.01$; $p = 0.96$) could be found in the respective volunteer modes.

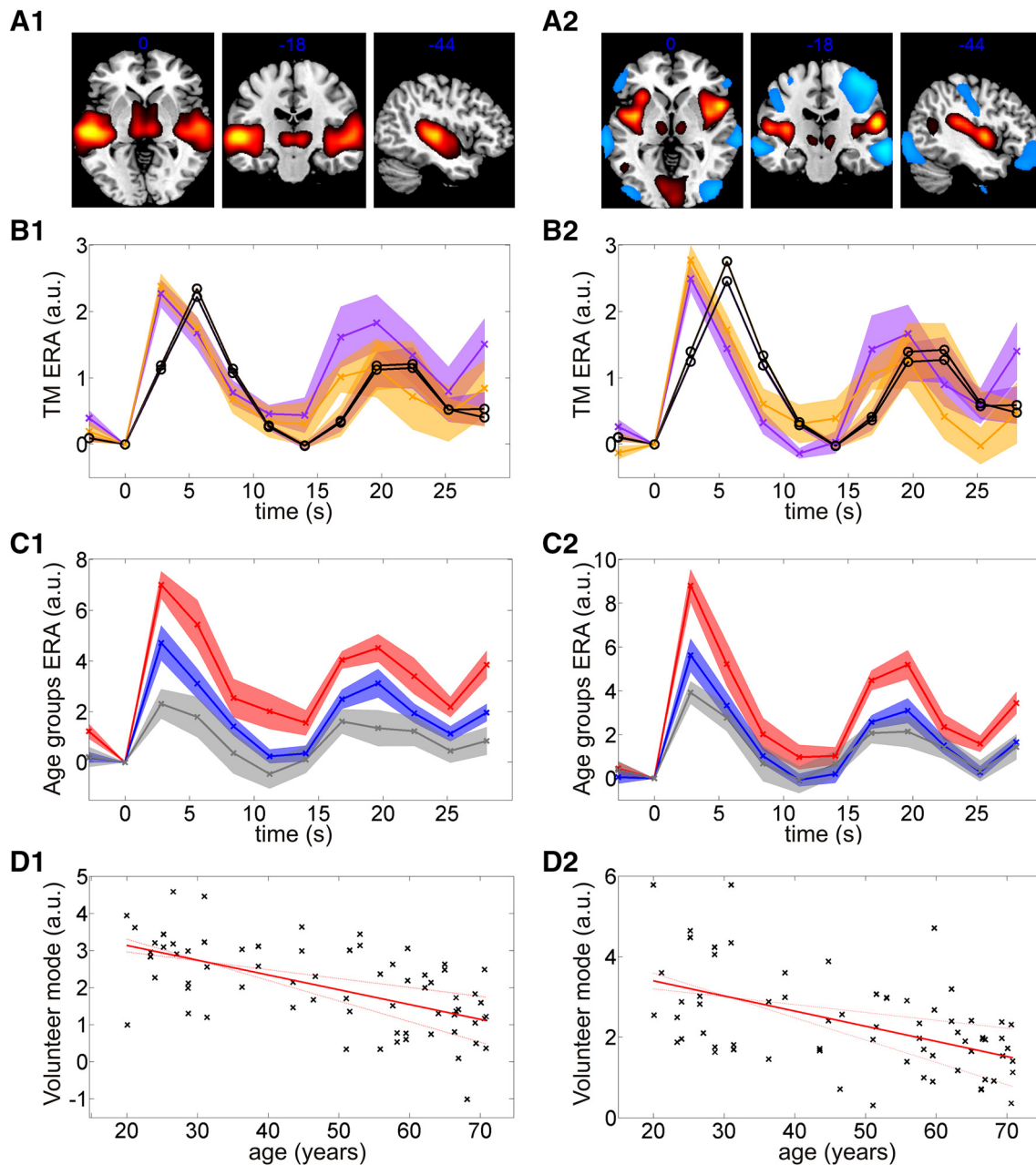


Fig. 2 Two exemplary ICs (IC-2 and IC-3, shown in **a**₁ and **a**₂, respectively) showing a significant age-related decrease in their respective volunteer mode (shown in **d**₁ and **d**₂, respectively) as well as a significant difference of the amplitudes of the event-related average (ERA) (shown in **c**₁ and **c**₂, respectively) between the age groups Group 1 and Group 3, [$p(\text{IC-2}) < 0.001$ and $p(\text{IC-3}) < 0.001$]. In **c**₁ and **c**₂, the ERA for the age groups Group 1, Group 2 and Group 3 are marked in *red*, *blue* and *gray*, respectively. In **c**₁ and **c**₂, the ERA is shown for left- and right-GVS averaged. The correlation coefficient between the volunteer mode and age was determined to be (**d**₁) $R(\text{IC-2}) = -0.64$ ($p < 0.001$) and (**d**₂) $R(\text{IC-3}) = -0.57$ ($p < 0.001$). In **d**₁ and **d**₂ the volunteer mode amplitudes are plotted as *black crosses* and the least squares regression line is plotted in *red*.

ERA of the temporal mode revealing the temporal response characteristics of these ICs with respect to left- and right-GVS (shown in purple and orange, respectively) are displayed in (**b**₁ and **b**₂) together with simulated BOLD-response curves (shown in *black*). The BOLD-response curves are simulated under the assumption of an event-like response to switching the direct current GVS ON convolved with the canonical hemodynamic response function. The amplitudes of the peaks of the ERA of the BOLD simulation have been manually adjusted to match the peak amplitude of the ERA of the ICs. *Shaded areas* in ERA plots indicate the standard error of the mean interval around the mean. All amplitudes are given in arbitrary units, time is given in seconds relative to the onset of stimulation and age is given in years since birth

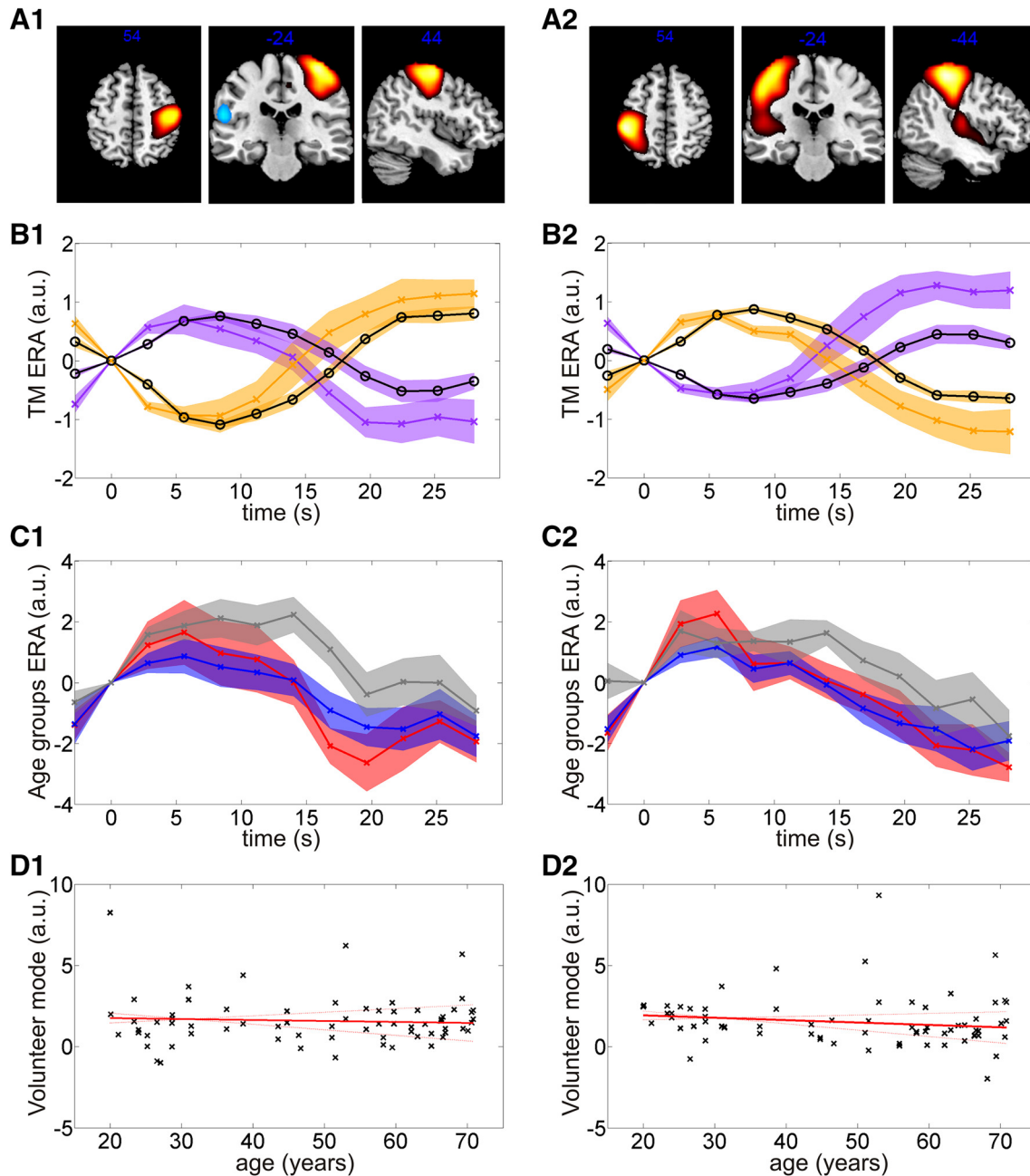


Fig. 3 Two exemplary ICs (IC-9 and IC-12, shown in **a**₁ and **a**₂, respectively) without a significant age-related change in their respective volunteer mode (shown in **d**₁ and **d**₂, respectively) as well as no significant difference of the amplitudes of the event-related average (ERA) (shown in **c**₁ and **c**₂, respectively) between the age groups Group 1 and Group 3, [$p(\text{IC-9}) < 0.85$ and $p(\text{IC-12}) < 0.31$]. In **c**₁ and **c**₂, the ERA for the age groups Group 1, Group 2 and Group 3 are marked in red, blue and gray, respectively. In **c**₁ only the ERA for left-GVS is shown and in **c**₂ only the ERA for right-GVS is shown (the positive response for the respective IC). The correlation coefficient between the volunteer mode and age was determined to be (**d**₁) $R(\text{IC-9}) = -0.072$ ($p = 0.66$) and (**d**₂) $R(\text{IC-12}) = -0.19$ ($p = 0.22$). In **d**₁ and **d**₂ the volunteer mode amplitudes are plotted as black crosses and the least squares regression line is plotted in red.

ERA of the temporal mode revealing the temporal response characteristics of these ICs with respect to left- and right-GVS (shown in purple and orange, respectively) are displayed in (**b**₁ and **b**₂) together with simulated BOLD-response curves (shown in black). The BOLD-response curves are simulated under the assumption of a block-like response to sustained continuous direct current stimulation of the skin, with a reciprocal relationship between left- and right-GVS. The amplitudes of the peaks of the ERA of the BOLD simulation have been manually adjusted to match the peak amplitude of the ERA of the ICs. Shaded areas in ERA plots indicate the standard error of the mean interval around the mean. All amplitudes are given in arbitrary units, time is given in seconds relative to the onset of stimulation and age is given in years since birth

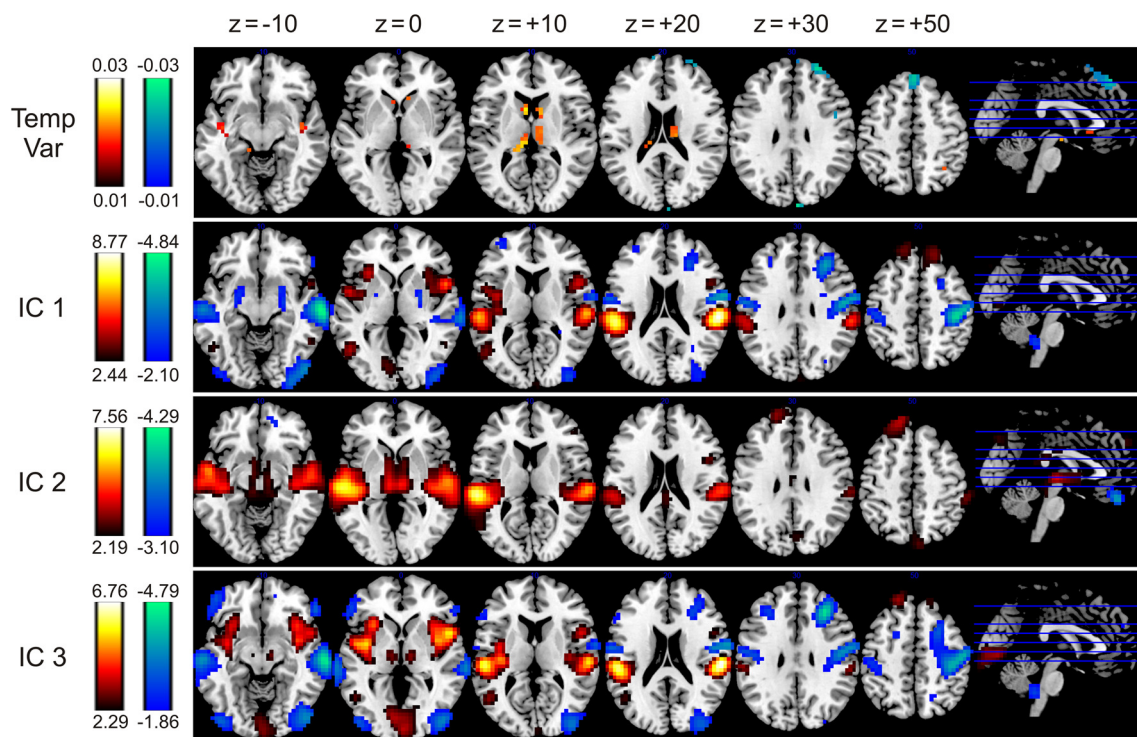


Fig. 4 Overlay of functional brain mapping results on a template brain for the resulting brain scores of the PLS temporal variability analysis method applied to the group-mean normalized data for the galvanic vestibular stimulation periods only ($R = 0.71$, $p = 0.016$). Additionally IC-1, IC-2 and IC-3 (the ICs describing the most amount

of total variance of the ICs of interest) are shown for comparison. *Color bars* indicate activity in terms of PLS brain scores for the temporal variability analysis or z statistic values of the alternative hypothesis test of the probabilistic ICA

Temporal variability analysis The variability of the BOLD signal, calculated as PLS brain scores in the same manner as for the GVS experiment, presented no significant correlation with age ($p > 0.5$). This demonstrates that the age-related changes in temporal BOLD-signal variability revealed in the GVS experiment are not due to generalized age-related changes affecting, i.e. the motor system.

Structural MRI data

Diffusion tensor imaging analysis

We detected a generalized decrease of fractional anisotropy with age across our sample of volunteers, but no correlations with the covariates from our behavioral data.

Voxel-based Morphometry: Age-related cerebral changes in volume

Cerebral volume decreased linearly with age, particularly in the primary somatosensory cortex, inferior parietal lobule and postcentral gyrus bilaterally. Furthermore, decreases in volume could be detected in the left anterior

intra-parietal sulcus, in the right operculum, in the left rectal and fusiform gyrus, in the left amygdala, the right middle and bilaterally in the inferior frontal gyrus, in the left entorhinal cortex, in the cingulate gyrus bilaterally, as well as bilaterally in the superior and in the right middle temporal gyri. For more detail, see Table 2.

Discussion

In the present study, galvanic vestibular stimulation (GVS) induced BOLD signal increases bilaterally in the posterior insula, the cerebellum, the hippocampus, the thalamus, the cingulus and the inferior and superior parietal lobe. This is consistent with previous studies, which found activity in this bihemispheric network induced by vestibular stimulation (Schneider et al. 2002; Stephan et al. 2005; Dieterich and Brandt 2008; Lopez et al. 2012). Balance and orientation being primarily multimodal, they seem destined for a network analysis. Furthermore, previous studies have shown the importance of investigating temporal variability in healthy aging (Garrett et al. 2010, 2011, 2013; Samanez-Larkin et al. 2010). We focused on whether the aging of vestibular processing would affect the BOLD-signal

Table 2 Significant decreases in cerebral volume with age as detected by Voxel-based morphometry analysis

MNI coordinates (x, y, z (mm))	Voxel	p (FWE corrected)	Anatomical location	BA
6, 42, 22	8,936	0.000	Right medial frontal gyrus	
15, 48, 7		0.000	Right medial frontal gyrus	
10, 44, 33		0.000	Right medial frontal gyrus	
−56, −12, 40	1,523	0.000	Left primary somatosensory cortex, inferior parietal lobule PFt and PFop	1, 2, 3b
−57, −27, 45		0.005	Left inferior parietal lobule PF, PFt and PFop, primary somatosensory cortex, anterior intra-parietal sulcus hIP2	1, 2
−46, −37, 46		0.012	Left anterior intra-parietal sulcus hIP2 and hIP3, primary somatosensory cortex, inferior parietal lobule PFt, PF and PFm	2
−63, −60, 19	1,441	0.001	Left inferior parietal lobule Pga, left superior temporal gyrus	22
−63, −42, 24		0.007	Left inferior parietal lobule PF and PFm	40
54, −15, 40	1,831	0.001	Right primary somatosensory cortex, inferior parietal lobule Pfof and PFt	1, 2, 3a, 3b
66, −13, 39		0.002	Right primary somatosensory cortex, right postcentral gyrus	3
66, −24, 21		0.005	Right secondary somatosensory cortex/parietal operculum OP1, inferior parietal lobule PFt, PF and Pfof right postcentral gyrus	40
34, 63, 13	152	0.003	Right middle frontal gyrus	
9, 33, −15	767	0.005	Right anterior cingulate gyrus	
−2, 38, −27		0.011	Left rectal gyrus	11
−60, 12, 1	143	0.005	Left inferior frontal gyrus	44, 45
2, −13, 43	237	0.009	Right and left cingulate gyrus	6
−36, −28, 67	191	0.014	Left primary somatosensory cortex, postcentral gyrus	1, 2, 3b 4a, 4p 6
−44, −25, 64		0.023	Left primary somatosensory cortex, left postcentral gyrus	1, 2, 3b, 4a, 6
68, −3, 3	116	0.015	Right superior temporal gyrus	22
28, −27, 63	183	0.015	Right primary somatosensory cortex, postcentral gyrus	1, 3b, 4a, 4p, 6
−15, −1, −20	48	0.021	Left superficial, amygdala	34
3, 12, 37	125	0.022	Right cingulate gyrus	24
46, 20, −2	38	0.024	Right inferior frontal gyrus	44, 45
−46, 26, 16	56	0.025	Left inferior frontal gyrus	44, 45
−40, 27, 9		0.036	Left inferior frontal gyrus	45
51, −16, −20	19	0.025	Right middle temporal gyrus	
−46, −57, −24	30	0.026	Left fusiform gyrus	
64, −22, −6	226	0.027	Right middle temporal gyrus	
54, −18, −2		0.040	Right superior temporal gyrus	
46, −2, −30	18	0.033	Right middle temporal gyrus	20
50, 26, 22	25	0.034	Right middle frontal gyrus	45

All results are FWE corrected for false positives. Clusters containing more than 15 voxels are displayed. Anatomical locations determined using the Juelich Histological Atlas and the Tailarach Demon Atlas as in the FSL Atlas toolbox

amplitude, functional connectivity or temporal variability. In the general linear model (GLM) analysis, we found no age-correlated changes in BOLD-signal amplitude. Tensor-independent component analysis (ICA) (Beckmann and Smith 2005), however, identified an age-related pattern of functional connectivity associated with vestibular networks. Furthermore, age-related changes in BOLD-signal variability were also associated with these vestibular networks.

The eight selected independent components (ICs) of interest could be separated into two groups, which were related to the two GVS-induced sensations. The

“vestibular” feeling of being tilted was represented by the “first six” ICs of interest, ICs 1-6, while the cutaneous pain was represented by the “last two” ICs of interest, IC 9 and IC 12, as could be inferred from the ICs time courses and the areas covered by their spatial maps. The “first six” were labeled the “multisensory vestibular networks” since they showed an event-like, transient temporal response characteristic associated with switching of the currents and thus corresponded best with the time course of the feeling of being tilted. These components included multisensory vestibular cerebral areas. The “last two” were labeled the “multisensory somatosensory networks”, because they

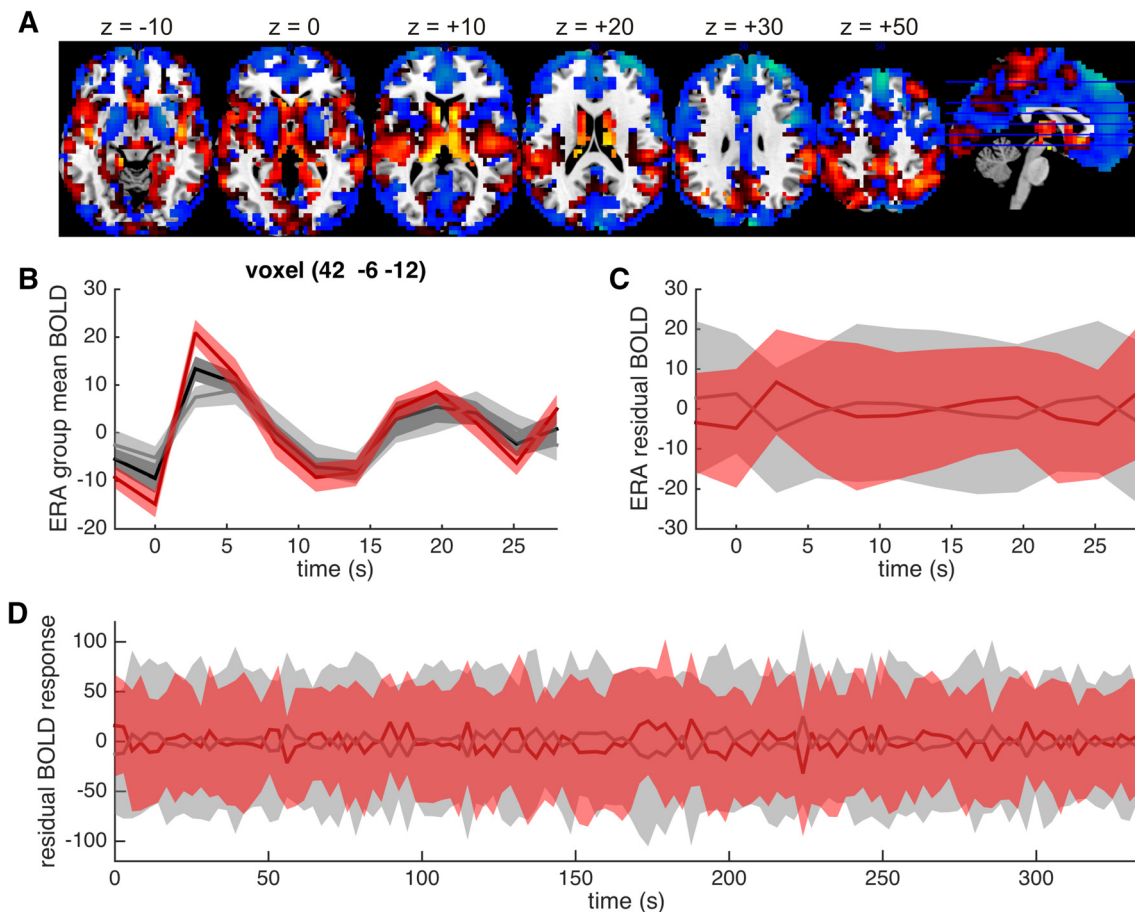


Fig. 5 In **a**, an overlay of functional brain mapping results on a template brain is displayed. It presents the resulting brain scores of the PLS temporal variability analysis method applied to the group-mean normalized data for the galvanic vestibular stimulation periods only, without threshold. In addition, an exemplary BOLD signal time series (**b**) and the variability (**c**) for a voxel in the posterior insula at MNI coordinate [42, -6, -12] are shown. This voxel contributes significantly and positively to the relation between variability and age. In **b**, the event-related average (ERA) group-mean time series (dark gray, shaded area SEM) is depicted, which displays a clear similarity to the “vestibular” ICs’ transient, event-like time course (for comparison see Fig. 2). The group-mean time series for young

participants (<50 years of age, red) and for old volunteers (≥ 50 years of age, light gray) present a similar event-related averaging increase or decrease relative to the overall mean, as suggested by the “vestibular” ICs. In **c**, the event-related average residual time series (after group-mean normalization) is shown separately for young and elderly (shaded area SD). The complete residual time series in **D** demonstrates that variability (shaded areas show SD over subjects) is larger for young than for elderly volunteers. As presented, this increase in variability occurs over the whole experiment, leading to an increased variability value over time for this voxel in older as compared to young volunteers. This effect, however, does not seem to be specific to GVS periods

showed a block-like, sustained temporal response characteristic associated with the constant stimulation of the skin during each block. These components were comprised predominantly of somatosensory areas. Thus, both networks overlapped but differed in their association with distinct phases of the time course governing network activation. The ICs constituting the multisensory vestibular network were bilateral, age correlated and associated with the rapid BOLD signal changes induced by switching of the stimulation currents to the states “on” and “off”. The age correlation was negative for the first six ICs, i.e. their relative weight decreased with age, indicating that the modulation of the “vestibular networks” by GVS declined with age. The ICs constituting the somatosensory network

showed a tonic time course and were divided into two components by lateralisation to the contralateral hemisphere; they were not age correlated. Since the “vestibular” and “somatosensory” networks partially overlapped in space, we defined them as multisensory, although they can be clearly separated by their distinct temporal characteristics; i.e. their event-like and block-like time courses, respectively.

Hence, age-related changes were found only in the “vestibular” network containing the superior, middle and inferior frontal and temporal gyri, the lingual gyrus, the insula, the superior and inferior parietal lobe, the parietal operculum, the posterior cingulate gyrus, the cuneus, the thalamus and the cerebellar tonsil. The “somatosensory

network” encompassed the middle and inferior frontal and temporal gyrus, the post- and precentral gyri, the lingual and fusiform gyrus, the paracentral lobule, the superior and inferior parietal lobe, the posterior insula, the cingulate gyrus and the thalamus.

The age dependency of the “vestibular” ICs was independent from anatomical changes: the decrease in fractional anisotropy demonstrated by DTI was global and not associated with any vestibular network in particular. No significant changes of fractional anisotropy associated with GVS current amplitude could be detected. This might be due to current amplitudes insufficiently reflecting vestibular perception in the group analysis. In this case, a measure of the intensity of perception might have revealed a possible correlation with anatomical measures. This has been shown previously in healthy individuals for an extensive white matter network that strongly correlated with a measure of vertigo perception (Nigmatullina et al. 2013) and an analogous approach might reveal similar correlations in future studies.

Changes in functional connectivity could also be due to changes in local gray matter volume or general vascular deterioration. In our study, voxel-based morphometry revealed an age-related decrease in volume in multiple anatomical areas bilaterally as has been previously described (Gonoi et al. 2010). Overlaps could be observed with all ICs of interest, whether age correlated or not. It is, therefore, unlikely that the age dependency of the vestibular networks could be solely attributed to the anatomical change in volume. Likewise, the decrease in fractional anisotropy with age was general and suggested that these changes were not due to age-related anatomical modifications. A simple motor paradigm (finger tapping) induced no age-related changes in functional connectivity, BOLD-signal amplitude or temporal variability. Thus, the age-dependent changes in functional connectivity appear to be particular to vestibular processing.

In the GVS experiment, we observed additional age-dependent modifications in temporal BOLD-signal variability, which have recently also been described in healthy volunteers (Garrett et al. 2010, 2011, 2013; Samanez-Larkin et al. 2010; Wutte et al. 2011). In our study, we specifically chose a task-free paradigm focusing on vestibular sensory perception and stimulated volunteers at low-level amplitudes. At this level, the level of perception could be assumed to be roughly matched among volunteers. Variability increased significantly with age in regions associated with the “vestibular” network (thalamus and posterior insula bilaterally), mostly during stimulation. Therefore, the spatial pattern of the variability associated with the vestibular network did coincide with the “mean signal”, i.e. the amplitudes of BOLD-signal responses. We added a motor experiment to control generalized changes

in temporal variability, connectivity or BOLD amplitude, allowing us to demonstrate age-related effects in our study that are specific to the vestibular system, and to distinguish them from generalized effects. Further studies should investigate the impact of task performance on the vestibular system, e.g. with a perceptual vestibular task. The rationale for this is that our findings here are for a vestibular sensory stimulation paradigm, which can be seen as roughly analogous in design to the first study of Garrett and co-authors (Garrett et al. 2010) which did not include task performance, and it would, therefore, be interesting to see if the inclusion of task performance in the study of aging effects might reveal a similar trend for the vestibular system as was found in the further studies of Garrett et al. (2011, 2013) that included task performance.

While the actual current intensity employed for GVS differed between individuals, the procedure to determine it strove to achieve a comparable intensity of perception. Notwithstanding, individually variable sensitivity to vestibular stimuli and different levels of pain tolerance may have affected standardization. However, behavioral data reported a brief vestibular sensation as opposed to an enduring somatosensory pain sensation, which corresponded to the analysis of time courses associated with the vestibular and somatosensory multimodal networks, respectively, and permitted us to distinguish between the two types of sensory input.

The observed age-dependent “vestibular” network cannot be attributed to the vestibular stimulation induced by the magnetic field of the MRI as recently described (Roberts et al. 2011). The magnetic field of the MRI is active also during rest periods. The main effect of magnetic vestibular stimulation (MVS) should thus be a constant activation level that is subtracted by filtering the removal of the mean signal over time and voxelwise variability normalization. Despite these common preprocessing steps, it is possible that the additivity principle of stimulus responses could be violated should the MVS effect be strong enough to cause non-linear effects like saturation to occur. However, inspecting the IC time courses and the event-related averages (ERA) plot amplitudes (see Figs. 2, 3), we conclude that this has not been the case. Furthermore, during the motor paradigm no vestibular activations could be observed with any of the analysis methods, therefore MVS should be considered negligible in our case.

Do the age-related changes reflect the aging of peripheral vestibular structures?

Peripheral vestibular structures such as hair cells, nerve fibers and otoconia have been demonstrated to decrease (Bergstrom 1973; Rosenhall 1973; Ross et al. 1976) and

Table 3 Significant increases in BOLD signal induced by GVS and detected by independent component and partial least squares (PLS) analysis

Voxels	Z MAX	MNI coordinates x, y, z (mm)	Anatomical location	BA
Independent component 2: positive clusters				
904	7.56	−58, −26, 8	Left primary auditory cortex TE1.0, secondary somatosensory cortex/parietal operculum OPI; superior temporal gyrus	
824	5.63	62, −26, 8	Right superior temporal gyrus	
341	4.3	6, −18, 0	Right thalamus	
277	4.04	−18, 54, 40	Left superior frontal gyrus	8
87	3.14	6, −82, 40	Right superior parietal lobule 7P, 7M, cuneus	19
35	2.65	2, −34, 20	Corpus callosum (posterior cingulum)	
19	2.54	46, −62, −56	Right cerebellar tonsil	
17	2.85	50, 10, 20	Right Broca's area, right inferior frontal gyrus	44
Independent component 2: negative clusters				
153	−4.29	10, 46, −20	Right medial frontal gyrus	
Independent component 3: positive clusters				
593	6.76	58, −22, 20	Right secondary somatosensory cortex/parietal operculum OP1, OP4, OP3; inferior parietal lobule PFop R, PFcm, PFT	
591	6.66	−54, −26, 16	Left secondary somatosensory cortex/parietal operculum OP1, OP4; inferior parietal lobule PFop, PFcm; primary auditory cortex TE1.0 L	40
228	3.48	2, −94, 0	Right visual cortex V1, V2, lingual gyrus	17, 18
119	3.28	−18, 46, 48	Left superior frontal gyrus	8
67	3.23	−50, −62, 8	Left visual cortex V5, inferior parietal lobule PGp, middle temporal gyrus	
54	3.03	18, 38, 56	Right superior frontal gyrus	
32	2.75	−26, −42, 80	Left primary somatosensory cortex, superior parietal lobule 5L, 7PC, 7A, primary motor cortex	1, 2, 3b, 4p, 4a
27	3.19	10, −14, −4	Right thalamic medial dorsal nucleus	
23	2.99	−10, −14, 0	Left thalamus	
Independent component 3: negative clusters				
897	−4.43	30, 34, 32	Right middle frontal gyrus	
598	−3.45	46, −78, −12	Right visual cortex V4, V3 V, fusiform gyrus	19
350	−2.99	−46, −86, −4	Left visual cortex V4, inferior occipital gyrus	
287	−4.79	66, −14, −12	Right middle temporal gyrus	21
261	−2.81	−38, 38, −28	Left middle frontal gyrus	
188	−3.53	−66, −18, −8	Left middle temporal gyrus	21
174	−3	−62, −6, 20	Left primary somatosensory cortex, secondary somatosensory cortex/parietal operculum OP4, Premotor cortex, inferior parietal lobule Pfop	3b, 1, 6, 44, 43
84	−2.94	58, 34, −8	Right Broca's area, inferior frontal gyrus	45
48	−2.57	−30, 34, 32	Left middle frontal gyrus	
24	−2.39	10, −42, 40	Right superior parietal lobule 5 Ci, 5 M, cingulate gyrus	31
20	−2.38	−18, 6, 52	Left premotor cortex, medial frontal gyrus	6
Independent component 9: positive clusters				
726	5.93	38, −18, 64	Right premotor cortex, primary motor cortex, primary somatosensory cortex	6, 4a, 3b
10	3.13	6, −22, 48	Right premotor cortex, primary motor cortex, superior parietal lobule 5 M, 5 Ci, paracentral lobule	6, 4a, 31
Independent component 9: negative clusters				
42	−4.42	−58, −22, 20	Left inferior parietal lobule PFop, PF; secondary somatosensory cortex/parietal operculum OPI, OP4	
Independent component 12: positive clusters				
1,353	6.63	−46, −34, 56	Left primary somatosensory cortex, inferior parietal lobule PF, PFT; superior parietal lobule 5L, 7PC;	2, 1, 3b, 40

Table 3 continued

Voxels	Z MAX	MNI coordinates x, y, z (mm)	Anatomical location	BA
Partial least-squared positive clusters (stimulus-phases only)				
42	0.0238	10, -14, 16	Right thalamic anterior nucleus	
26	0.0238	-10, -26, 12	Left hippocampal dentate gyrus, hippocampal cornu ammonis/posterior thalamus	
14	0.0246	-6, 10, 12	Left caput corpus caudatus	
8	0.0227	22, -38, 68	Right primary somatosensory cortex	3b, 1, 2, 4a
8	0.0237	42, -46, 36	Right anterior intra-parietal sulcus hIP1, hIP2; inferior parietal lobule Pga, supramarginal gyrus	
8	0.0201	-42, -6, -12	Left insula Id1, left temporal lobe	21
8	0.0237	42, -6, -12	Right insula Id, right temporal lobe	
7	0.0196	-38, 14, -24	Left inferior frontal gyrus	
5	0.0221	46, 6, -32	Right temporal pole; Middle temporal gyrus, anterior division	38
4	0.0199	34, -54, 48	Right anterior intra-parietal sulcus hIP3; hIP1; Superior parietal lobule 7A; anterior intra-parietal sulcus hIP2	
4	0.0178	54, -30, 28	Right inferior parietal lobule PFcm; PFop; PF; secondary somatosensory cortex/Parietal operculum OP1; Anterior intra-parietal sulcus hIP2	
4	0.0193	42, -18, 8	Right primary auditory cortex TE1.0; Insula Ig2; primary auditory cortex TE1.1; insula Ig1; Insula Id1	13
3	0.0193	18, -66, 60	Right superior parietal lobule 7P; 7A	7
Partial least-squared negative clusters (stimulus-phases only)				
44	-0.0258	2, 42, 52	Right superior frontal gyrus	
37	-0.0268	26, 54, 32	Right superior frontal gyrus	9
4	-0.0272	6, -94, 32	Right cuneus	
3	-0.0217	6, 58, 36	Right frontal pole; superior frontal gyrus	

All results are FWE corrected for false positives. Clusters containing more than 10 voxels are displayed, except for the PLS analysis where clusters of more than 3 voxels are displayed. Anatomical locations determined using the Juelich Histological Atlas, the Harvard-Oxford Cortical Structural Atlas and the Tailarach Demon Atlas as in the FSL Atlas toolbox

deteriorate with age as demonstrated by physiological testing (head thrust dynamic visual acuity testing, ocular and cervical vestibular evoked myogenic potentials) (Furman and Redfern 2001; Welgampola and Colebatch 2001; Agrawal et al. 2012). However, GVS is presumed to act directly on the vestibular nerve within the spike trigger zone (Goldberg et al. 1984; Fitzpatrick and Day 2004), bypassing the hair cells. The age-related changes in vestibular processing observed in our study are thus unlikely to be related to a loss of hair cells or otoconia, but could be associated with nerve fiber deterioration. Letting every volunteer choose their own amplitude assured a sufficiently perceptible stimulation in all subjects. If the number of nerve fibers decreases, the variability of the peripheral signal increases and could influence the BOLD-signal variability, possibly explaining why we found a stimulation-related increase in BOLD-signal variability in the thalamus and the posterior insula bilaterally, but not in the somatosensory areas. An increase in variability of the

vestibular sensory signal due to fiber loss should also affect the perceptual threshold (Cousins et al. 2013) and require an increase of GVS amplitude with age. Interestingly, this is in contrast to our behavioral data: volunteers' age did not correlate with self-chosen GVS amplitude. This might be due to amplitudes being individually very variable (range 1.25–2.75 mA), possibly masking age correlation. Alternatively, the elderly may rely more on multimodal mechanisms than the young (Mozolic et al. 2012), possibly causing a preservation of the threshold level with age despite a decline of unimodal pathways.

Differences between “vestibular” and “somatosensory” components

Previous studies suggest a common processing of somatosensory and vestibular sensations in the posterior insula (Penfield and Faulk 1955; Bottini et al. 1995, 2001; McGeoch et al. 2009; Baier et al. 2013; Ferre et al. 2012),

while others describe a functional vestibular network centered on the posterior insula and posterior parietal operculum (Eickhoff et al. 2006; zu Eulenburg et al. 2012). To our knowledge, age-related changes of functional connectivity have neither been described in the vestibular nor the somatosensory system. In the present study, the GVS-induced brain activity displayed no age-dependent changes in the somatosensory network, but revealed an age-dependent decrease in functional connectivity for the cerebral processing of vestibular information. The vestibular and the somatosensory systems give rise to partly overlapping cerebral networks. Compared to the processing of the vestibular network, however, somatosensory processing is mostly unimodal, while the vestibular network constantly integrates information from multiple sensory systems, i.e. visual, vestibular, and somatosensory input, besides enabling transfer from sensory input to motor reactions. Inhibitory reciprocal interaction between sensory systems deteriorates in old age (Zwergal et al. 2012) and with age, sensorimotor integration may affect the BOLD signal (Stefanova et al. 2013). The impaired inter-system inhibition may explain why functional connectivity in the vestibular system decreases with age: due to decreasing functional specificity, visual and other competing inputs are less inhibited and interfere with the vestibular information processing (Mozolic et al. 2012; Roski et al. 2014). Thus, vestibular activations and equivalent information from other sensory systems spread and may cause interference among the different sensory systems. The lack of inhibition may thereby increase the complexity of integration and cause a decrease in functional connectivity with age.

Likewise, the increased variability of the BOLD signal in the thalamus and posterior insula might be due to impaired inhibition. Changes in variability have previously been observed during visual fixation tasks (Garrett et al. 2010). BOLD variability could be attributed to various reasons ranging from sensory or internal neural noise (Faisal et al. 2008), over intrinsic brain activity such as the correlated fluctuations in resting state experiments (Birn 2012) to unaccounted for sensory input. We removed stimulus-related responses common to all subjects by group-mean regression, which accounts better for transient BOLD signal changes than the block normalization used by others (Garrett et al. 2010). In our study, modifications appear to be stimulation-specific considering that age-dependent variability increased significantly only during the GVS paradigm, but not during finger tapping.

In conclusion, we demonstrated a decrease in functional connectivity related to processing of GVS and restricted to the vestibular cortical network. The decrease in functional connectivity was not due to structural changes of the associated brain areas but to a decrease in response

amplitude undetected by GLM analysis. In parallel, we discovered an increase in the temporal variability of the BOLD signal in central areas of this vestibular network, which was predominantly linked to periods of stimulation, but without strongly reflecting stimulus-related aspects of the BOLD response. An increase in temporal BOLD-signal variability due to propagation of stimulus-induced sensory noise is possible, but does not fit in with the observed preservation of GVS current amplitudes over age and cannot explain changes in functional connectivity. Considering all these lines of evidence, another more likely reason for our results would be the deterioration of reciprocal cortico-cortical inhibition with age already observed in other studies (Zwergal et al. 2012; Stefanova et al. 2013), which might cause both the decrease in functional connectivity and the increase in variability observed in the current study.

Acknowledgments The authors are grateful for their support to the Bundesministerium für Bildung und Forschung (Grant Number BMBF—FKZ 01 E0 0901 and BMBFGrant—01GG0440 (BCCN)) and the Deutsche Stiftung Neurologie. The authors would like to thank the anonymous reviewers for their valuable comments and suggestions to improve the manuscript.

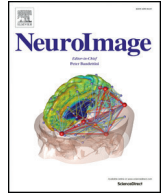
Conflict of interest The authors declare no competing financial interests.

References

- Agrawal Y, Zuniga MG, Davalos-Bichara M, Schubert MC, Walston JD, Hughes J, Carey JP (2012) Decline in semicircular canal and otolith function with age. *Otol Neurotol* 33:832–839
- Aizenstein HJ, Clark KA, Butters MA, Cochran J, Stenger VA, Meltzer CC, Reynolds CF, Carter CS (2004) The BOLD hemodynamic response in healthy aging. *J Cogn Neurosci* 16:786–793
- Allen EA et al (2011) A baseline for the multivariate comparison of resting-state networks. *Front Syst Neurosci* 5:2
- Andersson JLR, Jenkinson M, Smith S (2007a) Non-linear optimisation. In: FMRIB technical report TR07JA1 <http://www.fmrib.ox.ac.uk/analysis/techrep>. Accessed Jan 2013
- Andersson JLR, Jenkinson M, Smith S (2007b) Non-linear registration, aka Spatial normalisation. In: FMRIB technical report TR07JA2. <http://www.fmrib.ox.ac.uk/analysis/techrep>. Accessed Jan 2013
- Angelaki DE, Cullen KE (2008) Vestibular system: the many facets of a multimodal sense. *Annu Rev Neurosci* 31:125–150
- Ashburner J (2007) A fast diffeomorphic image registration algorithm. *Neuroimage* 38(1):95–113
- Ashburner J, Friston KJ (2000) Voxel-based morphometry—the methods. *Neuroimage* 11:805–821
- Ashburner J, Friston KJ (2005) Unified segmentation. *Neuroimage* 26:839–851
- Baier B, Zu Eulenburg P, Best C, Geber C, Müller Forell W, Birklein F, Dieterich M (2013) Posterior insular cortex—a site of vestibular-somatosensory interaction? *Brain Behav* 3(5): 519–524
- Barin K, Dodson EE (2011) Dizziness in the elderly. *Otolaryngol Clin North Am* 44:437–454, x

- Beckmann CF, C.E.M., Filippini N, Smith SM (2009) Group comparison of resting-state fMRI data using multi subject ICA and dual regression. In: Proceedings of HBM Vol. San Francisco
- Beckmann CF, Smith SM (2004) Probabilistic independent component analysis for functional magnetic resonance imaging. *IEEE Trans Med Imaging* 23:137–152
- Beckmann CF, Smith SM (2005) Tensorial extensions of independent component analysis for multisubject fMRI analysis. *Neuroimage* 25:294–311
- Beckmann C, Woolrich M, and Smith SM (2003) Gaussian/Gamma mixture modelling of ICA/GLM spatial maps. In: Ninth International Conference on Functional Mapping of the Human Brain
- Behrens TE, Woolrich MW, Jenkinson M, Johansen-Berg H, Nunes RG, Clare S, Matthews PM, Brady JM, Smith SM (2003) Characterization and propagation of uncertainty in diffusion-weighted MR imaging. *Magn Reson Med* 50:1077–1088
- Bense S, Stephan T, Yousry TA, Brandt T, Dieterich M (2001) Multisensory cortical signal increases and decreases during vestibular galvanic stimulation (fMRI). *J Neurophysiol* 85:886–899
- Bergstrom B (1973) Morphology of the vestibular nerve. II. The number of myelinated vestibular nerve fibers in man at various ages. *Acta Otolaryngol* 76:173–179
- Birn RM (2012) The role of physiological noise in resting-state functional connectivity. *Neuroimage* 62:864–870
- Biswal BB et al (2010) Toward discovery science of human brain function. *Proc Natl Acad Sci USA* 107:4734–4739
- Bottini G, Paulesu E, Sterzi R, Warburton E, Wise RJ, Vallar G, Frith CD (1995) Modulation of conscious experience by peripheral sensory stimuli. *Nature* 376:778–781
- Bottini G, Karnath HO, Vallar G, Sterzi R, Frith CD, Frackowiak RS, Paulesu E (2001) Cerebral representations for egocentric space: functional-anatomical evidence from caloric vestibular stimulation and neck vibration. *Brain* 124:1182–1196
- Brandt T, Dieterich M (1999) The vestibular cortex. Its locations, functions, and disorders. *Ann N Y Acad Sci* 871:293–312
- Cabeza R, Anderson ND, Locantore JK, McIntosh AR (2002) Aging gracefully: compensatory brain activity in high-performing older adults. *Neuroimage* 17(3):1394–1402
- Cousins SKD, Cutfield N, Seemungal B, Golding JF, Gresty M, Glasauer S, Bronstein AM (2013) Vestibular perception following acute unilateral vestibular lesions. *PLoS One* 8(5):e61862
- Dieterich M, Brandt T (2008) Functional brain imaging of peripheral and central vestibular disorders. *Brain* 131:2538–2552
- Eickhoff SB, Weiss PH, Amunts K, Fink GR, Zilles K (2006) Identifying human parieto-insular vestibular cortex using fMRI and cytoarchitectonic mapping. *Hum Brain Mapp* 27:611–621
- Faisal AA, Selen LP, Wolpert DM (2008) Noise in the nervous system. *Nat Rev Neurosci* 9:292–303
- Ferre ER, Bottini G, Haggard P (2012) Vestibular inputs modulate somatosensory cortical processing. *Brain Struct Funct* 217(4):859–864 (Epub 2012 Apr 1)
- Filippini N, MacIntosh BJ, Hough MG, Goodwin GM, Frisoni GB, Smith SM, Matthews PM, Beckmann CF, Mackay CE (2009) Distinct patterns of brain activity in young carriers of the APOE-epsilon4 allele. *Proc Natl Acad Sci USA* 106:7209–7214
- Fitzpatrick RC, Day BL (2004) Probing the human vestibular system with galvanic stimulation. *J Appl Physiol* 96:2301–2316
- Fox MD, Raichle ME (2007) Spontaneous fluctuations in brain activity observed with functional magnetic resonance imaging. *Nat Rev Neurosci* 8:700–711
- Frison L, Pocock SJ (1992) Repeated measures in clinical trials: analysis using mean summary statistics and its implications for design. *Stat Med* 11:1685–1704
- Furman JM, Redfern MS (2001) Effect of aging on the otolith-ocular reflex. *J Vestib Res* 11:91–103
- Garrett DD, Kovacevic N, McIntosh AR, Grady CL (2010) Blood oxygen level-dependent signal variability is more than just noise. *J Neurosci* 30:4914–4921
- Garrett DD, Kovacevic N, McIntosh AR, Grady CL (2011) The importance of being variable. *J Neurosci* 31(12):4496–4503
- Garrett DD, Kovacevic N, McIntosh AR, Grady CL (2013) The modulation of BOLD variability between cognitive states Vvries by age and processing speed. *Cereb Cortex* 23(3):684–693
- Goldberg JM, Smith CE, Fernandez C (1984) Relation between discharge regularity and responses to externally applied galvanic currents in vestibular nerve afferents of the squirrel monkey. *J Neurophysiol* 51:1236–1256
- Gonoi W, Abe O, Yamasue H, Yamada H, Masutani Y, Takao H, Kasai K, Aoki S, Ohtomo K (2010) Age-related changes in regional brain volume evaluated by atlas-based method. *Neuroradiology* 52:865–873
- Good CD, Johnsrude IS, Ashburner J, Henson RN, Friston KJ, Frackowiak RS (2001) A voxel-based morphometric study of ageing in 465 normal adult human brains. *Neuroimage* 14:21–36
- Grady CL, Garrett DD (2014) Understanding variability in the BOLD signal and why it matters for aging. *Brain Imaging Behav* 2:274–283
- Grady CL, Protzner AB, Kovacevic N, Strother SC, Afshin-Pour B, Wojtowicz M, Anderson JA, Churchill N, McIntosh AR (2010) A multivariate analysis of age-related differences in default mode and task-positive networks across multiple cognitive domains. *Cereb Cortex* 20(6):1432–1447
- Halmagyi GM (2005) Diagnosis and management of vertigo. *Clin Med* 5:159–165
- Halmagyi GM, Curthoys IS (1988) A clinical sign of canal paresis. *Arch Neurol* 45(7):737–739
- Jahn K, Naessl A, Schneider E, Strupp M, Brandt T, Dieterich M (2003) Inverse U-shaped curve for age dependency of torsional eye movement responses to galvanic vestibular stimulation. *Brain* 126:1579–1589
- Lobel E, Kleinschmidt JF, Bihan DL, Leroy-Willig A, Berthoz A (1998) Functional MRI of galvanic vestibular stimulation. *J Neurophysiol* 80:2699–2709
- Lopez C, Blanke O, Mast FW (2012) The human vestibular cortex revealed by coordinate-based activation likelihood estimation meta-analysis. *Neuroscience* 212:159–179
- Madhyastha TM, Grabowski TJ (2014) Age-related differences in the dynamic architecture of intrinsic networks. *Brain Connect* 4(4):231–241
- McGeoch PD, Williams LE, Song T, Lee RR, Huang M, Ramachandran VS (2009) Post-stroke tactile allodynia and its modulation by vestibular stimulation: a MEG case study. *Acta Neurol Scand* 119:404–409
- McIntosh AR, Bookstein FL, Haxby JV, Grady CL (1996) Spatial pattern analysis of functional brain images using partial least squares. *Neuroimage* 3:143–157
- Meier TB, Desphande AS, Vergun S, Nair VA, Song J, Biswal BB, Meyerand ME, Birn RM, Prabhakaran V (2012) Support vector machine classification and characterization of age-related reorganization of functional brain networks. *Neuroimage* 60:601–613
- Minka T (2000) Automatic choice of dimensionality for PCA. In: Technical Report 514: MIT Media Lab Vision and Modeling Group
- Mozolic J, Hugenschmidt C, Peiffer A, Laurienti P (2012) Multisensory Integration and Aging. In: Murray M, Wallace M (eds) *The Neural Bases of Multisensory Processes*. CRC Press, Boca Raton, pp 381–392
- Nasreddine ZS, Phillips NA, Bedirian V, Charbonneau S, Whitehead V, Collin I, Cummings JL, Chertkow H (2005) The Montreal Cognitive Assessment, MoCA: a brief screening tool for mild cognitive impairment. *J Am Geriatr Soc* 53:695–699

- Nichols TE, Holmes AP (2002) Nonparametric permutation tests for functional neuroimaging: a primer with examples. *Hum Brain Mapp* 15:1–25
- Nigmatullina Y1, Hellyer PJ, Nachev P, Sharp DJ, Seemungal BM (2013) The Neuroanatomical Correlates of Training-Related Perceptuo-Reflex Uncoupling in Dancers. *Cereb Cortex* (Epub ahead of print)
- Penfield W, Faulk ME Jr (1955) The insula; further observations on its function. *Brain* 78:445–470
- Roberts DC, Marcelli V, Gillen JS, Carey JP, Della Santina CC, Zee DS (2011) MRI magnetic field stimulates rotational sensors of the brain. *Curr Biol* 21:1635–1640
- Rosenhall U (1973) Degenerative patterns in the aging human vestibular neuro-epithelia. *Acta oto-laryngol* 76:208–220
- Roski C, Caspers S, Lux S, Hoffstaedter F, Bergs R, Amunts K, Eickhoff SB (2014) Activation shift in elderly subjects across functional systems: an fMRI study. *Brain Struct Funct* 219(2):707–718
- Ross MD, Peacor D, Johnsson LG, Allard LF (1976) Observations on normal and degenerating human otoconia. *Ann Otol Rhinol Laryngol* 85:310–326
- Rueckert D, Sonoda LI, Hayes C, Hill DL, Leach MO, Hawkes DJ (1999) Nonrigid registration using free-form deformations: application to breast MR images. *IEEE Trans Med Imaging* 18:712–721
- Salmaso D, Longoni AM (1985) Problems in the assessment of hand preference. *Cortex* 21:533–549
- Samanez-Larkin GR, Kuhnen CM, Yoo DJ, Knutson B (2010) Variability in nucleus accumbens activity mediates age-related suboptimal financial risk taking. *J Neurosci* 30:1426–1434
- Schlundwein P, Mueller M, Bauermann T, Brandt T, Stoeter P, Dieterich M (2008) Cortical representation of saccular vestibular stimulation: VEMPs in fMRI. *Neuroimage* 39:19–31
- Schneider E, Glasauer S, Dieterich M (2002) Comparison of human ocular torsion patterns during natural and galvanic vestibular stimulation. *J Neurophysiol* 87:2064–2073
- Smith SM (2002) Fast robust automated brain extraction. *Hum Brain Mapp* 17:143–155
- Smith SM, Nichols TE (2009) Threshold-free cluster enhancement: addressing problems of smoothing, threshold dependence and localisation in cluster inference. *Neuroimage* 44:83–98
- Smith SM, Jenkinson M, Woolrich MW, Beckmann CF, Behrens TE, Johansen-Berg H, Bannister PR, De Luca M, Drobnjak I, Flitney DE, Niazy RK, Saunders J, Vickers J, Zhang Y, De Stefano N, Brady JM, Matthews PM (2004) Advances in functional and structural MR image analysis and implementation as FSL. *Neuroimage* 23(Suppl 1):S208–S219
- Smith SM, Jenkinson M, Johansen-Berg H, Rueckert D, Nichols TE, Mackay CE, Watkins KE, Ciccarelli O, Cader MZ, Matthews PM, Behrens TE (2006) Tract-based spatial statistics: voxelwise analysis of multi-subject diffusion data. *Neuroimage* 31:1487–1505
- Smith SM, Johansen-Berg H, Jenkinson M, Rueckert D, Nichols TE, Miller KL, Robson MD, Jones DK, Klein JC, Bartsch AJ, Behrens TE (2007) Acquisition and voxelwise analysis of multi-subject diffusion data with tract-based spatial statistics. *Nat Protoc* 2:499–503
- Stefanova I, Stephan T, Becker-Bense S, Dera T, Brandt T, Dieterich M (2013) Age-related changes of blood-oxygen-level-dependent signal dynamics during optokinetic stimulation. *Neurobiol Aging* 34(10):2277–2286 (Epub 2013 Apr 28)
- Stephan T, Deutschlander A, Nolte A, Schneider E, Wiesmann M, Brandt T, Dieterich M (2005) Functional MRI of galvanic vestibular stimulation with alternating currents at different frequencies. *Neuroimage* 26:721–732
- Stephan T, Hüfner K, Brandt T (2009) Stimulus profile and modeling of continuous galvanic vestibular stimulation in functional magnetic resonance imaging. *Ann N Y Acad Sci* 1164:472–475
- Sturnieks DL, St George R, Lord SR (2008) Balance disorders in the elderly. *Neurophysiol Clin* 38:467–478
- Tzourio-Mazoyer N, Landeau B, Papathanassiou D, Crivello F, Etard O, Delcroix N, Mazoyer B, Joliot M (2002) Automated anatomical labeling of activations in SPM using a macroscopic anatomical parcellation of the MNI MRI single-subject brain. *Neuroimage* 15:273–289
- Welgampola MS, Colebatch JG (2001) Vestibulocollic reflexes: normal values and the effect of age. *Clin Neurophysiol* 112:1971–1979
- Woods RP (1996) Modeling for intergroup comparisons of imaging data. *Neuroimage* 4:S84–S94
- Wutte MG, Smith MT, Flanagan VL, Wolbers T (2011) Physiological Signal Variability in hMT+ Reflects Performance on a Direction Discrimination Task. *Front Psychol* 2:185
- zu Eulenburg P, Caspers S, Roski C, Eickhoff SB (2012) Meta-analytical definition and functional connectivity of the human vestibular cortex. *Neuroimage* 60:162–169
- Zwergal A, Linn J, Xiong G, Brandt T, Strupp M, Jahn K (2012) Aging of human supraspinal locomotor and postural control in fMRI. *Neurobiol Aging* 33:1073–1084



Full length articles

Magnetic vestibular stimulation modulates default mode network fluctuations



Rainer Boegle^{a,b,*}, Thomas Stephan^{a,b,c}, Matthias Ertl^{b,c}, Stefan Glasauer^{a,b,d}, Marianne Dieterich^{a,b,c,e}

^a German Center for Vertigo and Balance Disorders (DSGZ-IFB^{LMU}), Ludwig-Maximilians-University Munich, Germany

^b Graduate School of Systemic Neurosciences, Ludwig-Maximilians-University Munich, Germany

^c Department of Neurology, Ludwig-Maximilians-University Munich, Germany

^d Center for Sensorimotor Research, Ludwig-Maximilians-University Munich, Germany

^e SyNergy: Cluster for Systems Neurology, Munich, Germany

ARTICLE INFO

Article history:

Received 14 August 2015

Accepted 25 November 2015

Available online 5 December 2015

Keywords:

Magnetic vestibular stimulation

Vestibular imbalance

Resting-state networks

Resting-state fMRI

ABSTRACT

Strong magnetic fields (> 1 Tesla) can cause dizziness and it was recently shown that healthy subjects (resting in total darkness) developed a persistent nystagmus even when remaining completely motionless within a MR tomograph. Consequently, it was speculated that this magnetic vestibular stimulation (MVS) might influence fMRI results, as nystagmus is indicative of an imbalance in the vestibular system, potentially influencing other systems via multisensory vestibular interactions. The objective of our study was to investigate whether MVS does indeed modulate BOLD signal fluctuations. We recorded eye movements, as well as, resting-state fMRI of 30 volunteers in darkness at 1.5 T and 3.0 T to answer the question whether MVS modulated parts of the default mode resting-state network (DMN) in accordance with the Lorentz-force model for MVS, while distinguishing this from the known signal increase due to field strength related imaging effects. Our results showed that modulation of the default mode network occurred mainly in areas associated with vestibular and ocular motor function, and was in accordance with the Lorentz-force model, i.e., double than the expected signal scaling due to field strength alone. We discuss the implications of our findings for the interpretation of studies using resting-state fMRI, especially those concerning vestibular research. We conclude that MVS needs to be considered in vestibular research to avoid biased results, but it might also offer the possibility of manipulating network dynamics and may thus help in studying the brain as a dynamical system.

© 2015 Elsevier Inc. All rights reserved.

Introduction

Our sense of motion and orientation in space as well as stable visual perception is achieved by the vestibular system engaged in integration of information coming not only from the peripheral vestibular end-organs, but also from visual, proprioceptive and other sensory systems (Cullen and Sadeghi, 2008). Vertigo and dizziness may occur if these multisensory interactions are disturbed (Brandt et al., 2004; Dieterich and Brandt, 2008).

Dizziness in the presence of strong magnetic fields has been noticed ever since the first magnetic resonance experiments at high field

strengths (> 1 Tesla) have been conducted (Schenck, 1992). Recently, Roberts et al. (2011) showed that healthy subjects exposed to the static magnetic field of a MR machine in total darkness developed a persistent nystagmus, while patients with bilateral peripheral vestibular failure did not show any nystagmus. The authors argued that ionic currents coming from hair cells in the inner ear are diverted by a Lorentz-force. This creates pressure onto the cupula, “the rotatory motion sensor” of the inner ear, leading to nystagmus akin to a constant (accelerating) rotatory stimulation. This also explained why the nystagmus' slow phase velocity (SPV) depends on the subject's head orientation in the magnetic field. This model was further supported by various studies. A simulation study regarding the magneto-hydrodynamic forces acting on the cupula showed that the expected Lorentz-force is strong enough to cause nystagmus (Antunes et al., 2012). A study of patients with unilateral labyrinthine disorders showed that the nystagmus direction is dependent on the interaction of signals from the semicircular canals from both ears, further supporting the idea that the labyrinth is the part of the inner ear that is mainly affected by the magnetic field (Ward et al., 2014). Another study using healthy subjects showed that the temporal dynamics of the nystagmus' SPV are similar to those known from rotational stimulation or caloric irrigation studies (Glover

Abbreviations: MVS, magnetic vestibular stimulation; fMRI, functional magnetic resonance imaging; DMN, default mode resting-state network; BOLD, blood oxygen level-dependent; SPV, slow phase velocity; ICA, independent component analysis; IC, independent component; CSF, cerebrospinal fluid; AAL, automated anatomical labeling; ROI, region of interest.

* Corresponding author at: German Center for Vertigo and Balance Disorders (DSGZ-IFB^{LMU}), Ludwig-Maximilians-University Munich, Germany Klinikum Grosshadern der Universitaet Muenchen, Feodor-Lynen-Strasse 19, 81377 Munich, Germany.

E-mail address: Rainer.Boegle@googlemail.com (R. Boegle).

et al., 2014). Analogous behavioral effects were reported for animals (for review see: Saunders, 2005; Ward et al., 2015).

Consequently, it was speculated that this magnetic vestibular stimulation (MVS) might influence fMRI results (Roberts et al., 2011), as nystagmus is indicative of an imbalance in the vestibular system, potentially influencing also other systems via multisensory vestibular interactions.

The focus of the current study was to investigate whether MVS does indeed modulate BOLD signal fluctuations. We recorded spontaneous eye movements, as well as, resting-state fMRI of 30 healthy volunteers in darkness at 1.5 T and 3.0 T, focusing here on the question whether MVS disproportionately influences parts of the default mode resting-state network (DMN) (Raichle et al., 2001; Raichle and Snyder, 2007; Buckner et al., 2008). The DMN has been shown as a major network that is influenced in patients suffering from unilateral vestibular neuritis (Klingner et al., 2014), a disease which is marked by vestibular imbalance and a horizontal nystagmus that is similar to the horizontal nystagmus produced by MVS. Other recent studies comparing resting-state activity in patients with vestibular deficits to that of healthy controls showed widespread changes in various networks, also including the DMN (Göttlich et al., 2014; Klingner et al., 2014; Helmchen et al., 2014). Focusing on the DMN also serves as a demonstration of MVS influencing a network associated with higher cognitive functions. The role of the DMN for higher cognitive function and the interaction of the vestibular system with higher cognitive function, especially the impact of vestibular imbalance on cognitive disorders were discussed recently (Hanes and McCollum, 2006; Schilbach et al., 2008; Smith and Zheng, 2013; Mast et al., 2014).

Our hypothesis was that (i) the “unmodulated” parts of the DMN should scale in accordance with the well-known sublinear increase of fMRI signal between field strength (Triantafyllou et al., 2005; Duyn, 2012), when no additional neural effect related to field strength was present, i.e., MVS was not present. In contrast, (ii) the MVS “modulated” parts should scale more strongly (twice as much as the “unmodulated” parts), i.e., directly with the field strength in accordance with the proposed Lorentz-force model which is linear (Roberts et al., 2011). A comparison of the scaling of the resting-state fluctuations between field strength consequently uncovers if fluctuations were indeed modified as expected from MVS. To verify that MVS was present and scales linear as predicted from the Lorentz-force model, analyses of eye movements were done. This linear increase with field strength is essential as it should translate into the scaling of the resting-state fluctuations.

Methods

Overview: assumptions and reasons for the choice of methods

Spontaneous eye movements as well as resting-state fMRI in darkness were recorded in a group of healthy subjects ($N = 30$, 19 females) at field strengths of 1.5 T and 3.0 T.

The different field strengths were used to create conditions in which a possible MVS modulation of a network could be determined between the two field strengths. We verified that MVS was present by analyzing eye movements, and by analyzing resting-state fluctuations we revealed the modulatory influence of MVS on the DMN. The MVS effect is always present as long as a subject is in the magnetic field of a MR tomograph and cannot be switch “on” and “off” within an imaging run. We used a form of group independent component analysis (Beckmann and Smith, 2004) and dual regression (Beckmann et al., 2009; Filippini et al., 2009) to separate the DMN from other networks and other structured responses (artifacts) like cerebrospinal fluid (CSF) or white matter fluctuations.

It should be noted that many possible differences might exist between resting-state fluctuations recorded at two different field strengths (between two MR tomograph sites). A simple analysis for (any) statistically significant differences might therefore be misleading

or biased. The situation is further complicated because fMRI does not provide an absolute measure of activity.

However, the scaling of MVS is predicted to be linear with field strength, according to the Lorentz-model (Roberts et al., 2011) and should carry over to the scaling of the resting-state fluctuations that are related to MVS which is essential for our analysis. We therefore sought for a comparison of the scaling of the resting-state amplitude fluctuations between field strength for revealing modulations due to MVS. More specifically, we make a point-value prediction for the scaling value (of resting-state fluctuations) for areas that are influenced by MVS, based on the Lorentz-model for MVS (Roberts et al., 2011) and the known scaling of BOLD-signals as described in the literature (Triantafyllou et al., 2005; Duyn, 2012). We considered only those areas influenced by MVS that do not violate this prediction.

Our hypothesis for MVS modulation can be seen as predicting the overall scaling Λ of measured DMN amplitudes that occurs in the presence of MVS due to the change in field strength. This is the combined effect of the MVS scaling of the neuronal activity λ_{neural} (translated into blood flow effects, but independent of the imaging procedure) and the scaling of the BOLD-signal λ_{BOLD} from one MR tomograph to the other. We assume that the neuronal activity scaling can be determined from the scaling of eye movements and should be linear in B_0 , given that the Lorentz-force is linear in B_0 (Roberts et al., 2011), where B_0 denotes the magnetic field strength of the MRI. Therefore, $\lambda_{neural} = 3 \text{ T} / 1.5 \text{ T} = 2$ which we verified by analyzing the eye movements. The scaling of the BOLD-signal is taken from the literature (Triantafyllou et al., 2005; Duyn, 2012) and is sublinear in B_0 . More precisely, fMRI signal fluctuations should increase with $\sqrt{B_0}$, if only imaging constants and noise effects are affected by the magnetic field (Triantafyllou et al., 2005; Duyn, 2012). Therefore, $\lambda_{BOLD} = \sqrt{2} = \sqrt{3 \text{ T} / 1.5 \text{ T}}$. It is important to note that the BOLD-signal is an epiphenomenon of the neuronal effect and therefore the overall scaling Λ results from the composite of the neural scaling and the BOLD-scaling, i.e., the product $\Lambda = \lambda_{neural}\lambda_{BOLD} = 2\sqrt{2} = 3 \text{ T} / 1.5 \text{ T} \sqrt{3 \text{ T} / 1.5 \text{ T}}$.

Thus, we need to distinguish between two possible values for the scaling factor Λ relating resting-state fluctuations between field strengths. If no additional MVS modulation was present (approximately constant neuronal effect, $\lambda_{neural} \approx 1$) then Λ should be equal to $\Lambda = \lambda_{BOLD} = \sqrt{2}$. In the case of an additional MVS modulation Λ should be equal to $\Lambda = \lambda_{neural}\lambda_{BOLD} = 2\sqrt{2}$, if the Lorentz-force model is indeed correct. We will only consider those areas as modulated by MVS that follow $\Lambda \approx 2\sqrt{2}$ and consider that other values might be due to variability (session by session influences, CSF fluctuations or bias due to imaging system) or due to deviations from the assumptions in the prediction of the scaling values which should be investigated further in future studies.

Subjects

Thirty healthy volunteers (19 females) were recruited by ads on internet forums and email alert of the Ludwig-Maximilians-University, as well as word-of-mouth. The ethics committee of the medical faculty of the Ludwig-Maximilians-University approved the investigation. All subjects gave their written informed consent. Due to the reasons stated below 27 of these 30 subjects (19 females) were included in the final analysis.

None of the subjects had a known history of vestibular, psychiatric or neurological deficits. Furthermore, we recorded eye movements in total darkness also outside the MRI (see the section ‘Examination protocol’ below) as a control. For the 3.0 Tesla MRI, where the bed could be uncoupled from the MRI and moved outside the Faraday cage, no abnormal eye movements were observed for any of the included volunteers, suggesting that they had no vestibular imbalance or deficit. One volunteer did not partake (on own accord) in the second session, i.e., in the

other MRI after feeling unwell during the first session (MRI) and the complete data set was excluded from analysis. Two volunteers had to be excluded due to strong motion artifacts in one of the two MRI sessions, leaving 27 complete data sets from both MRI sessions for analysis of resting-state fluctuations and scaling relationships.

Behavioral experiments

Eye movement recording setup

The spontaneous eye movements of all subjects were recorded by 3D video-oculography (VOG), using an analog MR-compatible infrared camera (MRC Systems GmbH, Heidelberg, Germany) that was mounted on goggles to make the camera setup head-fixed. We applied artificial pigment markers on the sclera to be able to detect torsional eye movements (Schneider et al., 2002; Dera et al., 2006). The markers consist of an infrared-absorbing cosmetic pigment applied to the sclera by means of a sterile surgical pen (Schneider et al., 2002). EyeSeeCam software (www.eyesecam.com) was used for real-time image processing and recording of VOG data at a sampling frequency of 60 Hz. For transformation of the eye movement data into degrees of horizontal and vertical axes, a 5-point calibration was performed at the beginning of the recording. The 5-point calibration pattern, a central point and 4 lateral points in the horizontal and vertical axes with a distance between the points of 8.5°, was put on the ceiling directly above the MRI table, such that calibration could be done before entering the bore while lying supine with the head flat on the MRI bed. During calibration, subjects repeatedly fixated a sequence of given gaze directions. The pigment markers on the sclera were selected after calibration in the EyeSeeCam software manually once and are then tracked automatically while the software determines the 3D orientation of the eye (Dera et al., 2006). If the camera was moved, calibration and selection of the pigment markers on the sclera were repeated.

Examination protocol

We measured spontaneous eye movements in four different head positions. These ranged from (P1) subjects' having their head lifted upward resting on a cushion, bringing their jaw close to their chest, i.e., "chin down" position, (P2) the head placed in the head coil (this position was used for resting-state imaging), i.e., slightly lifted, (P3) the head lying flat on the bed of the MRI (also used for calibration of the EyeSeeCam software) and (P4) the head overstretched backwards similar to "looking above oneself" or "chin up" with a supportive cushion-roll under the neck. We recorded the head position by marking a line with a makeup-marker pen from the canthus (corner of the eye) to the tragus of the ear (fleshy prominent bulge at the front of the external opening of the ear canal) and measuring the angle of this line relative to a pendulum indicating gravity, i.e., the vertical line. Eye tracking measurements were done inside the MRI and outside of the MRI to control for spontaneous eye movements that might occur without the presence of a magnetic field.

The outside measurements were done outside of the Faraday cage at the 3.0 T MRI (here the bed was uncoupled from MRI) and at the 1.5 T MRI the outside measurements were done outside of the MRI bore with the MRI bed in the most outward and downward position, because the bed could not be uncoupled from the 1.5 T MRI. In the case of the 3.0 T MRI where the table could be undocked from the MRI and moved outside of the Faraday-cage, the field can be expected to be near the strength of the earth's magnetic field ($\leq 10^{-4}$ T) and the safety regulations for the 1.5 T MRI state that the fringe field (with the bed fully outside the MRI bore) should be ≤ 0.1 T.

Analysis of eye movement data

Analysis of eye movement data was done in MATLAB (MathWorks, Inc., Natick, MA, USA) with EyeSeeCam® scripts and self-written functions, in analogy to Roberts et al. (2011). Saccades (quick phases of nystagmus) were detected in the eye-tracking data and a linear fit of the

tracking data in-between the two saccades was done to determine the slow phase velocity as the trend between each two saccades. We calculated the median slow phase velocity for each subject in each head position from all linear fit slopes between each consecutive pair of detected saccades.

We assessed the scaling of the spontaneous eye movements between field strength by fitting the median slow phase velocities over all four head positions per subject with a linear model for the head angles, resulting in a beta-value per subject and field strength, i.e., a trend of the SPVs. This trend is therefore "independent" of a specific head position or the maximum angle that is covered between the most extreme head positions and dependent on the field strength only. The fraction of these beta-values per subject between field strengths of 3.0 T and 1.5 T is defined as the scaling parameter $\lambda = \text{beta}_{3T}/\text{beta}_{1.5T}$, i.e., signifying, per subject, how the effect scales between field strength. Determining the median of the scaling value λ over the whole group of subjects is an estimate of the scaling of MVS between field strengths of 1.5 T and 3 T and is ideally expected to have a value of 2 (see Methods section 'Overview: assumptions and reasons for the choice of methods' and Results section 'Behavioral results').

MRI setup and imaging protocols

Imaging was done on two MR tomographs with different field strengths, one with 1.5 T (MAGNETOM Aera Siemens, Erlangen, Germany) and the other with 3.0 T (Signa Excite Hdx; GE Medical Systems, Milwaukee, WI, USA) field strength. We verified that the nominal field strengths were reasonably close to 1.5 T and 3.0 T, respectively by inspecting the main resonance as indicated at the control console and dividing the respective values by the gyromagnetic ratio for hydrogen. We also verified the direction of the B_0 field using a pocket-compass. For both of the MRIs, used in this study, the south pole was at the foot-end (i.e., the compass needle will line up with the north pointing into the MRI) and by international convention the direction of the magnetic field is therefore from the feet to the head of the subjects, when entering head-first into the MRI. Note that this is the opposite direction relative to the Philips Achieva MRI that was used in the study of Roberts et al. (2011) and therefore the drifts are expected to be reversed.

For functional imaging we chose equal repetition times, equal voxel sizes and coverage of the whole brain including brain stem and cerebellum at both MR tomographs, but increased the effective echo time of the EPI sequence at 1.5 T to get a better BOLD contrast. Therefore we choose $TE_{\text{eff}} = 44$ ms for the 1.5 T MRI and $TE_{\text{eff}} = 30$ ms for the 3 T MRI. Although the fMRI signal scaling is also dependent on TE_{eff} of the EPI sequence (Triantafyllou et al., 2005; Duyn, 2012), we assume here that the approximation $\lambda \approx \sqrt{B_0^2/B_1^2} = \sqrt{3 \text{ T}/1.5 \text{ T}} = \sqrt{2}$ for the fMRI signal scaling holds, i.e., in our case we assume that the expected scaling solely depends on the field strengths of the MRIs. The resolution of both EPI sequences was 3.5 mm \times 3.5 mm \times 4.5 mm with a matrix of 64 \times 64 and 36 slices without any gap, i.e., a volume of 224 mm \times 224 mm \times 162 mm. The repetition time was 3000 ms and the flip angle was 90° for both MRIs. Two runs of resting-state fMRI were acquired each with 130 volumes, i.e., 6 min and 30 s of resting-state fMRI data for each run and additionally including four "dummy scans", i.e., volumes acquired but not reconstructed at the start of each run to account for T1 saturation.

The anatomical imaging sequences differed but had similar resolution. On the 1.5 T MRI we used a MPRAGE (magnetization prepared rapid gradient echo) sequence with TR = 1900 ms, TE = 2.67 ms, TI = 1100 ms, 160 slices per slab, 1 \times 1 \times 1 mm voxel, flip angle = 15°, FOV = 256 \times 256 mm covering the whole brain including brain stem and cerebellum. On the 3 T MRI we used a FSPGR (fast spoiled gradient echo) sequence with TE out of phase, preparation time 500 ms, flip angle 15°, FOV 220 mm, Locs per Slap 128, matrix 256 \times 256, with a resolution of 0.8 mm \times 0.8 mm \times 0.7 mm.

Preprocessing of MRI data

All preprocessing was done with SPM8 (www.fil.ion.ac.uk/spm/). Datasets from each MRI per subject were preprocessed separately, but in the same way, as follows. The functional data were corrected for motion via realignment of the whole time series to a reference volume that was chosen manually by looking for a relatively “motion free” part of the image time series. The mean of all realigned images of both runs after motion correction was used for coregistration of the functional data with the anatomical image. The functional and anatomical images were normalized to MNI space using the unified segmentation and normalization scheme implemented in SPM8 (Ashburner and Friston, 2005). The anatomical image (T1-weighted) was used in the segmentation step as the basis for estimating gray matter, white matter and CSF/other distributions using tissue probability maps provided with SPM8. The parameters obtained from the segmentation were then used to normalize the images (functional and anatomical) to the MNI space. The voxel size after normalization was $4 \times 4 \times 4 \text{ mm}^3$ for the functional, and $1 \times 1 \times 1 \text{ mm}^3$ for the anatomical image. All fMRI volumes were smoothed with an isotropic 3D gaussian kernel with a FWHM of 6 mm.

Analysis of resting-state data

Estimation and selection of resting-state networks with group ICA

We used FSL MELODIC (<http://www.fmrib.ox.ac.uk/fsl/melodic/>) (Beckmann and Smith, 2004) to perform group independent component analysis (ICA). This means applying spatial ICA to the temporal concatenation of all data of all runs of all subjects from both MRIs.

Before ICA was conducted, a voxel-wise de-meaning and normalization of the voxel-wise variance were performed and all drifts longer than 100 s were filtered out. Pre-processed data were whitened and projected into a subspace using probabilistic principal component analysis. The number of dimensions for the subspace was estimated using the Laplace approximation to the Bayesian evidence of the model order (Minka, 2000; Beckmann and Smith, 2004). Component maps were then estimated and afterwards normalized using the residual noise standard deviation. These normalized component maps were then thresholded by fitting a mixture model to the histogram of intensity values (Beckmann et al., 2003; Beckmann and Smith, 2004).

This results in a decomposition that is representative on the “global-level”, i.e., the whole-sample across both MRIs and all subjects. This was done to ensure that the network was present in both field strengths for the whole group. This has recently been shown to lead to a very accurate and reproducible detection of the DMN over various imaging sites and under varying imaging conditions (Jovicich et al., 2015). We then applied dual regression (Beckmann et al., 2009; Filippini et al., 2009) on the fMRI data based on all the group ICA spatial independent component maps. This allows us to obtain time courses and spatial amplitudes per individual subject, run and MRI for each independent component (IC) that can then be used for revealing MVS modulations. This also means that the detection of the DMN is not done for each run acquired in a MRI, but on all data and then related back to all runs of all subjects in both MR tomographs.

It should be noted that all independent components are used in the dual regression approach and therefore components of no interest, e.g., describing artifacts like white matter or cerebrospinal fluid (CSF) fluctuations are also accounted for in the data and should “absorb” at least some of these influences on the amplitudes of the component of interest (the DMN amplitudes), although any “nuisance removal” will probably never be perfect.

Independent component of interest describing the default mode network (DMN) was selected by visual inspection based on the proposed distributions taken from Beckmann et al. (2005) and Buckner et al. (2008).

Analysis of field strength influence on resting-state networks

Definition of scaling factor. We used the spatial amplitudes from the dual regression to calculate the scaling Λ as the magnitude of the fraction of the amplitudes at 3.0 T divided by the amplitudes at 1.5 T, both averaged over the runs, i.e., $\Lambda = \left| \frac{\widehat{\text{DMN-Amplitude}}_{3T}}{\widehat{\text{DMN-Amplitude}}_{1.5T}} \right|$, with Λ denoting the scaling value per subject at every individual voxel, $|\cdot|$ denoting the absolute value and $\widehat{\cdot}$ denoting the average over all runs per subject at every voxel individually.

It should be noted that Λ is from a ratio distribution (given that it is the ratio of amplitudes), and statistics are expected to suffer from long tails. Therefore, we chose to use robust statistics using the median of the scaling values as the measure of the average and the interquartile range (and derived confidence intervals) as the measure of dispersion, as this was proposed as a good approach when evaluating statistics on fractions (Brody et al., 2002), given that no closed form for the distribution function is known in our case.

For the case at hand we are only interested in finding those areas that do not violate the hypothesized Λ (i.e., areas with sufficiently small dispersion to not reject the null hypothesis $H_0(\Lambda = 2\sqrt{2})$). Hence, the median, the interquartile range and the Wilcoxon signed-rank test will suffice as statistical measures in this case and knowledge of the exact distribution function is not needed. Knowledge of the exact distribution function would make inference simpler and possibly reveal more about the nature of MVS or scaling values in general and would therefore be an interesting topic for a further mathematical-statistical treatment of the assumptions underlying the calculation of scaling-values.

ROI analysis step 1: determination of candidate areas of “modulation”. For defining regions of interest (ROIs) we first split the data spatially into parts that had their DMN amplitudes modulated significantly (statistically significant) between field strength and parts that did not modulate significantly (statistically not significant). For this we selected the estimated amplitudes from dual regression (stage 2) for all subjects including both MRIs for the DMN component and entered them into a paired t -test model using SPM8 to examine the subject-wise differences between “field strength” (MRIs) over the group and added behavioral covariates in the form of head angle of the subjects in the coil during imaging and their median horizontal slow phase velocity of the nystagmus for the corresponding head position.

This revealed modulations between field strengths using a threshold of $p \leq 0.05$ (FWE-corrected), which we call the candidate “modulated” areas of the DMN. All other parts of the DMN component (i.e., the significant voxels of the “global” group IC that was identified as the DMN) that were not covered by these voxels (of the modulated parts) are the candidate “unmodulated” areas of the DMN. Here, “unmodulated” means not statistically significant at $p \leq 0.05$ FWE-corrected in the analysis of differences in amplitudes, but significant in the “global” group IC that was identified as the DMN. This means that the “unmodulated” voxels are not simply the rest of the brain, but the rest of the significant voxels of the DMN group IC. We ensured that all voxels of the “unmodulated” and the “modulated” areas were present in the data of both MRI sessions.

Note that a “modulation” at this stage in the analysis does not necessarily imply that MVS is the underlying reason for the modulation. More precisely, at this point we are using a kind of “standard analysis for finding amplitude differences”, i.e., any kind of differences between the two settings (the two MR tomographs/the two field strengths). These differences can include biases from the two MRIs or insufficient modeling (and removal) of other fluctuations, e.g., from CSF or deviations from the assumptions for the prediction of the scaling of modulations. Therefore, we need a further step to identify modulations that stem from MVS, i.e., we have to analyze the scaling Λ for the hypothesized

point-value prediction of $\Lambda = 2\sqrt{2}$, as noted earlier (in the section ‘Overview: assumptions and reasons for the choice of methods’).

We used the automated anatomical labeling (AAL) atlas (Tzourio-Mazoyer et al., 2002) to split these regions of the candidate “modulated” and “unmodulated” voxels into smaller parts as labeled in the atlas (left and right sides were combined). This means that the significant voxels from the “modulated” areas are assigned AAL atlas labels and the voxels of the “unmodulated” areas (the significant voxels of the DMN component from the “global” group ICA without the voxel that are part of the “modulated” areas) are assigned AAL atlas labels to form separate ROIs. Any voxels that did not get a label initially were assigned to the nearest region of the AAL atlas. We then plotted the distribution of scaling values Λ in all these regions as boxplots.

ROI analysis step II: analysis and display of scaling values in ROIs. We chose to plot the distribution of the scaling data per region in three ways that allow us to visualize variability, distribution shape (via quartiles) and central tendency (via median) of the 4D scaling data (i.e., 3D spatial distribution of Λ over subjects).

We displayed (i) the spatial distribution of Λ within a given region for the “average subject”, i.e., the voxel-wise distribution of Λ for the “median subject”, as well as, (ii) all scaling data i.e., Λ of all voxels and all subjects, in a given region (“aggregate data”), and (iii) the distribution of subjects for the region, i.e., distribution of Λ of the subjects for the average voxel in the region, using the median over the voxels of the region, i.e., region average per subject (median over ROI).

The boxplot of the “aggregate” data, revealed the full variability and central tendency across all subjects and voxels in a given region (4D data) taken together. The distribution of voxels from the “median subject” aids in the understanding of the scaling behavior by revealing the contribution of the spatial-dispersion of Λ values to the variability and the central tendency to the “aggregate” data, for the “average” subject in each region. Finally, the distribution of subjects for the “median voxel” (or “region average”), aids in the understanding of the overall scaling behavior in the “aggregate data” by revealing the contribution of the “between subject variability” in Λ and its central tendency, i.e., it is the distribution of scaling values Λ between subject in a given region for an “average voxel” in that region of interest (ROI).

Mapping of Λ -statistics: searchlight based “ROI analysis at every voxel”

We also sought an approach for the analysis of the scaling behavior of the DMN that is independent from the previous definition of ROIs which used the candidate “modulated” and “unmodulated” regions (derived with the commonly used analysis for “statistically significant differences”), as well as the AAL atlas. Therefore we chose to employ a searchlight analysis. This means that a ROI was created for each of the N voxels in the brain. These N ROIs, called searchlights, contain (usually) 27 voxels each, i.e., the nearest neighbors ($3 \times 3 \times 3$ voxels) around the “center voxel”. If a “center voxel” falls on the edge of the brain mask then the searchlight was cropped and these searchlights have less than 27 voxels.

The preparation of the input data for each searchlight was analogous to the previous ROI analysis, i.e., in every searchlight we analyze the scaling behavior using the “aggregate” scaling data, the voxel-distribution of the “median subject” and the subject-distribution of the “median voxel” as input data for calculating the statistical parameters that are then assigned to the “center voxel”, such that they can be “mapped out” over the whole brain. Mapping of the “aggregate”, “median subject” as well as the “median voxel” scaling data enables the distinction of contributions to the variability in the scaling data analog to the boxplots described above.

We analyze the data in each searchlight using non-parametric robust statistics, like the median and interquartile range as well as the Wilcoxon signed-rank test. Robust statistics were used, because the scaling values Λ can be expected to be very noisy and will contain outliers because they are a fraction of resting-state fluctuation amplitudes derived from

fMRI, which is generally very noisy and taking the fraction will amplify the dispersion further (see the section ‘Definition of scaling factor’).

Given that we have a specific point-value prediction (i.e., $\Lambda = 2\sqrt{2}$) for our hypothesis that MVS has modulated parts of the DMN (on top of the modulation due to fMRI signal increase; Triantafyllou et al., 2005; Duyn, 2012), we can set the null hypothesis H_0 for the Wilcoxon signed-rank test to $H_0(\Lambda = 2\sqrt{2})$ and use the collected scaling data to reject this hypothesis (Meehl, 1967) and conversely look for areas where the null hypothesis was not rejected (i.e., where H_0 was retained). Note that although this formulation of the statistical null hypothesis test to falsify our theory is opposite to the familiar, but paradoxical way statistics is done in psychology and neuro-imaging, it is a common statistical practice in physics where point-value predictions are common and hypotheses are falsified instead of confirmed (Meehl, 1967; Cohen, 1994).

We visualized regions where our $H_0(\Lambda = 2\sqrt{2})$ was not rejected and those where it was rejected by plotting a “deviation measure” D as overlays on brain areas. D is defined as $D = \log_2(\text{CutOff}/|z|) = \log_2(D^*)$ where $|z|$ denotes the absolute value of the equivalent z -score obtained from the Wilcoxon signed-rank test and the “CutOff” defines the minimal (or larger) z -score value that amounts to a rejection, i.e., a falsification of our “MVS modulation” hypothesis. Note that a small value for the CutOff, rather than a large value will result in a more conservative estimate, given that larger z -scores indicate greater deviations from our null hypothesis $H_0(\Lambda = 2\sqrt{2})$ and rejecting our “MVS modulation” hypothesis will thus be “easier” when choosing a small CutOff value. We therefore chose a CutOff of $z = 1.96$ indicating a 95% confidence interval. Using the logarithm to base 2 on the deviations $D^* = \text{CutOff}/|z|$ allows us to transform D^* from the domain $(0 \dots 1 \dots \infty)$ to the domain $(-\infty \dots 0 \dots +\infty)$ for D that is symmetric and centered (on the value “ $D = 0$ ”) around the “CutOff”, i.e., $D^* = 1$ for $|z| = \text{CutOff}$. In case that the deviation is sufficiently large to reject our hypothesis, i.e., $|z| > \text{CutOff}$, we get $D^* < 1$ and therefore a negative D , which will be indicated by cyan-blue coloring in the overlays. Conversely in case of a small deviation which does not reject our hypothesis, i.e., $|z| < \text{CutOff}$, we get $D^* > 1$ and therefore a positive D , which will be indicated by yellow-red coloring in the overlays.

We also display the overlap of all regions where $H_0(\Lambda = 2\sqrt{2})$ was retained (positive D) for all preparations of the scaling data, i.e., the “aggregate” data, the voxel-distribution of the “median subject” and the subject-distribution of the “median voxel”, to indicate the most conservative inference on the regions for which we retain the null hypothesis $H_0(\Lambda = 2\sqrt{2})$, i.e., “MVS modulation is present”. The overlap is indicated by additive red-green-blue color mixing. We plot the distribution of scaling values for select regions that show full overlap of all statistics as boxplots.

In addition to the overlay plots of the statistical tests using the Wilcoxon signed-rank test, we also “map out” the median- Λ values and their deviation in form of the width of their confidence interval. The calculation of the confidence interval width was based on the 95% confidence interval determined from the interquartile range IQR by $\text{CIwidth} = 1.57 \times \text{IQR}/\sqrt{N}$, with N being the number of samples in the distribution. We plot overlays for the “aggregate” scaling data, the voxel-distribution of the scaling data of the “median subject” and the subject-distribution of the scaling data for the “median voxel” in each searchlight for indicating contributions to the variability in the scaling data analog to the boxplots described above.

Results

Behavioral results

All of our subjects showed a predominantly horizontal nystagmus in the MRI’s magnetic field analog to the results shown by Roberts et al. (2011). The nystagmus persisted as long as subjects remained in the MRI and little or no horizontal nystagmus was observed when outside the MRI bore where the magnetic field was weak (≤ 0.1 T at 1.5 T MR

tomograph site or near the earth's magnetic field, i.e., $\leq 10^{-4}$ T, at 3.0 T MR tomograph site, see Methods in the section 'Examination protocol'. Outside the Faraday-cage subjects did not show any horizontal nystagmus (or abnormal eye movements) after a brief period of reversed nystagmus, in contrast to the situation inside the MRI analog to previously published findings (Roberts et al., 2011). Some of the subjects reported the feeling of being moved, rotated as in "driving around a curve" or dizziness when entering or leaving the bore which subsided after a short time, while the nystagmus did not subside when inside the MRI for all subjects (except for some subjects when in the chin down position, P1 in Fig. 1A). Fig. 1A shows the distribution of the median horizontal slow phase velocities (SPVs) of all subjects in both MRIs and all four head positions. The nystagmus' SPV depended on the head orientation of the subjects and was positive, i.e., right-ward drift, for most subjects (more than 75%) for the head positioned in the coil e.g., during imaging, and increased further as the head was stretched more and more to the "chin up" position (i.e., P2, P3 & P4; Fig. 1A). The SPVs were reduced or zero for the "chin down" position and in some cases reversed, i.e., the nystagmus then had a left-ward drift (P1; Fig. 1A). The general trend of nystagmus SPV was the same for all subjects, i.e., increasing from "chin down" position (P1) to "chin up" position (P4) and these trends increased with field strength for almost all subjects (Fig. 1A).

The scaling of the trend between field strengths, i.e., the fraction λ of the nystagmus SPV trend over head-angle between field strengths, was found to be near the expected value of $\lambda = 2$ for group median, given the confidence interval for the median (Fig. 1B), indicating that MVS scales linearly with B_0 , as suggested by the Lorentz-model (Roberts et al., 2011).

Resting-state functional MRI results

The dimension estimation for the group ICA resulted in 21 components. We picked the default mode network via visual inspection as one component which described 7.48% of the total variance.

ROI analysis results

The spatial distribution of voxels of the DMN component are given in blue and green (Fig. 2A). Blue and green voxels are both significant parts of the DMN component and present in both MRI data. The green parts indicate voxels that were not (statistically) significantly modulated in their DMN amplitudes (taken from dual regression stage 2), while the blue parts indicate voxels with (statistically) significantly modulated

amplitudes of the DMN between field strength ($p \leq 0.05$ FWE-corrected; Fig. 2A).

Note that this does not necessarily reflect MVS modulations, but any kind of significant differences. Therefore we analyzed the scaling of amplitudes as noted in Methods section 'ROI analysis step I: Determination of candidate areas of "modulation"'. We hypothesized a specific scaling value ($\Lambda = 2\sqrt{2}$) for which we will accept that MVS modulation has occurred. Other values will not be considered as they might be due to deviations from our assumptions or other effects like bias between MRI settings or other fluctuations (e.g., CSF) that might be insufficiently modeled (see Methods sections 'ROI analysis step I: Determination of candidate areas of "modulation"' and 'Estimation and selection of resting-state networks with group ICA'). The ROI analysis results of the scaling Λ of the DMN amplitudes for the "unmodulated" parts are given in green and the "modulated" parts in blue (Fig. 2B). The three different boxplots for each part show different aspects of the scaling behavior Λ of the fMRI data (voxel distribution of "average subject", "aggregate data" and subject distribution of "average voxel" in every given region) as explained in the Methods section (the section 'ROI analysis step II: analysis and display of scaling values in ROIs'). The scaling factor of $\Lambda = \sqrt{2}$, expected for the case of no MVS influence on the modulation of amplitudes and increase only due to fMRI signal scaling with field strength (Triantafyllou et al., 2005; Duyn, 2012) is indicated by a black dotted line overlaying all boxplots. The scaling factor of $\Lambda = 2\sqrt{2}$, expected for the case of MVS influence due to field strength, in accordance with the Lorentz-force model describing the eye movements (Roberts et al., 2011), together with fMRI signal increase due to field strength (Triantafyllou et al., 2005; Duyn, 2012) is indicated by a red dotted line overlaying all boxplots.

The boxplots for the "unmodulated" parts of the DMN (Fig. 2B indicated in green) show a scaling behavior around the value $\sqrt{2}$ (considering the confidence interval for the median). This indicates that no MVS effect was present, according to the prediction that for this value only fMRI field strength effects are increasing the signal fluctuations.

For the "modulated" parts (Fig. 2B indicated in blue) we can show that the ROIs "anterior cingulum" and "cerebellar vermis" show a scaling behavior around the value $2\sqrt{2}$. This suggests that a MVS effect was present, according to the prediction that MVS would contribute linearly to the scaling, given that the Lorentz-force is linear in B_0 , i.e., resulting in a factor of 2 for 3.0 T relative to 1.5 T, while the fMRI signal scaling due to field strength contributes sub-linearly with an expected factor of $\sqrt{2}$. Furthermore, the areas "posterior cingulum" and the "precuneus" show a scaling behavior near the value $\sqrt{2}$ suggesting

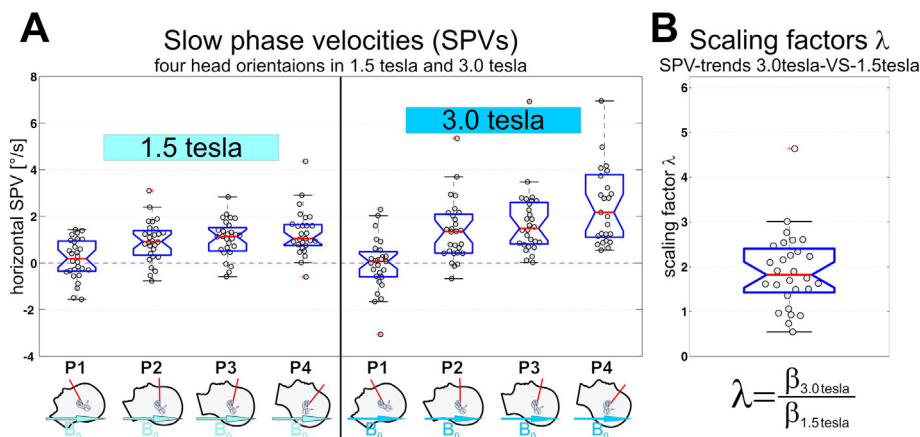
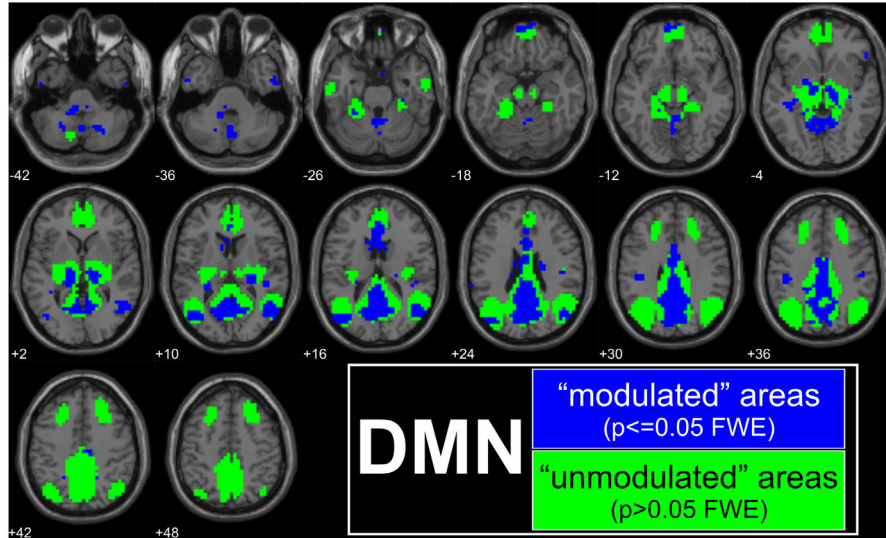


Fig. 1. A: Distribution of the median horizontal slow phase velocities (SPVs) of all subjects in both MR tomographs (1.5 T and 3.0 T) and all four head positions (P1 to P4). Head positions are indicated by P1 to P4 as a schematic drawing of the head and inner ear vestibular end-organ, including the marking of Reid's plane (red line) that was used for recording the head angle and the orientation of the magnetic field B_0 (blue arrow). The positions ranged from (P1) subjects' bringing their jaw close their chest, i.e., "chin down" position, (P2) the head placed in the head coil, i.e., only slightly lifted, (P3) the head lying flat on the bed of the MRI and (P4) the head overstretched backwards, i.e., "chin up". B: The scaling λ of the trends of the median horizontal SPVs between the two field strengths for all subjects (3.0 T relative to 1.5 T). The SPV trend was determined as the slope for the median SPVs over the head angle in all four head positions per subject and MRI.

A Amplitude modulations due to “field strength”



B ROI analysis of signal scaling Λ

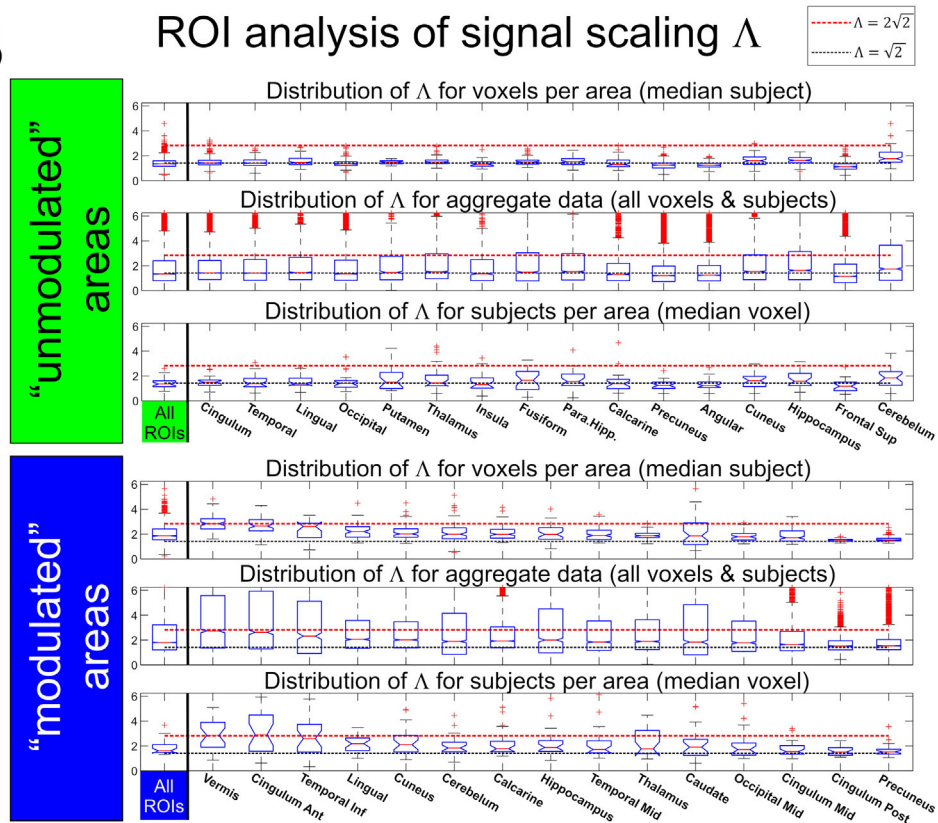


Fig. 2. A: Spatial distribution of voxels belonging to the DMN component shown in blue and green. Blue and green voxels are both significant parts of the DMN component and present in both MRI data. The green parts of Fig. 2A indicate voxels that were not statistically significantly modulated in their DMN amplitudes (taken from dual regression stage 2), while the blue parts indicate voxels with (statistically) significantly modulated amplitudes of the DMN between field strength ($p < 0.05$ FWE-corrected). Note that the modulated parts indicate any statistically significant difference, i.e., not necessarily that MVS modulation was present. MVS modulation (in accordance with our hypothesis) has to have a scaling value near $\Lambda = 2\sqrt{2}$ (see text and scaling analysis in B). B: ROI analysis results for the scaling Λ of the DMN amplitudes for the “unmodulated” parts (green) and the “modulated” parts (blue). The three different boxplots (top to bottom for each part) show different aspects of the scaling behavior Λ of the fMRI data: (top) voxel distribution of “average subject”, (middle) “aggregate data” and (bottom) subject distribution of “average voxel” in every given region. The black dotted line overlaying all boxplots indicates the predicted scaling factor of $\Lambda = \sqrt{2}$, expected for the case of no MVS influence on the modulation of amplitudes and increase only due to fMRI signal scaling with field strength. The red dotted line overlaying all boxplots indicates the predicted scaling factor of $\Lambda = 2\sqrt{2}$, expected for the case of signal modulation due to MVS influence, in accordance with the Lorentz-force model, together with fMRI signal increase due to field strength. The names of the ROI splits of the respective “modulated” or “unmodulated” parts of the DMN denote their spatial location as taken from the labels of the AAL atlas. The first column in each row of boxplots, separated from the ROI splits by a solid black line and also underlined with green or blue color, indicates the behavior of Λ for the complete region (all significant voxels) of the “unmodulated” or “modulated” parts of the DMN, respectively.

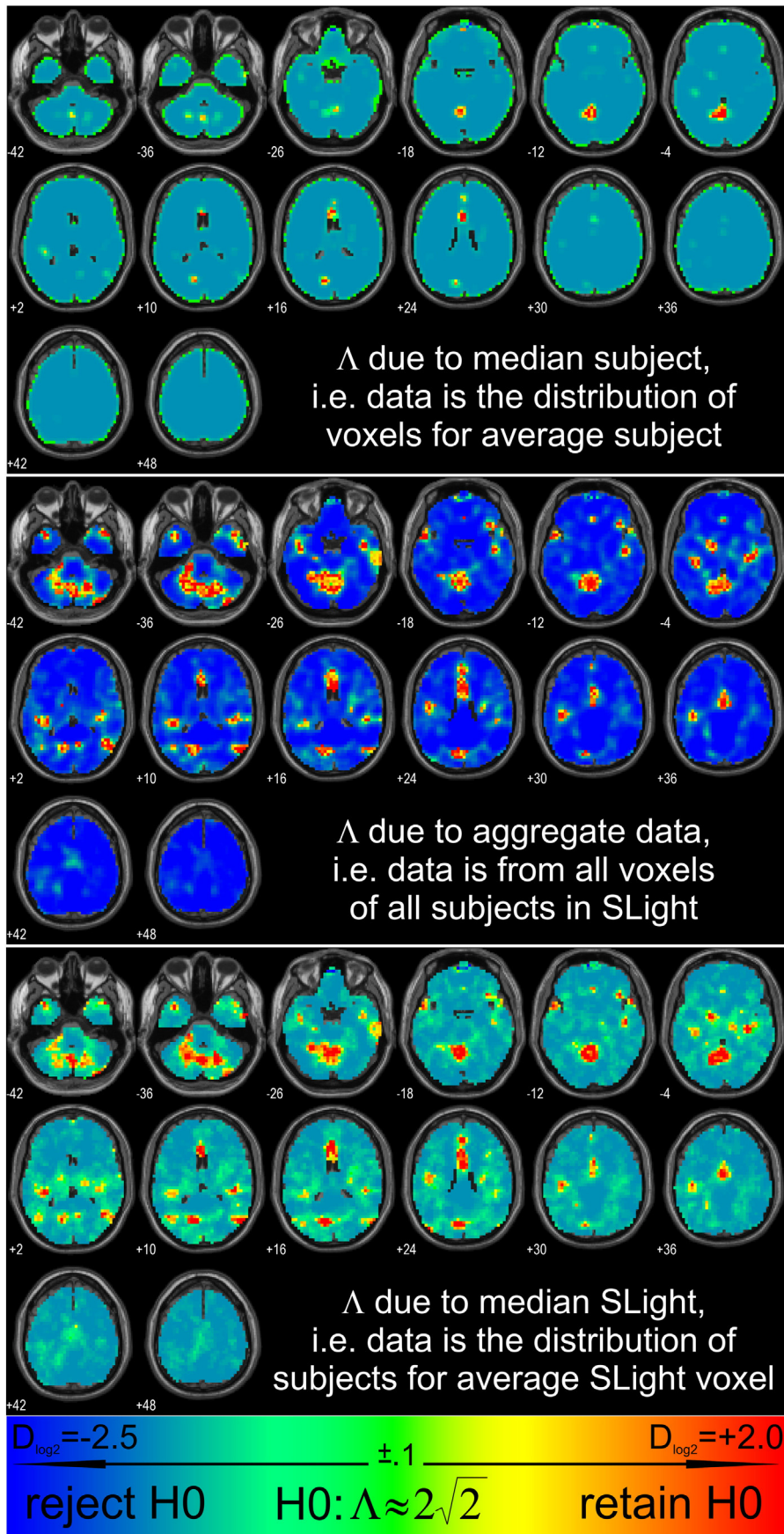


Fig. 3. Spatial distribution of the deviation measure D indicating regions where the null hypothesis $H_0(\Lambda = 2\sqrt{2})$ for the scaling values was retained ($D > 0$) and those where H_0 was rejected ($D < 0$) as colored overlays on a standard brain. The statistics for the voxel distribution of the “median subject” at each searchlight is shown at the top, the aggregate scaling data at each searchlight is shown in the middle and the subject distribution for the median voxel in each searchlight (“median searchlight”) is shown at the bottom.

that no MVS was present and signal increase was only due to fMRI field strength effects, i.e., the areas got (statistically) significant in the paired *t*-test between amplitudes, because the variability was relatively low. This demonstrates that the analysis for statistically significant differences between field strengths (indicated in blue; Fig. 2A) can be misleading when trying to analyze for MVS influences.

All other ROIs of the “modulated” areas (“inferior temporal gyrus”, “lingual gyrus”, “cuneus”, “cerebellum”, “calcarine”, “hippocampus”, “middle temporal gyrus”, “thalamus”, “caudate”, “middle occipital gyrus” and “middle cingulum”) showed a scaling that was significantly higher than $\sqrt{2}$, i.e., higher than expected for fMRI signal increase due to field strength without a MVS influence being present, but still lower than $2\sqrt{2}$ which would ideally be expected when a MVS effect was present (when considering the confidence interval of the median). Therefore, these areas were not considered as MVS modulated.

Searchlight analysis results

The spatial distribution of the deviation measures *D* that indicates where the null hypothesis $H_0(\Lambda = 2\sqrt{2})$, “MVS modulation is present”, was retained ($D > 0$) and where H_0 was rejected ($D < 0$) is depicted in Fig. 3. The results for the distribution of voxels for the average subject (median subject), the aggregate data (all voxels in searchlight, all subjects) and the distribution of subjects for the average voxel in the searchlight (median searchlight; indicated as “median SLight”) are depicted at the top, middle and bottom, respectively.

The overlap of all statistics where the null hypothesis $H_0(\Lambda = 2\sqrt{2})$, “MVS modulation is present”, was retained ($D > 0$) is shown in Fig. 4. The overlap is depicted as an additive red–green–blue color-mixing overlay on a standard anatomical brain, together with inlays showing the distribution of scaling values Λ as boxplots for the regions with the most consistent overlap, i.e., the most conservative estimate of $H_0(\Lambda =$

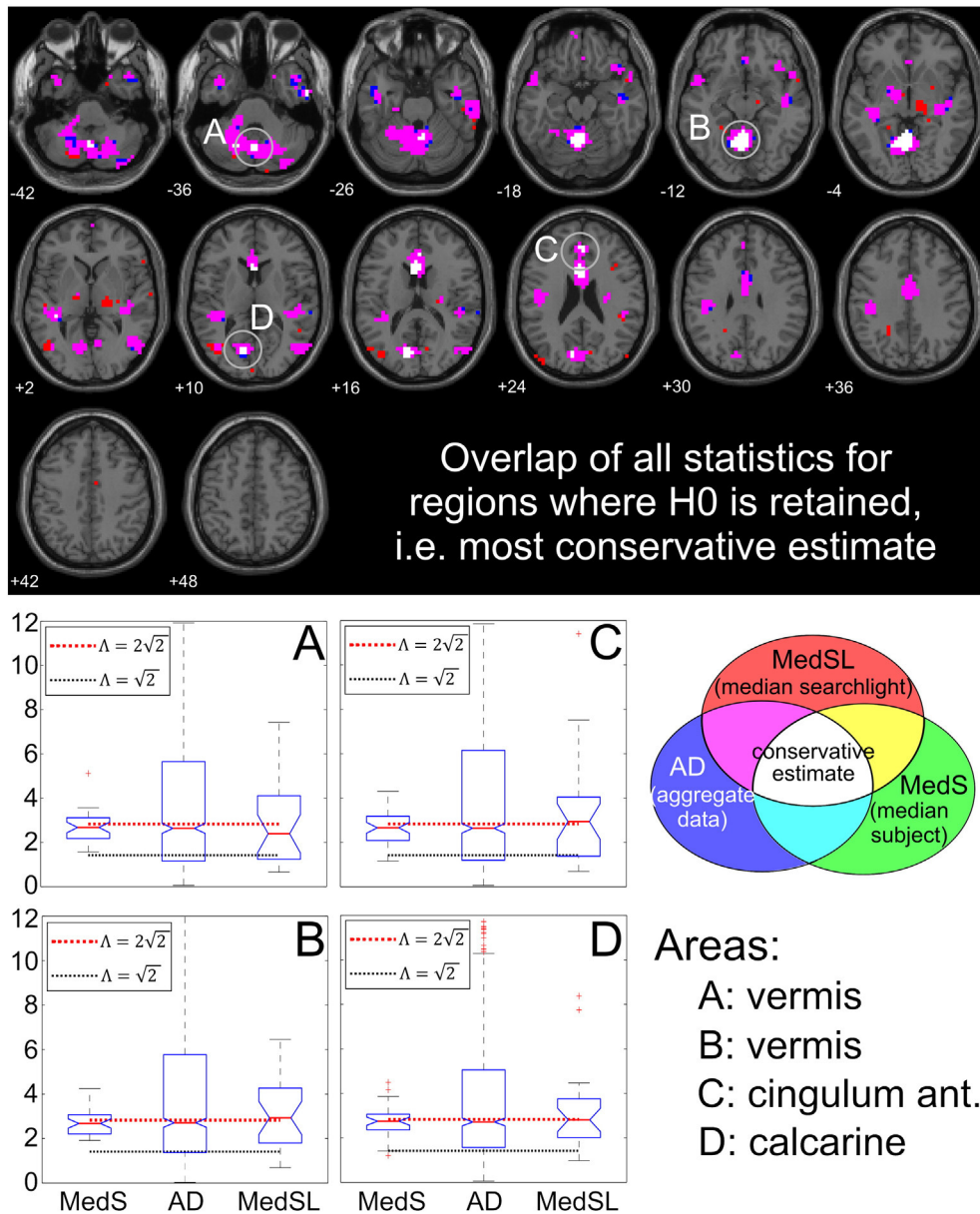


Fig. 4. The conservative estimate of the presence of the MVS modulation, including inlays showing the distribution of scaling values Λ for specific locations. The overlap of all statistics retaining ($D > 0$) the null hypothesis $H_0(\Lambda = 2\sqrt{2})$ “MVS modulation is present” is shown as an additive color-mixing overlay, showing the results from the “median subject” in green, the aggregate data in blue and the “median searchlight” in red and their overlaps in the respective additive color-mixing as indicated at the bottom. The overlap of all statistics is shown in white indicating the most conservative estimate, i.e., where all three possible statistics do not reject H_0 (i.e., $D > 0$). Inlays show boxplots of the scaling values Λ for four specific ROIs (upper and lower part of “cerebellar vermis”, “anterior cingulum” and “calcarine sulcus”) that were the main regions of the conservative estimate for the presence of the MVS effect.

$2\sqrt{2}$). These regions are the “cerebellar vermis”, the “anterior cingulum” and the “calcarine sulcus”.

The spatial distribution of median- Λ values and the associated confidence interval width, i.e., the range of uncertainty above and below the

median-value, is depicted in Fig. 5 on the left and right, respectively, as colored overlays on a standard brain. The color bar was designed to make the distinction of median- Λ values straightforward. The predicted value of $\Lambda = \sqrt{2}$, i.e., no MVS effect and only field strength related fMRI

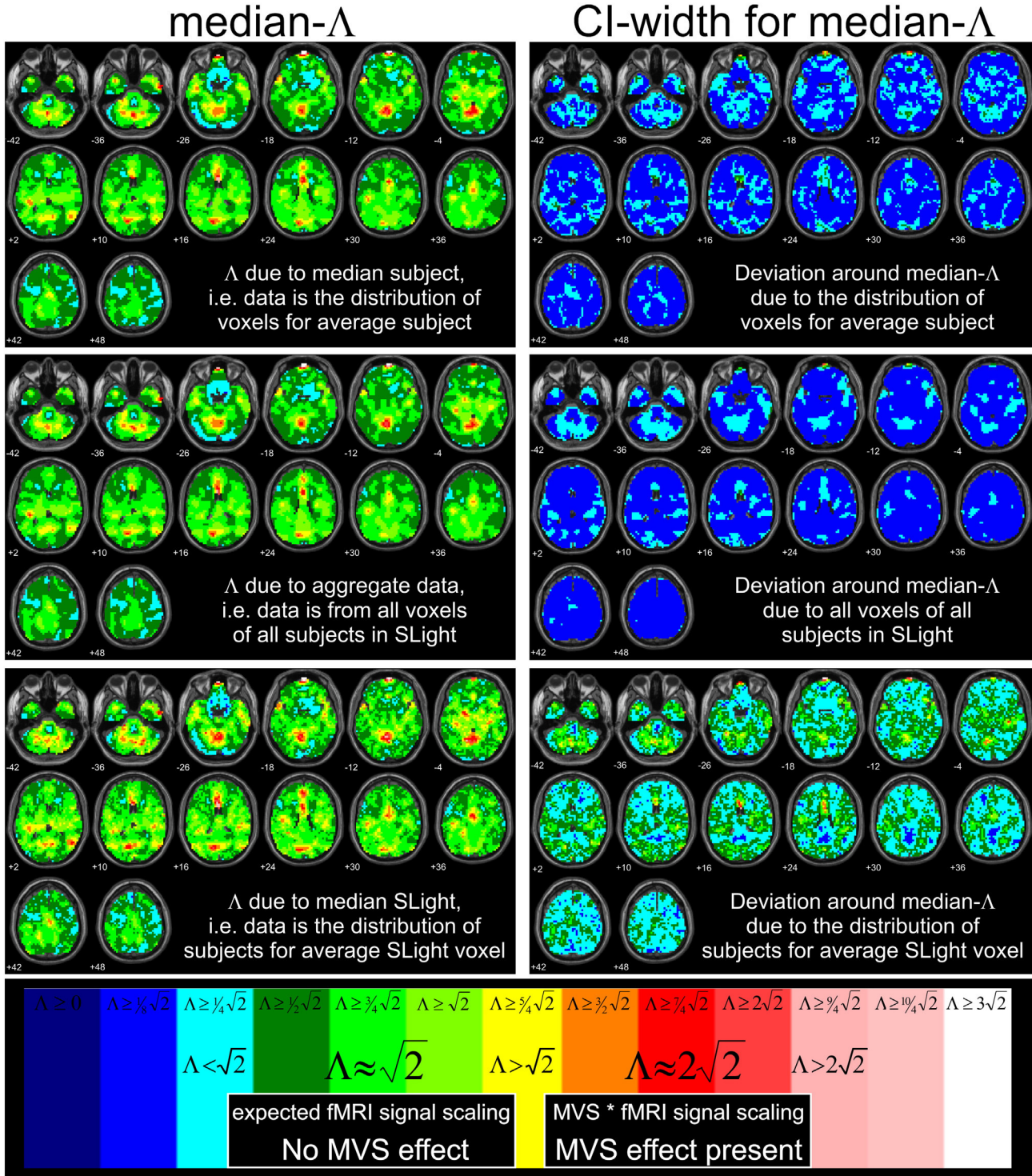


Fig. 5. Spatial distribution of scaling values Λ as colored overlays on a standard brain. Median- Λ is displayed on the left and the confidence interval width (95% CI), i.e., the range from the uncertainty limit above to the uncertainty limit below the median-value is displayed on the right. The color bar was designed to indicate values for the median- Λ around the predicted value of $\Lambda = \sqrt{2}$ in green, i.e., no MVS effect and only field strength related fMRI signal increases, and values of median- Λ around the predicted value of $\Lambda = 2\sqrt{2}$ in red, i.e., a MVS effect was present. The range of color display around the values $\Lambda = 2\sqrt{2}$ (red) and $\Lambda = \sqrt{2}$ (green) is in both cases $\delta = \pm 1/4\sqrt{2}$. Deviations from these predictions are colored in blue, yellow, orange or white respectively. The confidence interval width uses the same color bar, but the colors indicate the size of the width. The numbers at the top of the color bar for each color indicate the lower limit that a median- Λ or CI-width value at a certain voxel can have and still be plotted as the respective color. This means that a voxel with a median- Λ value $\Lambda \geq \sqrt{2}$ will be plotted as light green as long as it is not equal or larger than $\Lambda \geq 5/4\sqrt{2}$ which would result in being plotted in yellow, i.e., the upper end for each color is the lower end of the next color. Values of $\Lambda \geq 3\sqrt{2}$ are shown in white and considered outliers.

signal increases, is shown in green. A median- Λ around the predicted value of $\Lambda = 2\sqrt{2}$, i.e., “MVS effect was present”, is shown in red. Median- Λ scaling values that were significantly higher than $\sqrt{2}$, i.e., higher than expected for fMRI signal increase due to field strength alone without a MVS influence being present, but still lower than $2\sqrt{2}$, which would ideally be expected when a MVS effect was present, are shown in yellow and orange. This means the range of the color display around the values $\Lambda = 2\sqrt{2}$ (red) and $\Lambda = \sqrt{2}$ (green) is in both cases $\delta = \pm 1/4\sqrt{2}$.

It is interesting to note that the average scaling value over the whole brain was near $\Lambda = \sqrt{2}$ (labeled in green tones in Fig. 5) which is in accordance with the result published by Triantafyllou et al. (2005) who considered the average scaling of fMRI signals between field strengths. Local deviations from the value $\Lambda = \sqrt{2}$ were mostly in accordance with the prediction $\Lambda = 2\sqrt{2}$, derived from the Lorentz-force model (Roberts et al., 2011) and imaging physics (Triantafyllou et al., 2005; Duyn, 2012), e.g., “red regions” in slices at $z = -36$ mm to $z = -18$ mm or $z = +24$ mm in Fig. 5. All other regions that do not confirm to either of these two values for Λ were in parts of the brain that experienced imaging artifacts like field inhomogeneity effects which grow with field strength. These are therefore expected to have scaling values lower than $\Lambda = \sqrt{2}$, because signal reduction intensified at 3.0 T relative to the case at 1.5 T (e.g., “blue regions” in slices at $z = -26$ mm and $z = -18$ mm in Fig. 5). Statistical results of scaling analysis for selected clusters are listed in Table 1.

Discussion

Our goal in this study was to investigate if magnetic vestibular stimulation (MVS) does influence resting-state network fluctuations as measured with fMRI. We focused on the modulation of the default mode network (DMN) as an exemplary case and aimed on identifying

the modulatory influence of MVS on the DMN due to changes in magnetic field strength.

We validated that the MVS associated nystagmus was present and that its slow phase velocity (SPV) scales with field strength and head position as reported previously (Roberts et al., 2011). In the fMRI data, we chose to identify MVS modulations in the presence of other possible differences between field strengths (different MR tomographs, session effects, other fluctuations e.g., from CSF or white matter) by focusing on the analysis of scaling Λ of DMN amplitudes in accordance with the scaling of MVS under the assumption of the Lorentz-model (Roberts et al., 2011) and the scaling of the BOLD-signal (Triantafyllou et al., 2005; Duyn, 2012), which resulted in a specific point-value prediction, i.e., $\Lambda = 2\sqrt{2}$. This choice of methods is mainly due to the fact that fMRI only allows relative but no absolute measures of activity. Modulations of fMRI signals due to MVS can thus only be estimated by the evaluation of the scaling relationship between amplitudes of a chosen network, e.g., like the DMN, for different field strengths.

We found that those parts of the DMN which showed a scaling of amplitudes in accordance with the prediction made on the basis of the Lorentz model (Roberts et al., 2011) ($\Lambda = 2\sqrt{2}$) were associated with vestibular and ocular motor function (Dieterich and Brandt, 2008). These areas included the anterior cingulum, the cerebellar vermis and the calcarine sulcus. It should be noted that we did not expect to find all possible areas that have been described as vestibular in the literature before, or all areas that get vestibular input and that should therefore be influenced or “driven” by MVS, but only those “related to” the DMN. In other words, only those (MVS modulated) areas that have a “functional connection” (i.e., not effective connection) with the DMN can be detected, i.e., the relationship is correlative in nature (ICA identifies structured components in the data). Conversely, the direct effect of MVS on all areas that it “drives” cannot be estimated with fMRI, as possible for other stimulations, e.g., visual stimulation, which can be switched

Table 1

Coordinates in MNI-space of cluster peaks [x,y,z] as well as center of gravity (CoG) for cluster (x,y,z), both in mm, as well as cluster sizes, statistic values for amplitude scaling Λ and description of regions that are covered according to SUI-, Harvard-Oxford and Juelich Atlas. Statistic values are the estimated median Λ and the confidence interval for the median at the peak coordinate. Clusters 1 to 5 are part of the areas that are interpreted as MVS modulated, as all statistics (median subject, aggregate data and median searchlight) overlap with the prediction for $\Lambda = 2\sqrt{2}$ (see Fig. 4). Clusters 6 to 15 are areas where the prediction is matched in at least one statistic and are not interpreted as MVS modulated.

MNI-xyz in mm [Peak] & (CoG)	Cluster		$\Lambda = \text{Med} \pm \text{CI}$				Regions (SUIT; Harvard-Oxford; Juelich Atlas)
	No	size	“median subject”	“aggregate data”	“median SearchLight”		
[-2, -62, -36] (-2, -62, -32)	1.	64	2.64 + -0.27	2.58 + -0.26	2.42 + -0.86	Vermis VIIIb, VIIIa	
[-2, -58, -12] (-2, -58, -12)	2.	190	2.63 + -0.39	2.75 + -0.34	3.02 + -0.69	Cerebellum Left V, Left I-IV	
[2, 46, 24] (-2, 42, 24)	3.	23	2.57 + -0.25	2.68 + -0.23	2.96 + -0.73	Paracingulate gyrus, cingulate gyrus, anterior division	
[-2, 18, 24] (-2, 18, 20)	4.	80	2.80 + -0.34	2.66 + -0.32	2.99 + -1.56	Cingulate gyrus, anterior division (partly into corpus callosum)	
[-10, -74, 12] (-10, -74, 16)	5.	74	2.81 + -0.20	2.69 + -0.21	2.76 + -0.47	Intracalcarine cortex L, visual cortex V1 BA17 L	
[2, -10, 36] (-2, -6, 36)	6.	27	2.29 + -0.17	2.54 + -0.25	2.72 + -0.98	Cingulate gyrus, anterior division, posterior division	
[-2, -58, -48] (-2, -58, -48)	7.	31	2.54 + -0.26	2.41 + -0.24	2.69 + -0.65	Cerebellum left IX, vermis IX, VIIIb	
[-26, -46, -24] (-22, -50, -32)	8.	24	2.16 + -0.17	2.19 + -0.28	2.67 + -0.97	Cerebellum left VI, V	
[10, -54, -52] (10, -54, -52)	9.	10	2.36 + -0.17	2.53 + -0.23	2.64 + -0.66	Cerebellum right IX, VIIIb	
[18, -70, -36] (18, -62, -36)	10.	11	2.09 + -0.25	1.95 + -0.25	2.72 + -0.84	Cerebellum right crus II, crus I	
[10, -54, -24] (10, -54, -28)	11.	28	2.42 + -0.22	2.31 + -0.26	2.89 + -0.70	Cerebellum right V, I-IV	
[-18, -30, -36] (-22, -34, -36)	12.	4	2.10 + -0.37	1.99 + -0.33	2.69 + -1.03	Cerebellum/brainstem	
[-38, 6, -32] (-42, 10, -32)	13.	7	2.26 + -0.27	1.94 + -0.27	2.59 + -0.95	Temporal pole, inferior temporal gyrus, anterior division	
[58, -6, -36] (54, -6, -32)	14.	32	2.75 + -0.24	2.64 + -0.32	2.88 + -0.53	Inferior temporal gyrus, anterior division	
[54, -66, 8] (50, -66, 8)	15.	26	2.28 + -0.23	2.14 + -0.22	2.80 + -0.77	Lateral occipital cortex, visual cortex V5 R Middle temporal gyrus, temporooccipital part	

between “on” and “off” states during an imaging run, because MVS is always present throughout an imaging run. This suggests that the modulated DMN areas either have direct connections with the vestibular nuclei in the brain stem that process information coming from the vestibular end-organ, or if they don't have direct connections, they might get inputs from other vestibular areas that have connections to the brain stem nuclei.

Other parts of the DMN were not modulated by MVS as hypothesized (i.e., $\Lambda = 2\sqrt{2}$) with most of them modulated as expected for a constant neuronal effect under BOLD-signal scaling as described in the literature (Triantafyllou et al., 2005; Duyn, 2012), i.e., $\Lambda = \sqrt{2}$.

For the areas that modulated significantly above the prediction of fMRI signal increase, but less than expected from the Lorentz-force model it is possible that they were affected indirectly via vestibular areas, i.e., showed modulations because of vestibular interactions. On the other hand, our hypothesis that modulations should scale between field strengths as determined from the eye movements ($\Lambda = 2\sqrt{2}$) might only be appropriate for areas that are associated with vestibular subfunctions that are more closely related to ocular motor function. A third explanation could be that those deviations rather signify other kinds of modulations like CSF fluctuations or field inhomogeneity effects, leading to scaling values that are other than predicted for the constant case (i.e., $\Lambda = \sqrt{2}$; – no MVS modulation) or the MVS case (i.e., $\Lambda = 2\sqrt{2}$).

Our results raise questions about the influence of MVS on fMRI in general and in particular about fMRI studies on the function of the vestibular system and the influence of vestibular deficits. It is important to keep in mind that the effect of MVS is not like the constant acoustic noise stimulation during fMRI. MVS induces an imbalance state with a directional preponderance, i.e., has a signed difference effect, unlike acoustic noise that can be supposed to be equal and balanced for the auditory network and its connections. Thus, healthy subjects measured under MVS influence (i.e., in a MR tomograph) might be more like a “special patient group with a vestibular imbalance” but without lesions in the inner ear or central nervous system.

Recent studies comparing resting-state activity in patients with vestibular deficits to that of healthy controls showed widespread changes in various networks that also included the DMN (Göttlich et al., 2014; Klingner et al., 2014; Helmchen et al., 2014). Our results suggest caution when interpreting such studies, given that MVS can modulate brain areas differentially. In the case of bilateral vestibular loss (Göttlich et al., 2014), it should be noted that the patients will not show a MVS influence (Roberts et al., 2011), but the healthy control group will be under the influence of MVS. This might then lead to changes in the comparison of differences between the two groups as examined with fMRI that are not expected to appear in imaging methods without the use of strong magnetic fields. In this case, the healthy controls might be more akin to patients with acute unilateral vestibular neuritis, given that such patients also show a directional imbalance with a horizontal nystagmus, not unlike that evoked by MVS. For studies of vestibular neuritis patients versus healthy controls (e.g., Klingner et al., 2014; Helmchen et al., 2014), MVS effects should be expected for both, the patients and the healthy controls. However, MVS will affect patients with unilateral vestibular deficits differently than healthy controls (Ward et al., 2014), which will then further obscure the real differences between the two groups. This means that the reported differences at every time interval during the compensation period relative to the healthy control group will be obscured or biased by MVS. However, the trajectory of recovery of the patients and therefore the trajectory of associated relative differences to the healthy controls might not be affected by MVS influence. Thus, the trend of the change of the differences over the time intervals of compensation should be unaffected by MVS. This requires, however, that the subjects are imaged in, at least, very similar head positions and field strength at every time interval of compensation to stay comparable over the time intervals. In the resting-state study on vestibular neuritis patients (Klingner et al., 2014) it is

interesting to note that no significant correlations were found for the caloric testing covariate, although this is usually a good indicator of impairment or restoration of vestibular function. One might speculate that MVS had obscured this correlation, because MVS seems to share important characteristics in terms of temporal dynamics with caloric stimulation (Glover et al., 2014). Furthermore, MVS generally seems to increase the variability between subjects (e.g., in median SPV per head position) when field strength is increased from 1.5 T to 3 T, as the Lorentz-force model suggests a multiplicative relationship with field strength. Thus, studies at 3 T (and higher) will suffer from more “vestibular variability” between the measured subjects, as studies at 1.5 T. We suggest therefore that fMRI studies should monitor MVS via measurement of eye movements in darkness and adjust the head positions of all subjects and patients to keep the effects of MVS minimal or at least on the same level.

As a final note we want to stress that we do not see MVS as a nuisance for conducting research using fMRI, but as a tool for shifting balances in network dynamics. We urge the research community to see MVS as an opportunity to study the influence of vestibular imbalance in healthy subjects and in patients with the possibility to adjust the imbalance specifically, using the resulting nystagmus as an indicator for the imbalance level. Furthermore, MVS offers a way of studying network behavior and the behavior of the brain as a dynamic system in general by using its influence to shift the operation point of networks and examining the changes of these “shifted” networks either under rest or task conditions. This will also present an opportunity to study the influences of vestibular imbalance on higher cognitive functions and multisensory interaction that has been raised previously as an important research topic by various authors (Hanes and McCollum, 2006; Smith and Zheng, 2013; Mast et al., 2014).

Conclusion

The static magnetic field of the MRI influences default mode network resting-state fluctuations through the stimulation of vestibular areas and scales between field strengths of 1.5 T and 3.0 T in accordance with the Lorentz-force model for the stimulation of inner ear vestibular end-organs. We recommend that studies of the vestibular system using fMRI need to consider the influence of MVS and account for it if possible. A limitation of the current study is that differences in MVS had to be created by employing different field strengths using different MR tomographs which might have led to biases and raised variability in the results.

Acknowledgments

This work was supported by the Graduate School of Systemic Neuroscience, the German Federal Ministry of Education and Research (BMBF grant number 01 EO 0901) and the German Neurological Foundation (DSN grant number 80766090). We thank Sabine Esser for helpful suggestions regarding graphical presentation of the results. The content of this publication is solely the responsibility of the authors.

Conflict of interest

The authors declare no competing financial interests.

References

- Antunes, A., Glover, P.M., Li, Y., Mian, O.S., Day, B.L., 2012. Magnetic field effects on the vestibular system: calculation of the pressure on the cupula due to ionic current-induced Lorentz force. *Phys. Med. Biol.* 57 (14), 4477–4487. <http://dx.doi.org/10.1088/0031-9155/57/14/4477>.
- Ashburner, J., Friston, K.J., 2005. Unified segmentation. *NeuroImage* 26 (3), 839–851. <http://dx.doi.org/10.1016/j.neuroimage.2005.02.018>.
- Beckmann, C.F., Smith, S.M., 2004. Probabilistic independent component analysis for functional magnetic resonance imaging. *IEEE Trans. Med. Imaging* 23, 137–152.
- Beckmann, C.F., Woolrich, M., Smith, S.M., 2003. Gaussian/Gamma mixture modelling of ICA/GLM spatial maps. Ninth Int Conf on Functional Mapping of the Human Brain.

- Beckmann, C.F., DeLuca, M., Devlin, J.T., Smith, S.M., 2005. Investigations into resting-state connectivity using independent component analysis. *Philos. Trans. R. Soc. Lond. B Biol. Sci.* 360 (1457), 1001–1013.
- Beckmann, C.F., Mackay, C.E., Filippini, N., Smith, S.M., 2009. Group comparison of resting-state fMRI data using multi subject ICA and dual regression. *Proc HBM San Francisco*.
- Brandt, T., Dieterich, M., Strupp, M., 2004. *Vertigo and Dizziness—Common Complaints*. Springer, London.
- Brody, J.P., Williams, B.A., Wold, B.J., Quake, S.R., 2002. Significance and statistical errors in the analysis of DNA microarray data. *Proc. Natl. Acad. Sci. U. S. A.* 99 (20), 12975–12978. <http://dx.doi.org/10.1073/pnas.162468199>.
- Buckner, R.L., Andrews-Hanna, J.R., Schacter, D.L., 2008. The brain's default network anatomy, function, and relevance to disease. *Ann. N. Y. Acad. Sci.* 1124, 1–38. <http://dx.doi.org/10.1196/annals.1440.011>.
- Cohen, J., 1994. The earth is round ($p < 0.05$). *Am. Psychol.* 49, 997–1003.
- Cullen, K., Sadeghi, S., 2008. Vestibular system. *Scholarpedia* 3 (1), 3013. <http://dx.doi.org/10.4249/scholarpedia.3013> (revision #137650).
- Dera, T., Boening, G., Bardins, S., Schneider, E., Brandt, T., 2006. Low-latency video tracking of horizontal, vertical, and torsional eye movements as a basis for 3D of realtime motion control of a head-mounted camera. *Proceedings of the IEEE Conference on Systems, Man and Cybernetics (SMC2006)*, Taipei, Taiwan.
- Dieterich, M., Brandt, T., 2008. Functional brain imaging of peripheral and central vestibular disorders. *Brain* 131 (10), 2538–2552. <http://dx.doi.org/10.1093/brain/awn042>.
- Duyn, J.H., 2012. The future of ultra-high field MRI and fMRI for study of the human brain. *NeuroImage* 62 (2), 1241–1248. <http://dx.doi.org/10.1016/j.neuroimage.2011.10.065>.
- Filippini, N., MacIntosh, B.J., Hough, M.G., Goodwin, G.M., Frisoni, G.B., Smith, S.M., Matthews, P.M., Beckmann, C.F., Mackay, C.E., 2009. Distinct patterns of brain activity in young carriers of the APOE-epsilon4 allele. *Proc. Natl. Acad. Sci. U. S. A.* 106, 7209–7214.
- Glover, P.M., Li, Y., Antunes, A., Mian, O.S., Day, B.L., 2014. A dynamic model of the eye nystagmus response to high magnetic fields. *Phys. Med. Biol.* 59, 631–645. <http://dx.doi.org/10.1088/0031-9155/59/3/631>.
- Göttlich, M., Jandl, N.M., Wojak, J.F., Sprenger, A., von der Gablentz, J., Münte, T.F., Helmchen, C., 2014. Altered resting-state functional connectivity in patients with chronic bilateral vestibular failure. *NeuroImage: Clin.* 4, 488–499. <http://dx.doi.org/10.1016/j.nicl.2014.03.003>.
- Hanes, D.A., McCollum, G., 2006. Cognitive–vestibular interactions: a review of patient difficulties and possible mechanisms. *J. Vestib. Res.* 16 (3), 75–91.
- Helmchen, C., Zheng, Y., Sprenger, A., Münte, T.F., 2014. Changes in resting-state fMRI in vestibular neuritis. *Brain Struct. Funct.* 219 (6), 1889–1900. <http://dx.doi.org/10.1007/s00429-013-0608-5>.
- Jovicich, J., Minati, L., Marizzoni, M., Marchitelli, R., Sala-Llonch, R., Bartrés-Faz, D., Arnold, J., Benninghoff, J., Fiedler, U., Roccatagliata, L., Picco, A., Nobili, F., Blin, O., Bombois, S., Lopes, R., Bordet, R., Sein, J., Ranjeva, J.P., Didic, M., Gros-Dagnac, H., Payoux, P., Zoccatelli, G., Alessandrini, F., Beltramello, A., Bargalló, N., Ferretti, A., Caulo, M., Aiello, M., Cavaliere, C., Soricelli, A., Parnetti, L., Tarducci, R., Floridi, P., Tsolaki, M., Constantinidis, M., Drevelegas, A., Rossini, P.M., Marra, C., Schönknecht, P., Hensch, T., Hoffmann, K.T., Kuijter, J.P., Visser, P.J., Barkhof, F., Frisoni, G.B., PharmaCog Consortium, 2015. Longitudinal reproducibility of default-mode network connectivity in healthy elderly participants: a multicentric resting-state fMRI study. *NeuroImage* 124 (Pt A), 442–454. <http://dx.doi.org/10.1016/j.neuroimage.2015.07.010> (E-pub ahead of print).
- Klingner, C.M., Volk, G.F., Brodoehl, S., Witte, O.W., Guntinas-Lichius, O., 2014. Disrupted functional connectivity of the default mode network due to acute vestibular deficit. *NeuroImage: Clin.* 6, 109–114. <http://dx.doi.org/10.1016/j.nicl.2014.08.022>.
- Mast, F.W., Preuss, N., Hartmann, M., Grabherr, L., 2014. Spatial cognition, body representation and affective processes: the role of vestibular information beyond ocular reflexes and control of posture. *Front. Integr. Neurosci.* 27 (8), 44. <http://dx.doi.org/10.3389/fnint.2014.00044>.
- Meehl, P.E., 1967. Theory testing in psychology and in physics: a methodological paradox. *Philos. Sci.* 34, 103–115.
- Minka, T., 2000. Automatic choice of dimensionality for PCA. Technical Report 514. MIT Media Lab Vision and Modeling Group.
- Raichle, M.E., Snyder, A.Z., 2007. A default mode of brain function: a brief history of an evolving idea. *NeuroImage* 37 (4), 1083–1090.
- Raichle, M.E., MacLeod, A.M., Snyder, A.Z., Powers, W.J., Gusnard, D.A., Shulman, G.L., 2001. A default mode of brain function. *Proc. Natl. Acad. Sci. U. S. A.* 98 (2), 676–682.
- Roberts, D.C., Marcelli, V., Gillen, J.S., Carey, J.P., Della Santina, C.C., Zee, D.S., 2011. MRI magnetic field stimulates rotational sensors of the brain. *Curr. Biol.* 21, 1635–1640.
- Saunders, R., 2005. Static magnetic fields: animal studies. *Prog. Biophys. Mol. Biol.* 87 (2–3), 225–239. <http://dx.doi.org/10.1016/j.pbiomolbio.2004.09.001>.
- Schenck, J.F., 1992. Health and physiological effects of human exposure to whole-body four-Tesla magnetic fields during MRI. *Ann. N. Y. Acad. Sci.* 649, 285–301.
- Schilbach, L., Eickhoff, S.B., Rotarska-Jagiela, A., Fink, G.R., Vogeley, K., 2008. Minds at rest? Social cognition as the default mode of cognition and its putative relationship to the “default system” of the brain. *Conscious. Cogn.* 17 (2), 457–467. <http://dx.doi.org/10.1016/j.concog.2008.03.013>.
- Schneider, E., Glasauer, S., Dieterich, M., 2002. Comparison of human ocular torsion patterns during natural and galvanic vestibular stimulation. *J. Neurophysiol.* 87, 2064–2073.
- Smith, P.F., Zheng, Y., 2013. From ear to uncertainty: vestibular contributions to cognitive function. *Front. Integr. Neurosci.* 7, 84. <http://dx.doi.org/10.3389/fnint.2013.00084>.
- Triantafyllou, C., Hoge, R.D., Krueger, G., Wiggins, C.J., Potthast, A., Wiggins, G.C., Wald, L.L., 2005. Comparison of physiological noise at 1.5 T, 3 T and 7 T and optimization of fMRI acquisition parameters. *NeuroImage* 15 26 (1), 243–250. <http://dx.doi.org/10.1016/j.neuroimage.2005.01.007>.
- Tzourio-Mazoyer, N., Landeau, B., Papathanassiou, D., Crivello, F., Etard, O., Delcroix, N., Mazoyer, B., Joliot, M., 2002. Automated anatomical labeling of activations in SPM using a macroscopic anatomical parcellation of the MNI MRI single-subject brain. *NeuroImage* 15 (1), 273–289. <http://dx.doi.org/10.1006/nimg.2001.0978>.
- Ward, B.K., Roberts, D.C., Della Santina, C.C., Carey, J.P., Zee, D.S., 2014. Magnetic vestibular stimulation in subjects with unilateral labyrinthine disorders. *Front. Neurol.* 13, 5–28. <http://dx.doi.org/10.3389/fneur.2014.00028>.
- Ward, B.K., Roberts, D.C., Della Santina, C.C., Carey, J.P., Zee, D.S., 2015. Vestibular stimulation by magnetic fields. *Ann. N.Y. Acad. Sci.* 1343, 69–79. <http://dx.doi.org/10.1111/nyas.12702>.

SPRINGER LICENSE TERMS AND CONDITIONS

Apr 05, 2016

This is a License Agreement between Rainer E Boegle ("You") and Springer ("Springer") provided by Copyright Clearance Center ("CCC"). The license consists of your order details, the terms and conditions provided by Springer, and the payment terms and conditions.

All payments must be made in full to CCC. For payment instructions, please see information listed at the bottom of this form.

License Number	3842421110372
License date	Apr 05, 2016
Licensed content publisher	Springer
Licensed content publication	Brain Structure and Function
Licensed content title	Age-related decline in functional connectivity of the vestibular cortical network
Licensed content author	Carolin Anna Maria Cyran
Licensed content date	Jan 1, 2015
Volume number	221
Issue number	3
Type of Use	Thesis/Dissertation
Portion	Full text
Number of copies	5
Author of this Springer article	Yes and you are the sole author of the new work
Order reference number	None
Title of your thesis / dissertation	Modulation of vestibular networks by age and magnetic fields - Implications for the study of vestibular function in patients and healthy controls with functional magnetic resonance imaging
Expected completion date	Jan 2017
Estimated size(pages)	80
Total	0.00 EUR
Terms and Conditions	

Introduction

The publisher for this copyrighted material is Springer. By clicking "accept" in connection with completing this licensing transaction, you agree that the following terms and conditions apply to this transaction (along with the Billing and Payment terms and conditions established by Copyright Clearance Center, Inc. ("CCC"), at the time that you opened your Rightslink account and that are available at any time at <http://myaccount.copyright.com>).

Limited License

With reference to your request to reuse material on which Springer controls the copyright, permission is granted for the use indicated in your enquiry under the following conditions:

- Licenses are for one-time use only with a maximum distribution equal to the number stated in your request.
- Springer material represents original material which does not carry references to other sources. If the material in question appears with a credit to another source, this permission is

not valid and authorization has to be obtained from the original copyright holder.

- This permission
 - is non-exclusive
 - is only valid if no personal rights, trademarks, or competitive products are infringed.
 - explicitly excludes the right for derivatives.
- Springer does not supply original artwork or content.
- According to the format which you have selected, the following conditions apply accordingly:
 - **Print and Electronic:** This License include use in electronic form provided it is password protected, on intranet, or CD-Rom/DVD or E-book/E-journal. It may not be republished in electronic open access.
 - **Print:** This License excludes use in electronic form.
 - **Electronic:** This License only pertains to use in electronic form provided it is password protected, on intranet, or CD-Rom/DVD or E-book/E-journal. It may not be republished in electronic open access.

For any electronic use not mentioned, please contact Springer at permissions.springer@spi-global.com.

- Although Springer controls the copyright to the material and is entitled to negotiate on rights, this license is only valid subject to courtesy information to the author (address is given in the article/chapter).
- If you are an STM Signatory or your work will be published by an STM Signatory and you are requesting to reuse figures/tables/illustrations or single text extracts, permission is granted according to STM Permissions Guidelines: <http://www.stm-assoc.org/permissions-guidelines/>

For any electronic use not mentioned in the Guidelines, please contact Springer at permissions.springer@spi-global.com. If you request to reuse more content than stipulated in the STM Permissions Guidelines, you will be charged a permission fee for the excess content.

Permission is valid upon payment of the fee as indicated in the licensing process. If permission is granted free of charge on this occasion, that does not prejudice any rights we might have to charge for reproduction of our copyrighted material in the future.

-If your request is for reuse in a Thesis, permission is granted free of charge under the following conditions:

This license is valid for one-time use only for the purpose of defending your thesis and with a maximum of 100 extra copies in paper. If the thesis is going to be published, permission needs to be reobtained.

- includes use in an electronic form, provided it is an author-created version of the thesis on his/her own website and his/her university's repository, including UMI (according to the definition on the Sherpa website: <http://www.sherpa.ac.uk/romeo/>);
- is subject to courtesy information to the co-author or corresponding author.

Geographic Rights: Scope

Licenses may be exercised anywhere in the world.

Altering/Modifying Material: Not Permitted

Figures, tables, and illustrations may be altered minimally to serve your work. You may not alter or modify text in any manner. Abbreviations, additions, deletions and/or any other alterations shall be made only with prior written authorization of the author(s).

Reservation of Rights

Springer reserves all rights not specifically granted in the combination of (i) the license details provided by you and accepted in the course of this licensing transaction and (ii) these terms and conditions and (iii) CCC's Billing and Payment terms and conditions.

License Contingent on Payment

While you may exercise the rights licensed immediately upon issuance of the license at the end of the licensing process for the transaction, provided that you have disclosed complete and accurate details of your proposed use, no license is finally effective unless and until full

payment is received from you (either by Springer or by CCC) as provided in CCC's Billing and Payment terms and conditions. If full payment is not received by the date due, then any license preliminarily granted shall be deemed automatically revoked and shall be void as if never granted. Further, in the event that you breach any of these terms and conditions or any of CCC's Billing and Payment terms and conditions, the license is automatically revoked and shall be void as if never granted. Use of materials as described in a revoked license, as well as any use of the materials beyond the scope of an unrevoked license, may constitute copyright infringement and Springer reserves the right to take any and all action to protect its copyright in the materials.

Copyright Notice: Disclaimer

You must include the following copyright and permission notice in connection with any reproduction of the licensed material:

"Springer book/journal title, chapter/article title, volume, year of publication, page, name(s) of author(s), (original copyright notice as given in the publication in which the material was originally published) "With permission of Springer"

In case of use of a graph or illustration, the caption of the graph or illustration must be included, as it is indicated in the original publication.

Warranties: None

Springer makes no representations or warranties with respect to the licensed material and adopts on its own behalf the limitations and disclaimers established by CCC on its behalf in its Billing and Payment terms and conditions for this licensing transaction.

Indemnity

You hereby indemnify and agree to hold harmless Springer and CCC, and their respective officers, directors, employees and agents, from and against any and all claims arising out of your use of the licensed material other than as specifically authorized pursuant to this license.

No Transfer of License

This license is personal to you and may not be sublicensed, assigned, or transferred by you without Springer's written permission.

No Amendment Except in Writing

This license may not be amended except in a writing signed by both parties (or, in the case of Springer, by CCC on Springer's behalf).

Objection to Contrary Terms

Springer hereby objects to any terms contained in any purchase order, acknowledgment, check endorsement or other writing prepared by you, which terms are inconsistent with these terms and conditions or CCC's Billing and Payment terms and conditions. These terms and conditions, together with CCC's Billing and Payment terms and conditions (which are incorporated herein), comprise the entire agreement between you and Springer (and CCC) concerning this licensing transaction. In the event of any conflict between your obligations established by these terms and conditions and those established by CCC's Billing and Payment terms and conditions, these terms and conditions shall control.

Jurisdiction

All disputes that may arise in connection with this present License, or the breach thereof, shall be settled exclusively by arbitration, to be held in the Federal Republic of Germany, in accordance with German law.

Other conditions:

V 12AUG2015

Questions? customercare@copyright.com or +1-855-239-3415 (toll free in the US) or +1-978-646-2777.

ELSEVIER LICENSE TERMS AND CONDITIONS

Feb 17, 2017

This Agreement between Rainer E Boegle ("You") and Elsevier ("Elsevier") consists of your license details and the terms and conditions provided by Elsevier and Copyright Clearance Center.

License Number	3842461037038
License date	
Licensed Content Publisher	Elsevier
Licensed Content Publication	NeuroImage
Licensed Content Title	Magnetic vestibular stimulation modulates default mode network fluctuations
Licensed Content Author	Rainer Boegle,Thomas Stephan,Matthias Ertl,Stefan Glasauer,Marianne Dieterich
Licensed Content Date	15 February 2016
Licensed Content Volume	127
Licensed Content Issue	n/a
Start Page	409
End Page	421
Type of Use	reuse in a thesis/dissertation
Intended publisher of new work	other
Portion	full article
Format	both print and electronic
Are you the author of this Elsevier article?	Yes
Will you be translating?	No
Order reference number	
Title of your thesis/dissertation	Modulation of vestibular networks by age and magnetic fields - Implications for the study of vestibular function in patients and healthy controls with functional magnetic resonance imaging
Expected completion date	Jan 2017
Estimated size (number of pages)	80
Elsevier VAT number	GB 494 6272 12
Requestor Location	Rainer E Boegle Tölzer Straße 23c Holzkirchen, Bavaria 83607 Germany Attn: Rainer E Boegle
Billing Type	Invoice
Billing Address	Rainer E Boegle Tölzer Straße 23c Holzkirchen, Germany 83607 Attn: Rainer E Boegle

Total 0.00 EUR

Total 0.00 EUR

[Terms and Conditions](#)

INTRODUCTION

1. The publisher for this copyrighted material is Elsevier. By clicking "accept" in connection with completing this licensing transaction, you agree that the following terms and conditions apply to this transaction (along with the Billing and Payment terms and conditions established by Copyright Clearance Center, Inc. ("CCC"), at the time that you opened your Rightslink account and that are available at any time at <http://myaccount.copyright.com>).

GENERAL TERMS

2. Elsevier hereby grants you permission to reproduce the aforementioned material subject to the terms and conditions indicated.

3. Acknowledgement: If any part of the material to be used (for example, figures) has appeared in our publication with credit or acknowledgement to another source, permission must also be sought from that source. If such permission is not obtained then that material may not be included in your publication/copies. Suitable acknowledgement to the source must be made, either as a footnote or in a reference list at the end of your publication, as follows:

"Reprinted from Publication title, Vol /edition number, Author(s), Title of article / title of chapter, Pages No., Copyright (Year), with permission from Elsevier [OR APPLICABLE SOCIETY COPYRIGHT OWNER]." Also Lancet special credit - "Reprinted from The Lancet, Vol. number, Author(s), Title of article, Pages No., Copyright (Year), with permission from Elsevier."

4. Reproduction of this material is confined to the purpose and/or media for which permission is hereby given.

5. Altering/Modifying Material: Not Permitted. However figures and illustrations may be altered/adapted minimally to serve your work. Any other abbreviations, additions, deletions and/or any other alterations shall be made only with prior written authorization of Elsevier Ltd. (Please contact Elsevier at permissions@elsevier.com)

6. If the permission fee for the requested use of our material is waived in this instance, please be advised that your future requests for Elsevier materials may attract a fee.

7. Reservation of Rights: Publisher reserves all rights not specifically granted in the combination of (i) the license details provided by you and accepted in the course of this licensing transaction, (ii) these terms and conditions and (iii) CCC's Billing and Payment terms and conditions.

8. License Contingent Upon Payment: While you may exercise the rights licensed immediately upon issuance of the license at the end of the licensing process for the transaction, provided that you have disclosed complete and accurate details of your proposed use, no license is finally effective unless and until full payment is received from you (either by publisher or by CCC) as provided in CCC's Billing and Payment terms and conditions. If full payment is not received on a timely basis, then any license preliminarily granted shall be deemed automatically revoked and shall be void as if never granted. Further, in the event that you breach any of these terms and conditions or any of CCC's Billing and Payment terms and conditions, the license is automatically revoked and shall be void as if never granted. Use of materials as described in a revoked license, as well as any use of the materials beyond the scope of an unrevoked license, may constitute copyright infringement and publisher reserves the right to take any and all action to protect its copyright in the materials.

9. Warranties: Publisher makes no representations or warranties with respect to the licensed material.

10. Indemnity: You hereby indemnify and agree to hold harmless publisher and CCC, and their respective officers, directors, employees and agents, from and against any and all claims arising out of your use of the licensed material other than as specifically authorized pursuant to this license.

11. No Transfer of License: This license is personal to you and may not be sublicensed, assigned, or transferred by you to any other person without publisher's written permission.

12. **No Amendment Except in Writing:** This license may not be amended except in a writing signed by both parties (or, in the case of publisher, by CCC on publisher's behalf).

13. **Objection to Contrary Terms:** Publisher hereby objects to any terms contained in any purchase order, acknowledgment, check endorsement or other writing prepared by you, which terms are inconsistent with these terms and conditions or CCC's Billing and Payment terms and conditions. These terms and conditions, together with CCC's Billing and Payment terms and conditions (which are incorporated herein), comprise the entire agreement between you and publisher (and CCC) concerning this licensing transaction. In the event of any conflict between your obligations established by these terms and conditions and those established by CCC's Billing and Payment terms and conditions, these terms and conditions shall control.

14. **Revocation:** Elsevier or Copyright Clearance Center may deny the permissions described in this License at their sole discretion, for any reason or no reason, with a full refund payable to you. Notice of such denial will be made using the contact information provided by you. Failure to receive such notice will not alter or invalidate the denial. In no event will Elsevier or Copyright Clearance Center be responsible or liable for any costs, expenses or damage incurred by you as a result of a denial of your permission request, other than a refund of the amount(s) paid by you to Elsevier and/or Copyright Clearance Center for denied permissions.

LIMITED LICENSE

The following terms and conditions apply only to specific license types:

15. **Translation:** This permission is granted for non-exclusive world **English** rights only unless your license was granted for translation rights. If you licensed translation rights you may only translate this content into the languages you requested. A professional translator must perform all translations and reproduce the content word for word preserving the integrity of the article.

16. **Posting licensed content on any Website:** The following terms and conditions apply as follows: Licensing material from an Elsevier journal: All content posted to the web site must maintain the copyright information line on the bottom of each image; A hyper-text must be included to the Homepage of the journal from which you are licensing at <http://www.sciencedirect.com/science/journal/xxxxx> or the Elsevier homepage for books at <http://www.elsevier.com>; Central Storage: This license does not include permission for a scanned version of the material to be stored in a central repository such as that provided by Heron/XanEdu.

Licensing material from an Elsevier book: A hyper-text link must be included to the Elsevier homepage at <http://www.elsevier.com>. All content posted to the web site must maintain the copyright information line on the bottom of each image.

Posting licensed content on Electronic reserve: In addition to the above the following clauses are applicable: The web site must be password-protected and made available only to bona fide students registered on a relevant course. This permission is granted for 1 year only. You may obtain a new license for future website posting.

17. **For journal authors:** the following clauses are applicable in addition to the above:

Preprints:

A preprint is an author's own write-up of research results and analysis, it has not been peer-reviewed, nor has it had any other value added to it by a publisher (such as formatting, copyright, technical enhancement etc.).

Authors can share their preprints anywhere at any time. Preprints should not be added to or enhanced in any way in order to appear more like, or to substitute for, the final versions of articles however authors can update their preprints on arXiv or RePEc with their Accepted Author Manuscript (see below).

If accepted for publication, we encourage authors to link from the preprint to their formal publication via its DOI. Millions of researchers have access to the formal publications on ScienceDirect, and so links will help users to find, access, cite and use the best available version. Please note that Cell Press, The Lancet and some society-owned have different preprint policies. Information on these policies is available on the journal homepage.

Accepted Author Manuscripts: An accepted author manuscript is the manuscript of an article that has been accepted for publication and which typically includes author-

incorporated changes suggested during submission, peer review and editor-author communications.

Authors can share their accepted author manuscript:

- immediately
 - via their non-commercial person homepage or blog
 - by updating a preprint in arXiv or RePEc with the accepted manuscript
 - via their research institute or institutional repository for internal institutional uses or as part of an invitation-only research collaboration work-group
 - directly by providing copies to their students or to research collaborators for their personal use
 - for private scholarly sharing as part of an invitation-only work group on commercial sites with which Elsevier has an agreement
- after the embargo period
 - via non-commercial hosting platforms such as their institutional repository
 - via commercial sites with which Elsevier has an agreement

In all cases accepted manuscripts should:

- link to the formal publication via its DOI
- bear a CC-BY-NC-ND license - this is easy to do
- if aggregated with other manuscripts, for example in a repository or other site, be shared in alignment with our hosting policy not be added to or enhanced in any way to appear more like, or to substitute for, the published journal article.

Published journal article (JPA): A published journal article (PJA) is the definitive final record of published research that appears or will appear in the journal and embodies all value-adding publishing activities including peer review co-ordination, copy-editing, formatting, (if relevant) pagination and online enrichment.

Policies for sharing publishing journal articles differ for subscription and gold open access articles:

Subscription Articles: If you are an author, please share a link to your article rather than the full-text. Millions of researchers have access to the formal publications on ScienceDirect, and so links will help your users to find, access, cite, and use the best available version. Theses and dissertations which contain embedded PJAs as part of the formal submission can be posted publicly by the awarding institution with DOI links back to the formal publications on ScienceDirect.

If you are affiliated with a library that subscribes to ScienceDirect you have additional private sharing rights for others' research accessed under that agreement. This includes use for classroom teaching and internal training at the institution (including use in course packs and courseware programs), and inclusion of the article for grant funding purposes.

Gold Open Access Articles: May be shared according to the author-selected end-user license and should contain a [CrossMark logo](#), the end user license, and a DOI link to the formal publication on ScienceDirect.

Please refer to Elsevier's [posting policy](#) for further information.

18. For book authors the following clauses are applicable in addition to the above: Authors are permitted to place a brief summary of their work online only. You are not allowed to download and post the published electronic version of your chapter, nor may you scan the printed edition to create an electronic version. **Posting to a repository:** Authors are permitted to post a summary of their chapter only in their institution's repository.

19. Thesis/Dissertation: If your license is for use in a thesis/dissertation your thesis may be submitted to your institution in either print or electronic form. Should your thesis be published commercially, please reapply for permission. These requirements include permission for the Library and Archives of Canada to supply single copies, on demand, of the complete thesis and include permission for Proquest/UMI to supply single copies, on demand, of the complete thesis. Should your thesis be published commercially, please reapply for permission. Theses and dissertations which contain embedded PJAs as part of

the formal submission can be posted publicly by the awarding institution with DOI links back to the formal publications on ScienceDirect.

Elsevier Open Access Terms and Conditions

You can publish open access with Elsevier in hundreds of open access journals or in nearly 2000 established subscription journals that support open access publishing. Permitted third party re-use of these open access articles is defined by the author's choice of Creative Commons user license. See our [open access license policy](#) for more information.

Terms & Conditions applicable to all Open Access articles published with Elsevier:

Any reuse of the article must not represent the author as endorsing the adaptation of the article nor should the article be modified in such a way as to damage the author's honour or reputation. If any changes have been made, such changes must be clearly indicated.

The author(s) must be appropriately credited and we ask that you include the end user license and a DOI link to the formal publication on ScienceDirect.

If any part of the material to be used (for example, figures) has appeared in our publication with credit or acknowledgement to another source it is the responsibility of the user to ensure their reuse complies with the terms and conditions determined by the rights holder.

Additional Terms & Conditions applicable to each Creative Commons user license:

CC BY: The CC-BY license allows users to copy, to create extracts, abstracts and new works from the Article, to alter and revise the Article and to make commercial use of the Article (including reuse and/or resale of the Article by commercial entities), provided the user gives appropriate credit (with a link to the formal publication through the relevant DOI), provides a link to the license, indicates if changes were made and the licensor is not represented as endorsing the use made of the work. The full details of the license are available at <http://creativecommons.org/licenses/by/4.0>.

CC BY NC SA: The CC BY-NC-SA license allows users to copy, to create extracts, abstracts and new works from the Article, to alter and revise the Article, provided this is not done for commercial purposes, and that the user gives appropriate credit (with a link to the formal publication through the relevant DOI), provides a link to the license, indicates if changes were made and the licensor is not represented as endorsing the use made of the work. Further, any new works must be made available on the same conditions. The full details of the license are available at <http://creativecommons.org/licenses/by-nc-sa/4.0>.

CC BY NC ND: The CC BY-NC-ND license allows users to copy and distribute the Article, provided this is not done for commercial purposes and further does not permit distribution of the Article if it is changed or edited in any way, and provided the user gives appropriate credit (with a link to the formal publication through the relevant DOI), provides a link to the license, and that the licensor is not represented as endorsing the use made of the work. The full details of the license are available at <http://creativecommons.org/licenses/by-nc-nd/4.0>. Any commercial reuse of Open Access articles published with a CC BY NC SA or CC BY NC ND license requires permission from Elsevier and will be subject to a fee.

Commercial reuse includes:

- Associating advertising with the full text of the Article
- Charging fees for document delivery or access
- Article aggregation
- Systematic distribution via e-mail lists or share buttons

Posting or linking by commercial companies for use by customers of those companies.

20. Other Conditions:

v1.8

Questions? customercare@copyright.com or +1-855-239-3415 (toll free in the US) or +1-978-646-2777.

SHUTTERSTOCK
Terms of Service
Shutterstock License Agreement(s)

Dear Shutterstock Customer:

The following is a legal agreement between you or the employer or other entity on whose behalf you are entering into this agreement ("you" or "Customer") and: i) if you are an existing customer or a new customer in the United States or Canada, Shutterstock, Inc., a Delaware corporation with its office at Shutterstock, Inc., 350 Fifth Avenue, 21st Floor, New York, NY 10118, United States; or ii) if you are a new customer not located in the United States or Canada, Shutterstock Netherlands, B.V., incorporated under the laws of the Netherlands, having its principal place of business at Hoogte Kadijk 391018 BE Amsterdam, the Netherlands (in either instance, referred to hereafter as "Shutterstock"). By entering into this agreement, you verify that your country of residence is the same as your billing address.

"Image(s)" means photographs, vectors, drawings and the like available for license from the Shutterstock website.

"Footage" means any moving images, animations, films, videos or other audio/visual representations, excluding still images, recorded in any format that are available for license from the Shutterstock website.

"Visual Content" shall refer collectively to Images and Footage.

The following Terms of Service ("TOS") constitutes an agreement between Customer and Shutterstock setting forth the rights and obligations with respect to any Visual Content licensed by you. By agreeing to the TOS, you agree that these terms control your rights and obligations with respect to all Visual Content licenses set forth herein, notwithstanding the subscription or license you may be purchasing today. Please revisit these TOS when you purchase any Visual Content.

UNLESS YOU PURCHASE A ["TEAM SUBSCRIPTION"](#) OR ["PREMIER LICENSE"](#), THIS IS A SINGLE SEAT LICENSE AUTHORIZING ONE NATURAL PERSON TO LICENSE, DOWNLOAD AND USE VISUAL CONTENT. IF YOU PURCHASE A TEAM SUBSCRIPTION THE RIGHT TO LICENSE, DOWNLOAD AND USE VISUAL CONTENT IS LIMITED TO THE NUMBER OF USERS PERMITTED BY THAT TEAM SUBSCRIPTION. THE PREMIER LICENSE AND PLATFORM PROVIDES THESE AND ADDITIONAL RIGHTS TO AN UNLIMITED AMOUNT OF USERS. SOME LICENSES SET FORTH HEREIN MAY NOT BE AVAILABLE FOR TEAM SUBSCRIPTION PURCHASE. *If you require a multi-user account, please contact Customer Service (Phone: Inside US 1-866-663-3954, Outside US 1-646-419-4452 Email: [Customer Support](#) or our [Premier Team](#)).*

Part I Visual Content Licenses

- a. Image Licenses
- b. Footage Licenses
- c. Restrictions on Use of Visual Content

Part II Warranties and Representations

Part III Indemnification and Liability

Part IV Additional Terms

PART I VISUAL CONTENT LICENSES

Shutterstock hereby grants you a non-exclusive, non-transferable right to use, modify and reproduce Visual Content worldwide, in perpetuity, as expressly permitted by the applicable license and subject to the limitations set forth herein:

a. IMAGE LICENSES

i. A STANDARD IMAGE LICENSE grants you the right to use Images:

1. As a digital reproduction, including on websites, in online advertising, in social media, in mobile advertising, mobile "apps", software, e-cards, e-publications (e-books, e-magazines, blogs, etc.), and in online media (including on video-sharing services such as YouTube, Dailymotion, Vimeo, etc., subject to the budget limitations set forth in sub-paragraph I.a.i.4 below);
2. Printed in physical form as part of product packaging and labeling, letterhead and business cards, point of sale advertising,

billboards, CD and DVD cover art, or in the advertising and copy of tangible media, including magazines, newspapers, and books provided no Image is reproduced more than 500,000 times in the aggregate;

3. As part of an "Out-of-Home" advertising campaign, provided the intended audience for such campaign is less than 500,000 gross impressions.
 4. Incorporated into film, video, television series, advertisement, or other multimedia productions for distribution in any medium now known or hereafter devised (each a "Production"), without regard to audience size, provided the budget for any such Production does not exceed USD \$10,000;
 5. For your own personal, non-commercial use (not for resale, download, distribution, or any commercial use of any kind).
- ii. AN ENHANCED IMAGE LICENSE grants you the right to use Images:
1. In any manner permitted under a Standard Image License, without any limitation on the number of reproductions, impressions, or budget;
 2. Incorporated into merchandise or promotional items for sale or distribution (collectively "Merchandise"), including, without limitation, textiles, artwork, magnets, wall-art, calendars, toys, stationery, greeting cards, and any other physical reproduction for resale or distribution, provided that such Merchandise incorporates material creative or functional elements apart from the Image(s).
 3. In wall art (and without requiring further creative or functional elements) for decorative purposes in a commercial space owned by you or your client, and not for sale.
 4. Incorporated as elements of digital templates for sale or distribution.

If the Standard or Enhanced Image licenses do not grant the rights you require please contact Customer Service. (Phone: Inside US 1-866-663-3954, Outside US 1-646-419-4452 Email: [Customer Support](#))

b. FOOTAGE LICENSES

i. A FOOTAGE USE LICENSE grants you the right to use Footage:

1. in Productions (i.e., a film, video, television series, advertisement, or other multimedia production) displayed or distributed to the public by any means now known or hereafter devised;
2. in connection with a live performance;
3. on websites.

If the Footage Use License does not grant the rights you require, please contact Customer Service. (Phone: Inside US 1-866-663-3954, Outside US 1-646-419-4452 Email: [Customer Support](#))

ii. A FOOTAGE COMP LICENSE grants you the right to use watermarked, low resolution Footage as a comp (the "Comp Footage") solely in test, sample, comp, or rough cut evaluation materials. Footage Comp Licenses do not permit you to display or distribute to the public or incorporated into any final materials any such Footage. Comp Footage can be edited, but you may not remove or alter the Shutterstock watermark.

c. RESTRICTIONS ON USE OF VISUAL CONTENT

YOU MAY NOT:

- i. Use Visual Content other than as expressly provided by the license you purchased with respect to such Visual Content.
- ii. Portray any person depicted in Visual Content (a "Model") in a way that a reasonable person would find offensive, including but not limited to depicting a Model: a) in connection with pornography, "adult videos", adult entertainment venues, escort services, dating services, or the like; b) in connection with the advertisement or promotion of tobacco products; c) in a political context, such as the promotion, advertisement or endorsement of any party, candidate, or elected official, or in connection with any political policy or viewpoint; d) as suffering from, or medicating for, a physical or mental ailment; or e) engaging in immoral or criminal activities.
- iii. Use any Visual Content in a pornographic, defamatory, or deceptive context, or in a manner that could be considered libelous, obscene, or illegal.
- iv. Use Visual Content designated "Editorial Use Only" for commercial purposes.
- v. Resell, redistribute, provide access to, share or transfer any Visual Content except as specifically provided herein.
- vi. Use Visual Content in a manner that infringes upon any third party's trademark or other intellectual property, or would give rise to a claim of deceptive advertising or unfair competition.
- vii. Use any Visual Content (in whole or in part) as a trademark, service mark, logo, or other indication of origin, or as part thereof.
- viii. Use "stills" derived from Footage except solely in connection with the in-context marketing, promotion, and advertising of your derivative works incorporating Footage.
- ix. Falsely represent, expressly or by way of reasonable implication, that any Visual Content was created by you or a person other than the copyright holder(s) of that Visual Content.

If you require any of the foregoing rights, please contact Customer Service. (Phone: Inside US 1-866-663-3954, Outside US 1-646-

419-4452 Email: [Customer Support](#))

d. CREDIT AND COPYRIGHT NOTICES

- i. The use of Visual Content in an "editorial" context, shall be accompanied by an adjacent credit to the Shutterstock contributor and to Shutterstock in substantially the following form:
"Name of Artist/Shutterstock.com"
- ii. If and where commercially reasonable, the use of Visual Content in Merchandise or a Production shall be accompanied by a credit to Shutterstock in substantially the following form:
"Image(s) or Footage (as applicable), used under license from Shutterstock.com"
- iii. Credit attributions are not required in connection with any other use of Images unless another stock content provided is afforded credit in connection with the same use.
- iv. In all cases the credit and attribution shall be of such size, color and prominence so as to be clearly and easily readable by the unaided eye.

PART II WARRANTIES AND REPRESENTATIONS

- a. Shutterstock warrants and represents that:
 - i. Shutterstock's contributors have granted Shutterstock all necessary rights in and to the Visual Content to grant the rights set forth in Part I as applicable.
 - ii. Visual Content in its original unaltered form and used in full compliance with these TOS and applicable law, will not: i) infringe any copyright, trademark or other intellectual property right; ii) violate any third parties' rights of privacy or publicity; iii) violate any US law, statute, ordinance, or regulation; or iv) be defamatory, libelous, pornographic or obscene.
- b. While Shutterstock makes commercially reasonable efforts to ensure the accuracy of keywords and descriptions, as well as the integrity of Visual Content designated "Editorial Use Only", SHUTTERSTOCK MAKES NO WARRANTIES AND/OR REPRESENTATIONS REGARDING ANY: I) KEYWORD, TITLES OR DESCRIPTIONS; II) AUDIO IN FOOTAGE; OR III) VISUAL CONTENT DESIGNATED "EDITORIAL USE ONLY". For the sake of clarity, Shutterstock will not indemnify or have any liability in respect of any claims arising from inaccurate keyword, titles or descriptions, any audio in Footage, or the use of Visual Content designated Editorial Use Only.
- c. SHUTTERSTOCK MAKES NO REPRESENTATIONS OR WARRANTIES WHATSOEVER OTHER THAN THOSE EXPRESSLY MADE IN THIS "WARRANTIES AND REPRESENTATIONS" SECTION.

PART III Indemnification and Liability:

- a. Subject to the terms hereof, and provided that you have not breached the terms of this or any other agreement with Shutterstock, Shutterstock will defend, indemnify, and hold you harmless up to the applicable "Limit of Liability" set forth below. Such indemnification is solely limited to Customer's direct damages arising from a third-party claim directly attributable to Shutterstock's breach of the express warranties and representations made in Part II hereof, together with associated expenses (including reasonable attorneys' fees). Indemnification is conditioned upon you notifying Shutterstock, in writing, of any such claim or threatened claim, no later than five (5) business days from the date you know or reasonably should have known of the claim or threatened claim. Such notification must include all details of the claim then known to you (e.g., the use of Visual Content at issue, the name and contact information of the person and/or entity making the claim, copies of any correspondence received and/or sent in connection with the claim). The notification must be emailed or faxed to Shutterstock at counsel@shutterstock.com or 1-646-786-4782, with a hard copy to Shutterstock, 350 5th Avenue, 21st Floor, New York, New York, 10118, Attention: General Counsel, via certified mail, return receipt requested; or ii) overnight courier, recipient's signature required. Shutterstock shall have the right to assume the handling, settlement or defense of any claim or litigation to which this indemnification applies. You agree to cooperate with Shutterstock in the defense of any such claim and shall have the right to participate in any litigation at your own expense. You agree that Shutterstock is not liable for any legal fees and/or other costs incurred by you or on your behalf prior to Shutterstock having a reasonable opportunity to analyze such claim's validity.
- b. Shutterstock shall not be liable for any damages, costs or losses arising as a result of modifications made to the Visual Content or due to the context in which the Visual Content is used by you.
- c. Limits of Liability: Shutterstock's total maximum aggregate obligation and liability (the "Limit of Liability") arising out of each of

Customer's:

- i. Standard Image Licenses shall be USD \$10,000.
- ii. Enhanced Image Licenses shall be USD \$250,000.
- iii. Footage Use Licenses shall be USD \$10,000.

If you have questions about the foregoing, please contact Customer Service. (Phone: Inside US 1-866-663-3954, Outside US 1-646-419-4452 Email: Customer Support)

- d. You will indemnify and hold Shutterstock, its officers, employees, shareholders, directors, managers, members and suppliers, harmless against any damages or liability of any kind arising from any use of the Visual Content other than the uses expressly permitted by these TOS. You further agree to indemnify Shutterstock for all costs and expenses that Shutterstock incurs in the event that you breach any of the terms of this or any other agreement with Shutterstock.

PART IV ADDITIONAL TERMS

- a. Except when required by law, Shutterstock shall be under no obligation to issue refunds under any circumstances. In the event that Shutterstock determines that you are entitled to a refund of all or part of the fees you paid, such refund shall be made using the payment method originally used by you to make your purchase. If you reside in the European Union and you cancel your account within seven (7) days of making payment to Shutterstock Netherlands, B.V., provided that you have not yet licensed any Visual Content, Shutterstock Netherlands, B.V., will refund the payment made by you in connection with such cancelled account. To cancel your account, contact support@shutterstock.com.
- b. "Non-transferable" as used herein means that except as specifically provided in these TOS, you may not sell, rent, load, give, sublicense, or otherwise transfer to anyone, Visual Content or the right to use Visual Content. You may however, make a one-time transfer of Visual Content to a third party for the sole purpose of causing such third party to print and/or manufacture your goods incorporating Visual Content subject to the terms and conditions herein. If you become aware that any Social Media Website uses any Visual Content in a manner that exceeds your license hereunder, you agree to remove all derivative works incorporating Visual Content from such Social Media Site, and to promptly notify Shutterstock of each such Social Media Website's use. You agree to take all commercially reasonable steps to prevent third parties from duplicating any Visual Content. If you become aware of any unauthorized duplication of any Visual Content please notify us via email at support@shutterstock.com.
- c. If you use any Visual Content as part of work product created for or delivered to a client or customer, you will disclose the identities of such clients or customers to Shutterstock, upon Shutterstock's reasonable request.
- d. The validity, interpretation and enforcement of these TOS, matters arising out of or related to these TOS or their making, performance or breach, and related matters shall be governed by the internal laws of the State of New York (without reference to choice of law doctrine). Any legal action or proceeding concerning the validity, interpretation and/or enforcement of these TOS, matters arising out of or related to these TOS or its making, performance or breach, or related matters shall be brought exclusively in the State or Federal courts located in the State and County of New York. All parties consent to the exclusive jurisdiction of those courts, waiving any objection to the propriety or convenience of such venues. The United Nations Convention on Contracts for the International Sale of Goods does not apply to or otherwise affect these TOS. You agree that service of process in any actions, controversies and disputes arising from or relating to these TOS may be effected by mailing a copy thereof by registered or certified mail (or any substantially similar form of mail), postage prepaid, to the other party however, nothing herein shall affect the right to effect service of process in any other manner permitted by law.
- e. If you are entering into these TOS on behalf of your employer or other entity, you warrant and represent that you have the full right and authority to do so. In the event that you do not have such authority, you agree that you will be personally liable to Shutterstock for any breaches of the terms of these TOS.
- f. The number of Visual Content downloads available to you is determined by the product you purchase. For the purposes of these TOS, a day is defined as the twenty four (24) hour period beginning at the time your product is purchased. A month is defined as thirty (30) consecutive days beginning on and including the date that you purchase your product.
- g. If any individual term of these TOS is found to be invalid or unenforceable by any legal or regulatory body of competent jurisdiction, such finding will be limited solely to such invalid or unenforceable part, without affecting the remaining parts of such individual term, or any other part of the TOS, so that these TOS shall otherwise remain in full force and effect.
- h. **It is expressly understood and agreed that this TOS is entered into solely for the mutual benefit of the parties herein and that**

no benefits, rights, duties, or obligations are intended by this TOS as to third parties.

- i. In the event that you breach any of the terms of this or any other agreement with Shutterstock, Shutterstock shall have the right to terminate your account without further notice, in addition to Shutterstock's other rights at law and/or equity. Shutterstock shall be under no obligation to refund any fees paid by you in the event that your account is terminated by reason of a breach.
- j. Except as expressly set forth herein, Shutterstock grants no rights and makes no warranties, with regard to the use of personally identifiable information that may be visible in the Visual Content, music or other audio in footage, trademarks, trade dress or copyrighted designs or works of art or architecture depicted in any Visual Content. Shutterstock only has model or property releases where expressly indicated on the Shutterstock website.
- k. Shutterstock's liability under any individual license purchased hereunder shall not exceed the "Limit of Liability" applicable to the license in effect at the time customer knows or should have known of the claim, and is without regard to the number of times the subject Visual Content is licensed or used by you.
- l. Except as specifically provided in Part III hereof, in no event, will Shutterstock's total aggregate liability to you or any third party claiming through you, arising out of or in connection with your use of or inability to use the Shutterstock websites and/or Visual Content contained thereon (whether in contract, tort or otherwise) exceed the monetary amount actually received by Shutterstock from you for the applicable Visual Content license.
- m. Neither Shutterstock nor any of its officers, employees, managers, members, shareholders, directors or suppliers shall be liable to you or to any other person or entity for any general, punitive, special, indirect, consequential or incidental damages, or lost profits or any other damages, costs or losses arising out of your use of the Visual Content, Shutterstock's breach of this agreement, or otherwise, unless expressly provided for herein, even if Shutterstock has been advised of the possibility of such damages, costs or losses.
- n. Except as expressly set forth in Part II, all Visual Content is provided "as is" without warranty of any kind, either express or implied, including, but not limited to the implied warranties of non-infringement, merchantability, or fitness for a particular purpose. Some Visual Content may contain elements that require additional clearance if the Visual Content is modified or used in a particular context. If you make such modification or use Visual Content in such context, you are solely responsible for obtaining any additional clearances thereby required.
- o. Shutterstock does not warrant that the Visual Content, Shutterstock websites, or other materials will meet your requirements or that use will be uninterrupted or error free. The entire risk as to the quality, performance and use of the Visual Content is solely with you.
- p. In the event that you use fraudulent credit card information to open an account or otherwise engage in any criminal activity affecting Shutterstock, Shutterstock will promptly file a complaint with www.ic3.gov, the internet crime complaint center, a partnership between the [Federal Bureau of Investigation \(FBI\)](#) and the [National White Collar Crime Center](#).

Effective August 3, 2015

Affidavit – Eidesstattliche Versicherung

I, Rainer Boegle, hereby confirm that the dissertation

“Modulation of the central vestibular networks through aging and high-strength magnetic fields - implications for studies of vestibular function with functional magnetic resonance imaging”

is the result of my own work and that I have only used sources or materials listed and specified in the dissertation.

Hiermit versichere ich, Rainer Boegle, an Eides statt, dass ich die vorliegende Dissertation

“Modulation of the central vestibular networks through aging and high-strength magnetic fields - implications for studies of vestibular function with functional magnetic resonance imaging”

selbstständig angefertigt habe, mich außer der angegebenen keiner weiteren Hilfsmittel bedient und alle Erkenntnisse, die aus dem Schrifttum ganz oder annähernd übernommen sind, als solche kenntlich gemacht und nach ihrer Herkunft unter Bezeichnung der Fundstelle einzeln nachgewiesen habe.

München, den 20.02.2017
Munich, 20.02.2017

Unterschrift
signature

Declaration of author contributions

Age-related decline in functional connectivity of the vestibular cortical network

*C.A.M. Cyran, *R. Boegle, T. Stephan, M. Dieterich, S. Glasauer

*C.A.M. Cyran and R. Boegle contributed equally to the study.

Author contribution:

The Author of this thesis participated in measuring the subjects, analyzed the functional imaging data for functional connectivity and performed the data denoising for the analysis of temporal variability, as well as writing substantial parts of the manuscript, and created figures 2, 3, and 4 of the attached publication.

Signatures

Shared first author: C.A.M. Koriath (C.A.M. Cyran)

Shared first author: R. Boegle

1st supervisor: M. Dieterich

Magnetic vestibular stimulation modulates default mode network fluctuations

R. Boegle, T. Stephan, M. Ertl, S. Glasauer, and M. Dieterich

Author contribution

The Author of this thesis planned the experiment, measured the subjects, performed the data analysis, wrote major parts of the manuscript, and created all figures.

Signatures

First author: R. Boegle

1st supervisor: M. Dieterich